CHALMERS

Analyses of EMC- & Grid-connected Filters in an Electric Power-train

Measurements & Improvements

Bachelor's thesis in Electrical Engineering

TOBIAS EKBORG
ANDREAS ERIKSSON

DEPARTMENT OF ELECTRICAL ENGINEERING

CHALMERS UNIVERSITY OF TECHNOLOGY
Gothenburg, Sweden 2024
www.chalmers.se

Bachelor's thesis 2024

Analyses of EMC- & Grid-connected Filters in an Electric Power-train

Measurements & Improvements

TOBIAS EKBORG
ANDREAS ERIKSSON

CHALMERS

Department of Electrical Engineering
Chalmers University of Technology
Gothenburg, Sweden 2024

Analyses of EMC- & Grid-connected Filters in an Electric Power-train
Measurements & Improvements
TOBIAS EKBORG
ANDREAS ERIKSSON

Supervisor: Emil Andersson, Epiroc AB
Examiner: Rob Maaskant, Department of Electrical Engineering, Chalmers University of Technology

Bachelor's Thesis 2024
Department of Electrical Engineering
Chalmers University of Technology
SE-412 96 Gothenburg
Telephone +46 31 772 1000

Typeset in LaTeX
Printed by Chalmers Reproservice
Gothenburg, Sweden 2024

Analyses of EMC- & Grid-connected Filters in an Electric Power-train
Measurements & Improvements
TOBIAS EKBORG
ANDREAS ERIKSSON
Department of Electrical Engineering
Chalmers University of Technology 4

Abstract

Epiroc have had a need to investigate the EMC and LCL-filters that are currently placed and operating in a lot of their vehicles. They have questioned whether or not their currently used capacitor and inductor-based filters are working adequately in filtering unwanted noise or if there could be a risk of wear to the system with prolonged operation and if any improvements could be made.

This thesis has, with the help of Epiroc and extensive research, examined these questions in detail by conducting measurements on a drill rig vehicle at Epiroc's facilities in Örebro. The thesis dives into areas such as Electromagnetic interference, electrical noise prevention methods and signal processing.

The measurements indicated that both of the filters work and do filter unwanted noise, differences can be seen in the overall noise level. There are however some ideas outlined in this thesis that potentially could help increase the noise suppression of the filters.

Keywords: EMC, LCL, filters, noise, vehicle.

Acknowledgements

This thesis was written by two aspiring electrical engineers in their third year of their bachelor's programme at Chalmers University of Technology. The project was a joint venture together with the company Epiroc located in Örebro and is connected to the concept of electrical engineering in many ways by covering topics such as electromagnetic interference, electrical filters and data processing.

The two of us would like to lend our greatest appreciation to a few different people that contributed to this thesis in many ways. Without these people, the project would likely never have seen the light of day. Firstly, we would like to thank Emil Andersson for his unwavering conviction to see this project through to the end. We would also like to thank Niklas Sundin for always being available for any questions we had regarding the project. Thirdly, we would like to thank Thomas Tierney for always thinking about solutions rather than problems and being an invaluable help in order to get across the finish line. Lastly, we would thank every other person that contributed to this project in some way, but were not mentioned specifically.

Tobias Ekborg, Andreas Eriksson, Gothenburg, May 2024

List of Acronyms

CM	Common-mode
CMC	Common-mode choke
DM	Differential-mode
EMC	Electromagnetic compatibility
EMI	Electromagnetic interference
THD	Total harmonic distortion

Contents

List of Figures

List of Tables

1

Introduction

1.1 Background

Electromagnetic interference (EMI) or electromagnetic noise is prevalent in all electrical circuits, whether it stems from internal sources or external sources. If not properly handled, the noise can disturb the circuit's processes and even damage its components. There is also a possibility that the noise manifests itself in other circuits through radiation or conduction.

A common problem in electric vehicles is the radiated noise through stray capacitance that originates from the traction inverter driving the motor. For electric cars driving on the road, the possibility of transmitting EMI to other vehicles is low due to galvanic isolation and radiation shielding. But for electric drill-rigs connected to the grid, conducted interference to other grid-connected devices and internally is much more likely. It is therefore of great importance to attenuate this noise.

For conducted EMI, filtering is the main method of attenuation, where the filter components, the arrangement of those components and their values determine the filters capability to attenuate a certain type of noise. This thesis aims to examine what causes this EMI, and how it can be prevented by, together with Epiroc AB, conducting measurements on already existing filters in the power train of one their vehicle.

1.2 Purpose

With different capacitor values for a Y-capacitor filter, measure and analyse the noise in the drive-train of one of Epiroc's vehicles. This is done in order to determine what capacitor value works the best and if that value attenuates the noise to an acceptable level. If not, come up with ideas for a solution.

Analyse how the noise between the power-train and the grid is attenuated by the vehicle's LCL-filter. If not to an acceptable level, come up with ideas on how improve the filter.

1.3 Limitations

This report only covers the measurements and analysis of one drill rig vehicle due to the lack of time and availability of other vehicles. Therefore this thesis specifically targets this one vehicle.

All measuring points wished for were not possible to measure at the same time, which is of importance due to the possible variability of electromagnetic noise. The reason for this was that there was not enough equipment at hand, more specifically, not enough oscilloscope ports that could transfer the data into a computer easily. Some parts of the power-train have therefore not been analysed.

The different capacitor values used for the Y-capacitor filter are predetermined from earlier tests done by the company. As a consequence, the measurements covered in this report were also done using these capacitor values.

1.4 Key questions

- Why is noise being generated in Epiroc's vehicle and how can it be suppressed?
- How does common mode current affect the different components of the power train?
- Do the current EMC and LCL-filters already attenuate the noise to an acceptable level?
- Can the filters be improved?

1.5 Thesis outline

The thesis is divided into the following chapters. Ch. 2 covers relevant theory regarding the emergence of electromagnetic interference and its varying properties, how it manifests itself in a circuit, common filtering methods and standards of emitted interference towards the electrical grid. Methods are covered in Ch. 3. Here, courses of action such as simulations and measurements are described. In Ch. 4 the results are presented and, finally, in Ch. 5 the conclusions and ways of improvement are discussed.

2
Theory

In the following section, the theory and background of electromagnetic interference (EMI) is described and the general methods with which this noise can be attenuated are described, but also a brief explanation of harmonics and the Swedish standard with regards to electricity distribution in the grid. The Swedish standard is used to put the data into context of what is an acceptable level of interference output from the vehicle to the grid. Additionally, information about the power train in the examined vehicle is provided.

2.1 Power-train

A simplified sketch of the power-train of the vehicle M2C MK10 Boomer can be seen in Fig. 2.1 below. A battery pack is connected to DC-lines. The battery can be charged from the AC/DC inverter/charger, also mentioned as a multi-inverter throughout the report, that is connected to an LCL-filter and the electric power grid. To use the traction motor, the battery can power the traction inverter, converting the DC-voltage to AC-voltage. The DC/DC converter can convert the high voltage from the battery to 24 V for other systems in the vehicle. Lastly, the Y-capacitor filter can be seen in the upper right corner, connected from the DC-lines to the common ground. All components are connected to this common ground rail.

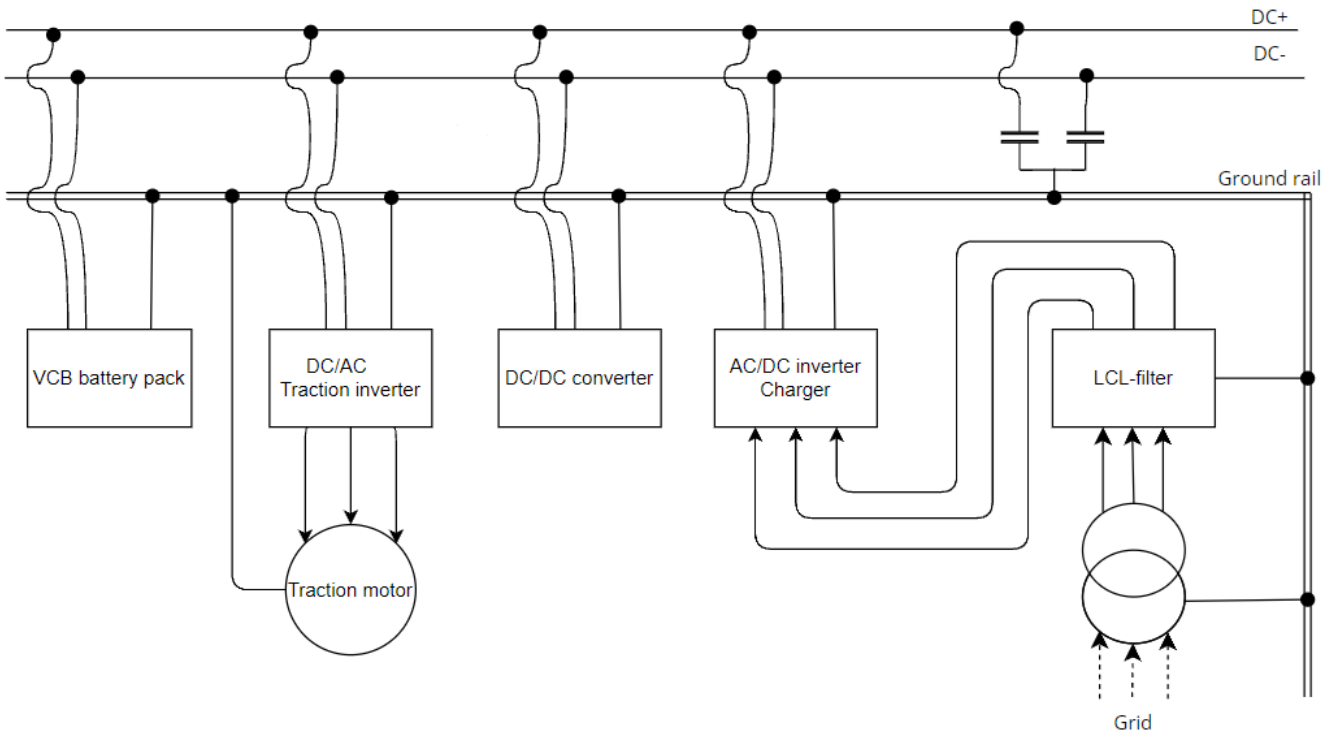

Figure 2.1: Power-train of Epiroc's vehicle.

2.2 Electromagnetic Interference

EMI is a phenomenon that exists in almost all electrical circuitry and all voltage and current levels to some extent. It is unwanted electrical signals that affect and disturb electrical components, which, in certain scenarios and with sufficient quantities can make some sensitive electrical equipment completely dysfunctional.

2.2.1 Sources of EMI

EMI can be caused by a number of different things, even natural sources such as solar storms or lightning impulses [1]. A frequent source for EMI in circuits with power electronics, such as the one in this thesis, is switching operations. By switching, a component like the inverter which uses pulse width modulation (PWM) will create frequency components at high frequency ranges. The reason for this is that the switch wants to instantly change the voltage and current when switching on or off but is hindered by capacitive and inductive elements in the circuit which makes this impossible [2]. The faster the switching, the larger the noise [3]. For the time delay, switching from one voltage level to another, to be as small as possible it requires high frequency components to exist. These frequency components are usually called harmonics and are discussed further in Sec. 2.4. Cables and circuits can also interfere with each other through multiple different coupling paths which is mentioned in Sec. 2.2.3.

2.2.2 Common mode and Differential mode current

Common mode (CM) and differential mode (DM) current are two ways in which current can manifest in a circuit. CM and DM current are two very important concepts when discussing EMI. Knowing what type of modes have the largest impact in the circuit is usually a prerequisite before designing counter measurements such as filters, since different noise attenuation methods target the two modes differently.

2.2.2.1 Differential mode current

DM current works in the same way to how conventional current characteristics work in a circuit, i.e. the current flows through the line and returns through the neutral with an opposite sign [4]. This can be seen represented in a simple circuit in Fig. 2.2 below.

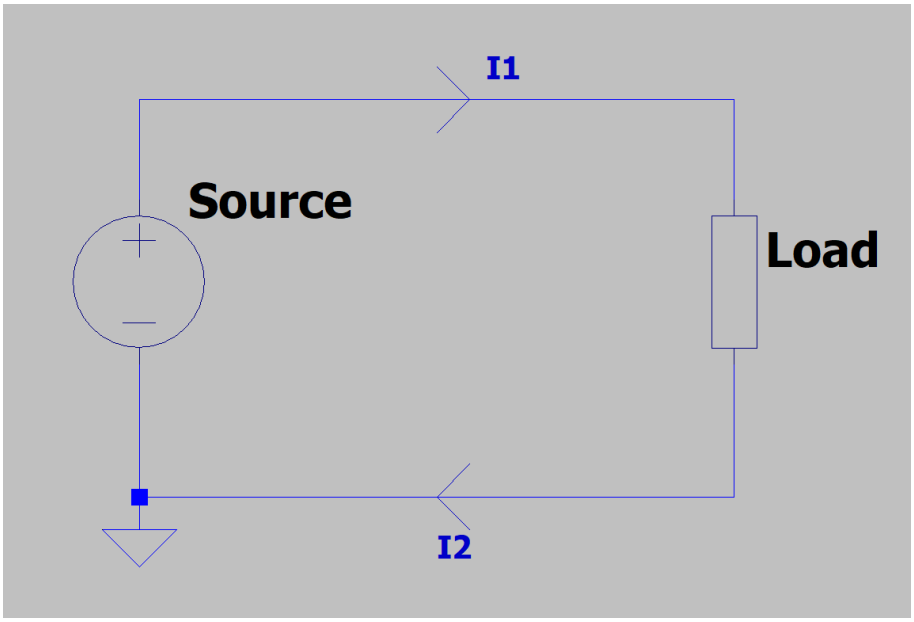

Figure 2.2: Differential mode current.

I_1 in this case is the current in the line while I_2 is the current with opposite sign through the neutral. This can also be explained through a current equation. But first it is necessary to make an assumption that the lines are balanced [5], which means that the characteristic impedance $Z_0 = \frac{1}{2}$, so the impedance is the same for both lines according to the equations

$$Z_{01} = \frac{Z_1}{Z_1 + Z_2} \text{ and } Z_{02} = \frac{Z_2}{Z_1 + Z_2} \tag{2.1}$$

The current equation can then be derived through the use of both Eq. (2.1) and Fig. 2.2 which gives the equation below [4] [5].

$$I_{DM} = I_1 \cdot Z_{01} - I_2 \cdot Z_{02} = \frac{I_1}{2} - \frac{I_2}{2} = \frac{I_1 - I_2}{2} \tag{2.2}$$

So it can be seen that the DM current is the difference of current between the lines divided by two in a balanced system.

Noise that takes this path path is called differential mode noise. As seen in the equation, this noise can only appear if the neutral and the line have different current magnitudes since the currents would otherwise negate each other [6]. The simplest method to attenuate differential-mode noise is by incorporating an LCL-filter into the circuit [7]. The filtering method is expanded upon in Sec. 2.2.4.

2.2.2.2 Common mode current

Common mode current is instead current that flows through the line and neutral in the same direction throughout the circuit [4]. The current pathway for CM current can be seen in Fig. 2.3 below.

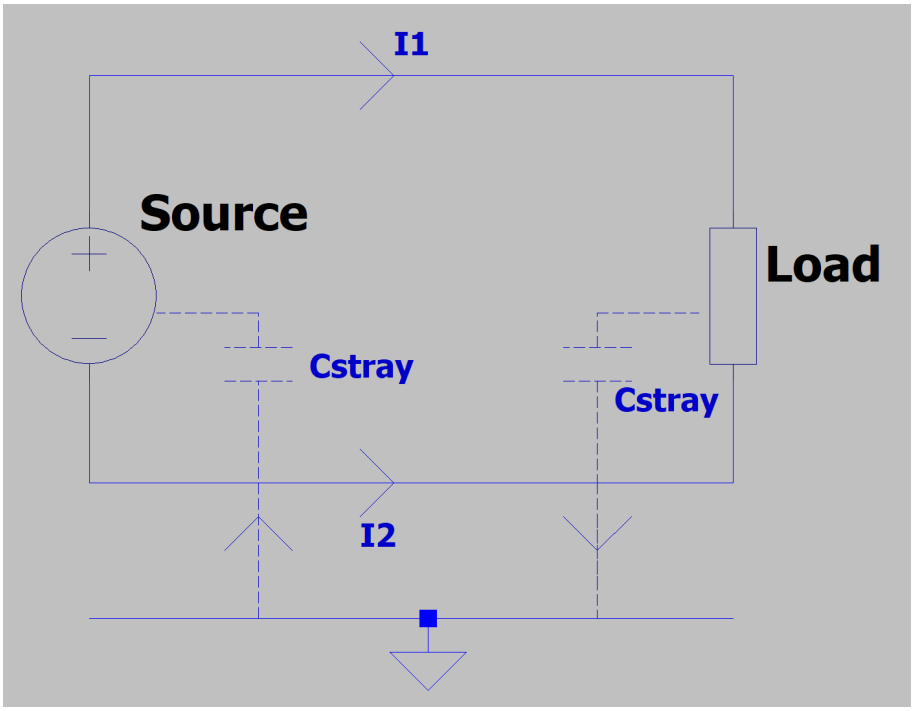

Figure 2.3: Common-mode current path.

The current equation for CM current is very simple compared to DM current, it is simply the addition of the currents according to the equation [5],

$$I_{CM} = I_1 + I_2 \tag{2.3}$$

CM is generally the most problematic form that noise can take, since it usually consists of high frequency harmonic impulse components [8]. This is due to CM noise generally being capacitively coupled noise, and thus interfering more effectively at higher frequencies [8]. It takes a path through the lines and then through parasitic capacitances to the ground plane and then again out into the circuit. This coupling path is further explained in Sec. 2.2.3.3. CM noise is generally introduced in a

circuit if, as mentioned in Sec. 2.2.1, switching power electronics are used, but it can also be due to improper grounding causing ground loops [8]. Grounding loops are caused due to differences in potential between different grounding planes. One of the simplest methods of reducing CM noise is to use a shield around components and cables [4]. Stray capactiance leads CM current to the surface of the shield, completely bypassing the cables and circuits inside and is then led back to the source via the grounding system. This shield is visualised in Fig. 2.6. Similarly to differential mode noise, filtering is another effective method of noise reduction, which is explained further in Sec. 2.2.4.

2.2.3 Coupling paths

There are a number of different ways that EMI can arise in circuits, namely through conductive coupling, inductive coupling, capacitive coupling and radiated coupling. These coupling paths are dependent on the circuits, their components and at what frequencies they operate at.

2.2.3.1 Conductive coupling

The first coupling path is conductive coupling. It happens when two circuits or lines share an impedance through a common point in the circuit. This is usually a common cable to ground that is shared between the two systems or lines. If one of the lines or circuits is very noisy this will also extend to the other, through a common current path [9]. This issue has an easy solution as it can be entirely solved by electrically isolating the two circuits or lines from each other and by doing that not share a common point in the circuit. This has been illustrated in Fig. 2.4 below [9].

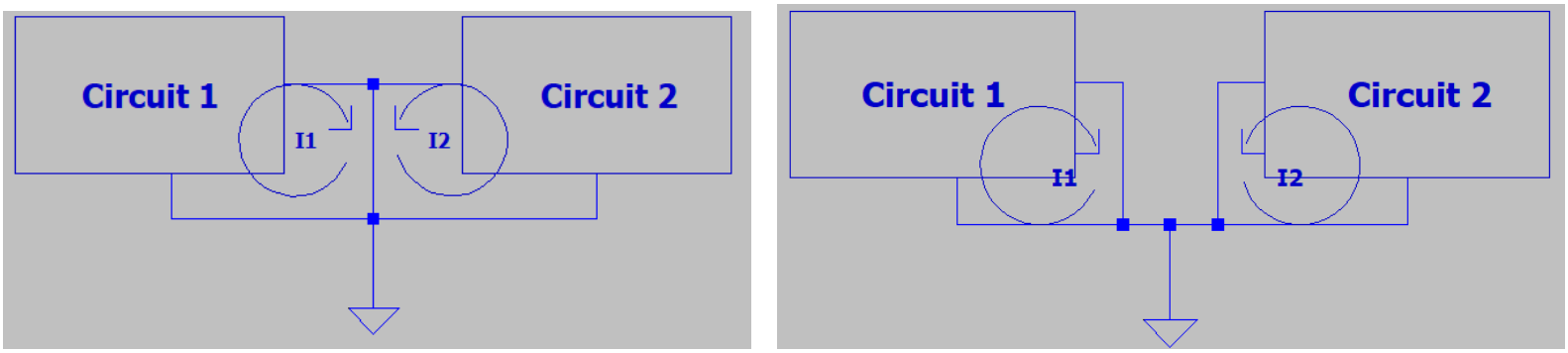

(a) Without electrical isolation. **(b)** With electrical isolation

Figure 2.4: Conductive coupling and its solution.

Fig. 2.4a shows that I_1 and I_2 share the same earthing line, so both of the currents travel through the same cable and thus, will share conductive noise signals. Fig. 2.4b shows that both of the circuits are isolated from each other and share no current and therefore no conductive EMI.

2.2.3.2 Inductive coupling

Inductive coupling occurs when cables or components in different circuits are located in close proximity to each other [4]. It couples them together by a magnetic field. This coupling path is illustrated in Fig. 2.5 below.

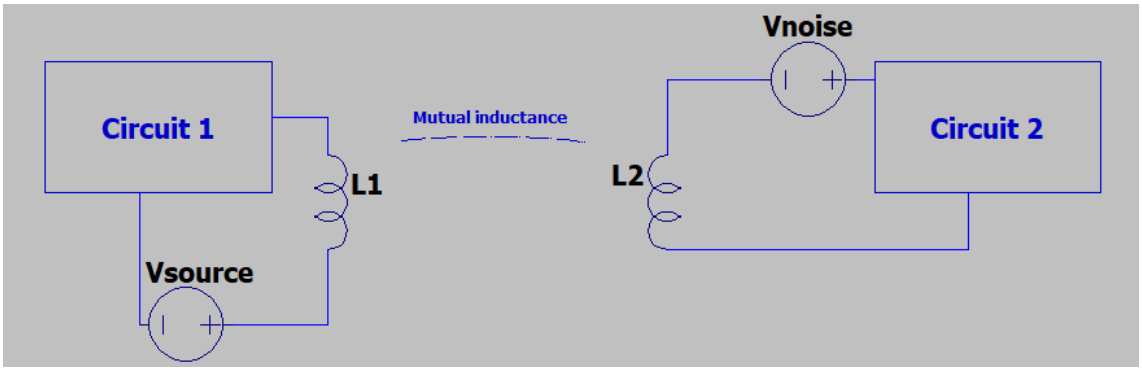

Figure 2.5: Simplified circuit showing inductive coupling.

In this case V_{source} is the noise source and V_{noise} is the resulting noise in the victim circuit (circuit 2). The inductance in the figure is a representation of inductive properties in the circuit or cable, it does not necessarily mean that there has to be an inductor in the circuit. Inductive coupling occurs due to fact that the current that goes through the source circuit will induce a voltage over the inductance in the victim circuit. This is done through mutual inductance between the victim and source circuits. The relation for inductive coupling can be seen in the following equation [9],

$$V_{\text{noise}} = M_{\text{mutual}} \cdot \frac{dI_{\text{noise}}}{dt} \tag{2.4}$$

where M_{mutual} is the mutual inductance. This means that the mutual inductance has a big impact on the noise in the victim circuit and is the reason that this coupling occurs when cables and circuits are close to each other. Similarly, the noise also depends on how fast the noise current changes.

There are multiple solutions to limit inductive coupling and usually a combination of at least some of these are necessary in order to get the desired reduction effect [4]. The first method can be to use shielding to isolate circuits and cables from interfering with each other and significantly reducing the mutual inductance between them. This shield has to be grounded in both ends for frequencies greater than 1 MHz [4] in order to have any effect on the magnetic field, which is shown in Fig. 2.6.

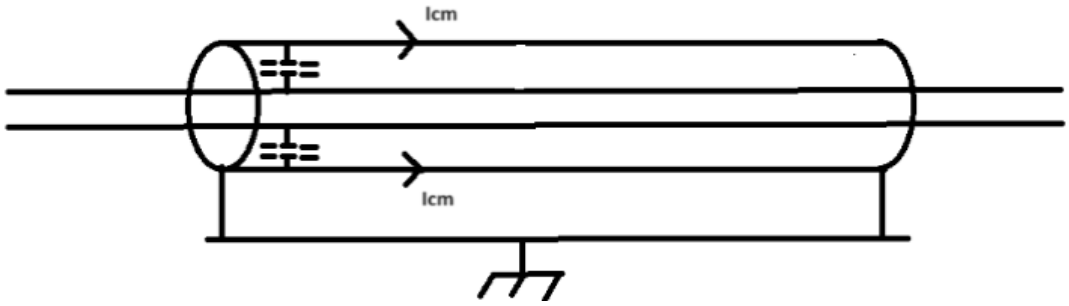

Figure 2.6: CM current flowing through the surface of a shield with both ends grounded.

The second method with which inductive coupling can be reduced is to reduce the area of the current loop [4]. This usually consists of having shorter cables and having components close together. This relation can be seen in Eq. (2.5) below [10] [11].

$$M_{\text{mutual}} = \frac{B \cdot A \cdot \cos\phi}{i} \tag{2.5}$$

Where i is the current in the source circuit and A is the area of the current path in the victim circuit. As seen in the equation, the mutual inductance depends on the loop area. And as shown in Eq. (2.5) the noise depends on the mutual inductance and thus, the noise also depends on the loop area of the current.

The third method is to physically separate the cables or circuits from each other, since magnetic field strength decreases with distance and will therefore reduce the inductive coupling [4].

The final part of reducing inductive coupling is done through filters that attenuate the noise signal which prevents it from affecting the equipment in the circuit. This method is further explained in Sec. 2.2.4.

2.2.3.3 Capacitive coupling

Capacitive coupling, similar to inductive coupling occurs when two cables or circuit are close together. It the case of capacitive coupling however, instead of a magnetic field as in the inductive case, it uses an electric field to create noise [4][9]. This electric field creates what is effectively stray capacitance that lets noise pass from source to victim. A simplified circuit illustrating this can be seen in Fig. 2.7 below.

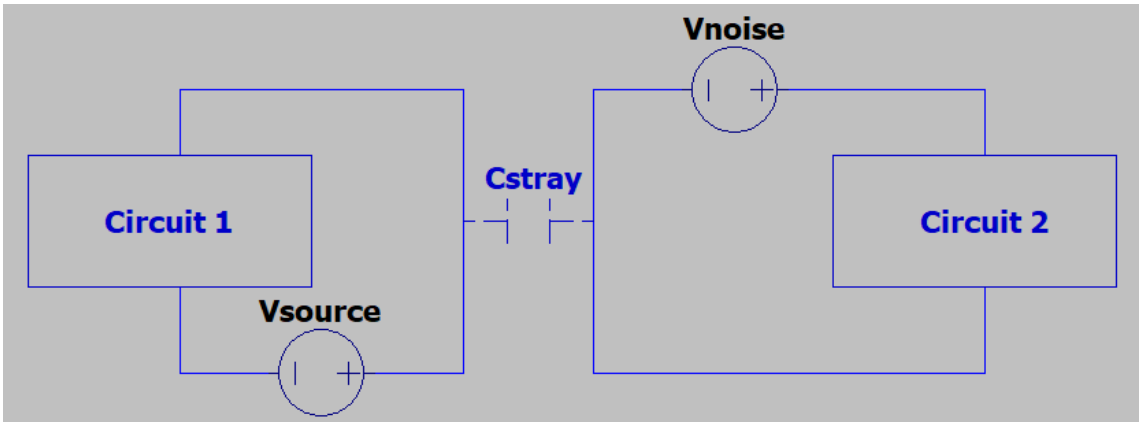

Figure 2.7: Simplified circuit showing capacitive coupling.

C_{stray} represents the stray capacitance that couples the two circuits, V_{source} represents the noise source voltage and V_{noise} is the noise that is induced in the victim circuit. The mathematical relation in this coupling path can be seen in Eq. (2.6) [4].

$$I_{\text{noise}} = C_{\text{stray}} \cdot \frac{dV_{\text{noise}}}{dt} \tag{2.6}$$

As can be seen in the equation, the noise current increases with increasing stray capacitance but also with increasing derivatives for noise voltage, which means that the noise current increases at higher frequencies.

Noise reduction methods for capacitive coupling consists of shielding, physical separation of cables and filtering [4]. The shielding method is the same as for the inductive case, to cut off the coupling path by removing the electrical field that creates capacitances between the source and the victim circuits. The only difference in shielding method is that it does not matter if the shield is grounded in one or both ends, as opposed to the requirement of both ends being grounded for inductive coupling [12]. Physical separation of cables works similarly in this case as for the inductive case, the electrical field strength decreases with distance.

2.2.3.4 Radiated coupling

Radiated coupling can, unlike the other coupling paths, interfere with circuits over long distances, as the noise source sends out electromagnetic waves toward the victim [4]. The source and the victim components act as antennas to each other which is what makes this long distance interference possible. This is illustrated in Fig. 2.8 below.

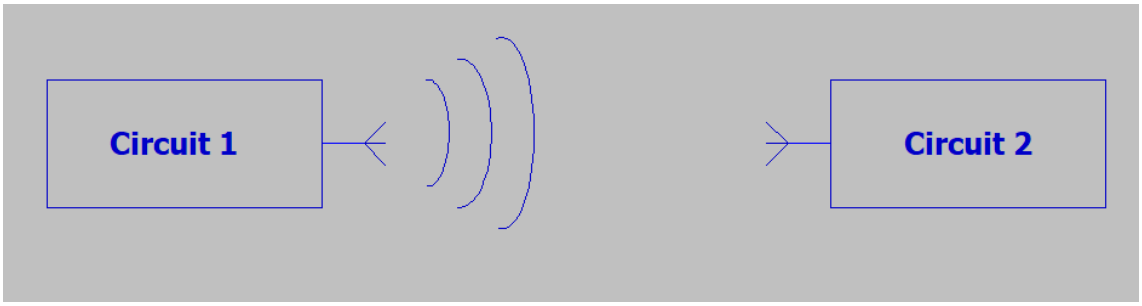

Figure 2.8: Radiated coupling path

Radiated coupling can be reduced with a lot of methods that have already been mentioned in previous sections, such as proper earthing, filtering and shielding of the circuits [4].

2.2.4 EMI-filters

When designing a filter, there are a couple aspects to consider. For example, what type of noise and how much of it needs to be suppressed. These questions are important to answer, since certain filter configurations work the best for a certain type of noise.

2.2.4.1 X-capacitors

For DM noise, typically an X-capacitor is placed line-to-line. A resistor may also be placed in parallel to discharge the X-capacitor when the power to the circuit is turned off [13]. The purpose of an X-capacitor is to create a low impedance path from line-to-line back to the source. The impedance of reactive components such as capacitors or inductors vary with frequency and capacitance/inductance. This means that for a capacitor, the impedance will be very high at low frequencies and decrease when the frequency increases. For the general low frequency desired signal, the impedance of the capacitor is high, passing this signal to the load. For the high frequency noise the impedance is low, passing the noise back to the source.

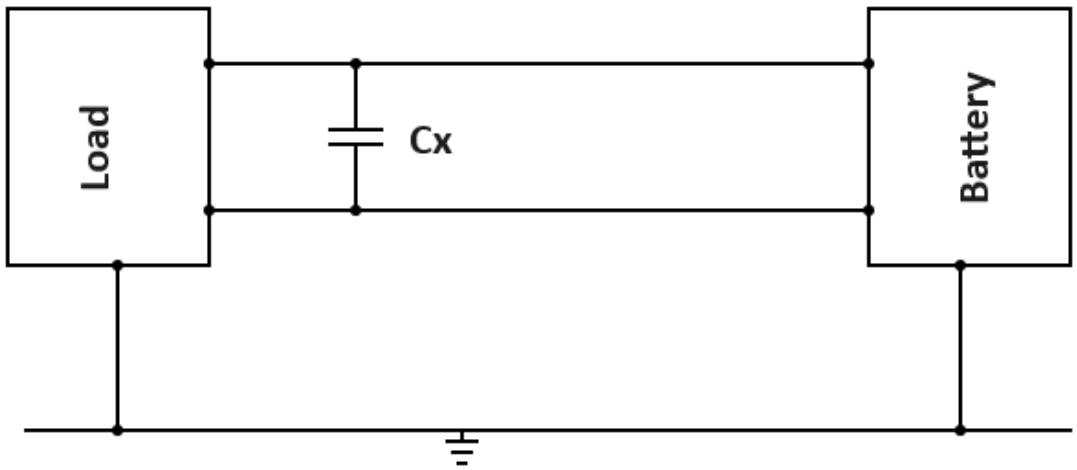

Figure 2.9: X-capacitor.

2.2.4.2 Y-capacitors

If the most prevalent noise is CM noise, then Y-capacitors need to be installed. Two capacitors in a line-to-ground formation, as seen in Fig. 2.10. The purpose of Y-capacitors is to create a low impedance path from the lines to a grounded chassis for the high frequency CM current to pass through [14]. Usually CM noise has higher frequency than DM noise, which is why the Y-capacitor values usually are lower than X-capacitor values [15]. Another reason for not having too high Y-capacitor values is due to the safety concerns. The noise current is filtered to the ground or chassis and if this connection is faulty, it can become dangerous. Therefore, this leakage current is regulated by standards and thus the Y-capacitor values as well [16][15].

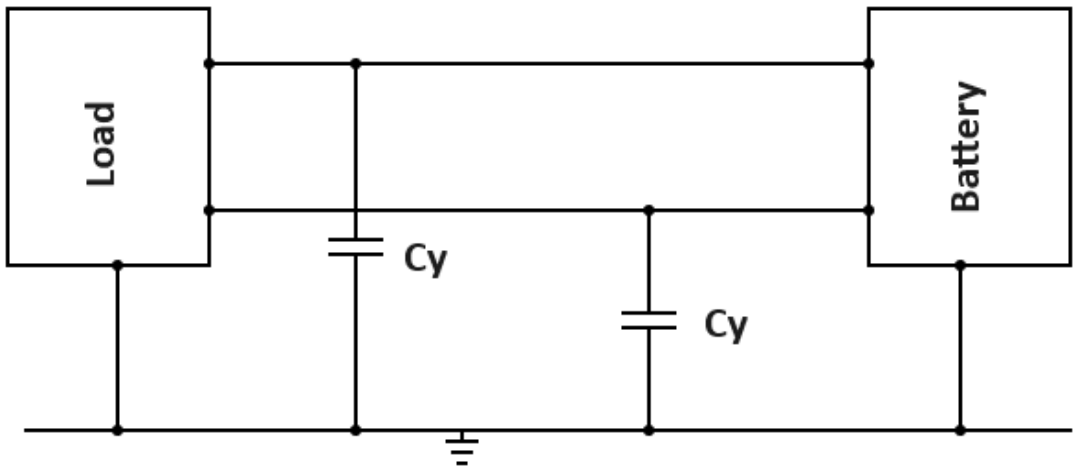

Figure 2.10: Y-capacitors.

2.2.4.3 Common-mode choke

A common-mode choke (CMC) refers to when the two lines are wound around a ferromagnetic core. It is especially effective against CM noise due to the magnetic field of the CM currents enhancing each other. This can be confirmed using the right-hand rule, where the thumb goes in the direction of the current and the rest of the fingers show how the induced magnetic field circulates. When the magnetic field is enhanced, the impedance is increased for the high frequency CM noise, and thus it is attenuated. For DM noise the formed magnetic fields from the two currents cancel each other, resulting in low impedance and no attenuation [17].

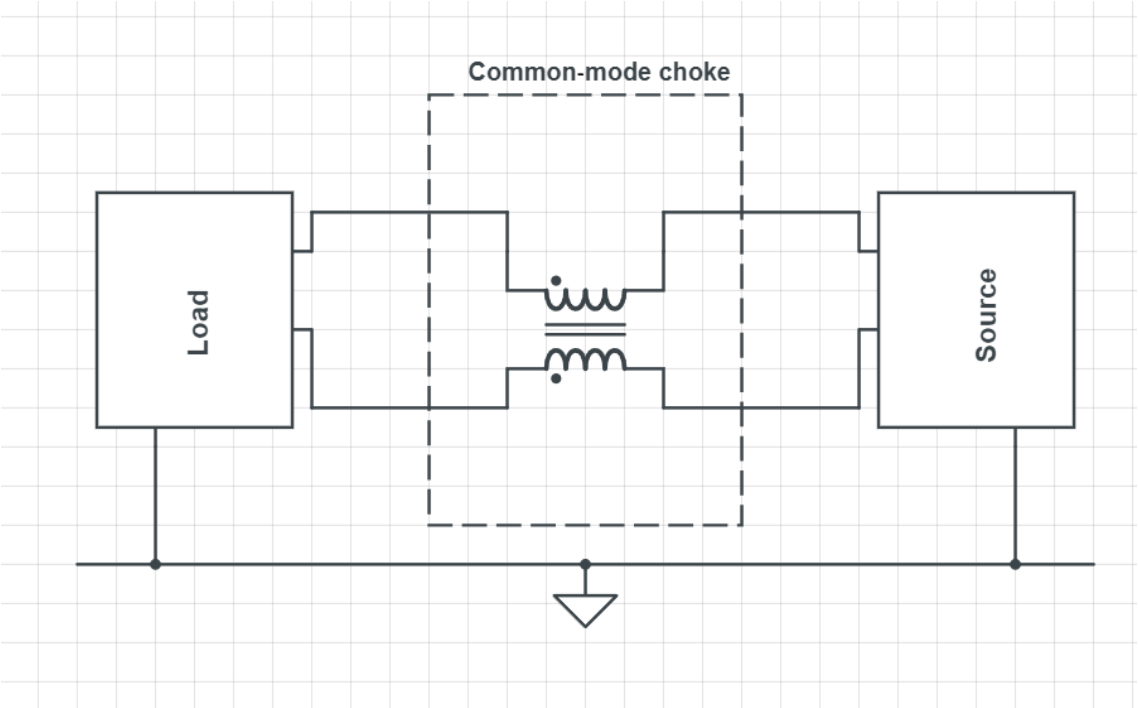

Figure 2.11: Common-mode choke.

2.2.4.4 Filter configuration

Filters can be divided into different orders. For example 1st-order, 2nd-order or 3rd-order filters and so on. The order depends on how many elements the filter consists of and theoretically the filter can attenuate the noise by 20 dB/decade for each element, which is why higher-order filters are better at suppressing noise [15]. If a filter consists of a CMC and Y-capacitors, then theoretically it should attenuate the noise by 40 dB/decade after the cutoff frequency. In practice the amount of attenuation is actually smaller due to parasitic effects of the elements [15].

2.2.4.5 Grid-connected filters

The most common types of grid-connected filters are low pass filters due to the wanted signal having a low frequency. In Sweden this is 50 Hz. They are used to filter out disturbances coming from the grid and going out to the grid. One such filter is the LCL-filter, which is also the one used in Epiroc's vehicles. It is a 3rd-order filter, meaning that it theoretically can attenuate the noise by 60 dB/decade.

Two formulas when constructing an LCL-filter is one for determining the resonance frequency, Eq. (2.7), and one for determining the cutoff frequency, Eq. (2.8).

$$f_r = \frac{\sqrt{\frac{L_i + L_g}{L_i \cdot L_g \cdot C_1}}}{2 \cdot \pi} \tag{2.7}$$

$$f_c = \frac{\sqrt[3]{\frac{1}{L_i \cdot L_g \cdot C_1}}}{2 \cdot \pi} \tag{2.8}$$

L_g is the grid side filter inductance, L_i is the inverter side filter inductance and C_1 is the filter capacitance [18].

2.3 Rogowski coils

A Rogowski coil is a type of measuring instrument that is used when measuring currents and can be seen in Fig. 2.12.

Figure 2.12: Rogowski coil.

It is a coil that is placed around the conductor that is to be measured, thereby inducing a voltage in the Rogowski coil [19]. This induced voltage has a relation to the current derivative and inductance. From this relation the current can be calculated [19].

2.4 THD and harmonics

In an AC circuit, harmonics are the result of voltage distortion due to non-linear elements such as inductance and capacitance. The harmonics appear as multiples of the fundamental frequency at higher frequencies and depend on the characteristics of the input signal and of the circuit. When too substantial, harmonics can cause problems such as power loss or component damage [20]. The total harmonic distortion (THD) is a measurement of the percentage amount of harmonics in a signal. THD can be divided into two definitions, THD_F and THD_R, where the harmonic content is compared with the fundamental wave or the RMS value of the signal, respectively. This thesis uses the first of the two and the calculation is as follows,

$$THD_F = \frac{\sqrt{\sum_{n=2}^{\infty} I_n^2}}{I_1} \tag{2.9}$$

I_1 is the fundamental wave and I_n are the multiples of the fundamental wave [21].

2.4.1 Swedish standard

The standard SS-EN 50160 covers the Swedish version of the European standard regarding the allowed amount of EMI that can be conducted to the power grid. Epiroc's vehicles operate in the low voltage range, with a nominal voltage of up to 1 kV. The THD in the low voltage range, up to the 40th harmonic, should not exceed 8 %. The individual harmonic voltage levels should themselves not exceed a certain percentage of the fundamental voltage level. This applies to normal operation conditions over the period of a week divided into 10 minute intervals, where 95 % of the mean values of these intervals should not exceed the values in the table below. Since the harmonics above the 25th order tend to be insignificant and behave randomly, they are not specified in the table [22].

Table 2.1: The relative voltage levels of each harmonic up to the 25th order[22].

Odd harmonics				Even harmonics	
Non-multiples of 3		Multiples of 3			
Order n	Relative voltage	Order n	Relative voltage	Order n	Relative voltage
5	6,0 %	3	5,0 %	2	2, %
7	5,0 %	9	1,5 %	4	1,0 %
11	3,5 %	15	0,5 %	6...24	0,5 %
13	3,0 %	21	0,75 %		
17	2,0 %				
19	1,5 %				
23	1,5 %				
25	1,5 %				

3
Methods

This chapter explains what steps were taken in order to progress the thesis work and how they were conducted.

3.1 Simulations

3.1.1 Y-capacitor filter

To get a sense of what to expect from the filters, simple filter models and simulations on the models were conducted in LTspice. The results of the simulations can be taken into account when analyzing the results of the real measurements in order to establish a conclusion and possible improvements of the filters. Firstly, the model of the Y-capacitor filter was made and is shown in Fig. 3.1 below. The model is not a direct simplification of the real circuit, it was mainly used to see how the filter reacts to the change of parameter values and frequency. Vsource is an AC voltage source. Vcm1 and Vcm2 simulate CM noise on the lines. Rsource and Rload simulate impedance matched source- and load resistances.

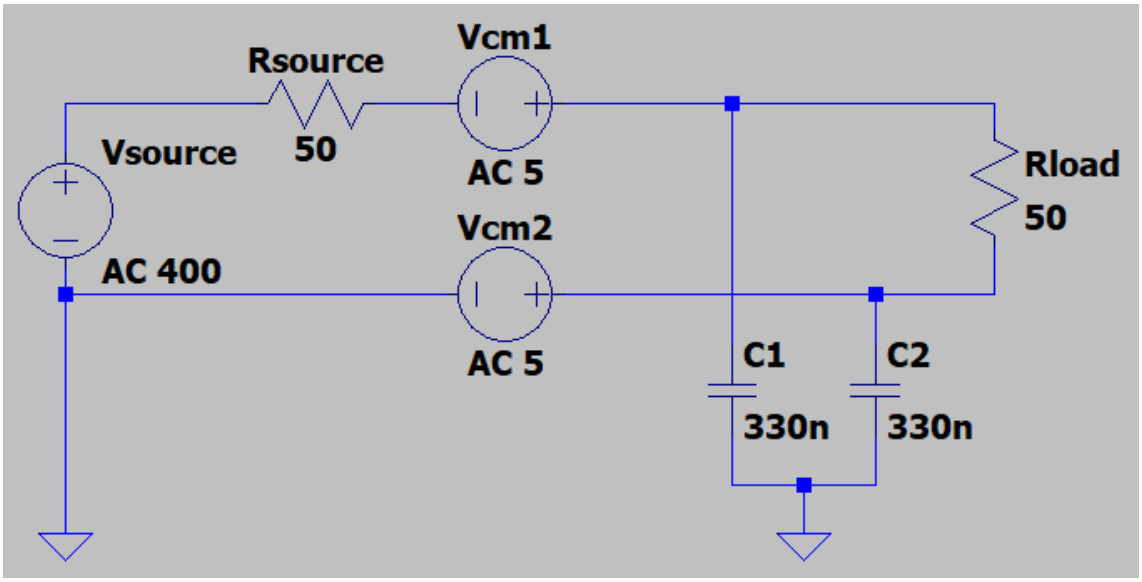

Figure 3.1: Simulation model for the Y-capacitor filter.

To see how the filter reacts over a large frequency range, AC analyses were conducted from 1 Hz to 100 MHz. Simulations were made on the capacitor values 330 nF and 47 nF, which are two of the values used in the measurements. One more value of 1 μF was simulated. Simulations on 220 nF capacitors are not shown since the results did not differ much from 330 nF.

3.1.2 Common mode choke

A few simulations where also conducted for the possible improvements of the filters. A CMC was added to the circuit in Fig. 3.1 and is shown in Fig. 3.2 below. This was done to get a feeling of what to expect when adding a choke to the filter.

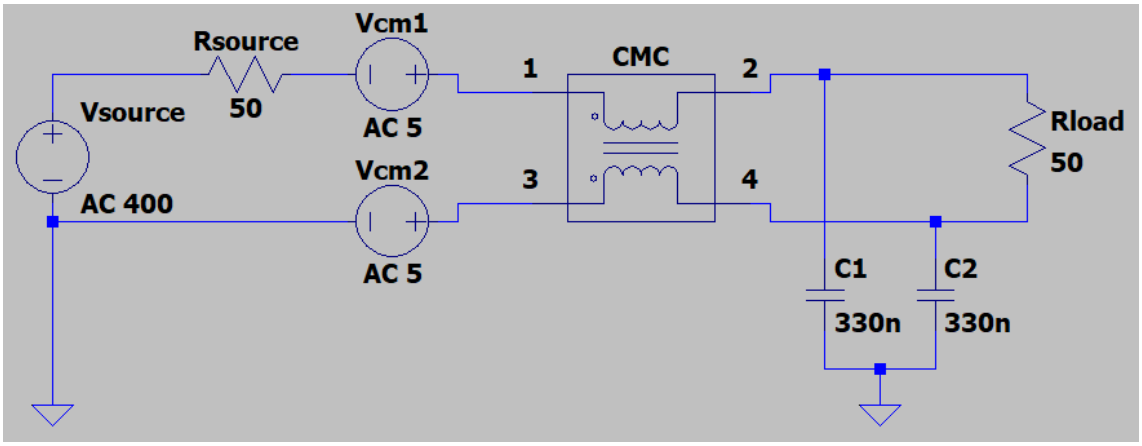

Figure 3.2: Simulation model for the Y-capacitor filter with an added common mode choke.

3.1.3 LCL-filter

The simulation model for the LCL-filter can be seen below in Fig. 3.3. It is a simplified version of a three phase system. In reality the 1000 V grid is connected to a transformer that converts the voltage to 400 V. A transformer is not shown in the model, but Vsource, Rsource and L3 represent the secondary side of the transformer. Rsource and Rload both are set to 1,4 Ω because of the current in the secondary side of the transformer. They are set to the same value due to impedance matching. L3 is the inductance of the secondary side of the transformer. The inductance values of L1 and L2, as well as the capacitance of C1 have all been set by the company. For clarification, the model is likely not completely accurate to the real circuit, but like the other simulations, is made to get a feeling of what to expect from the filter.

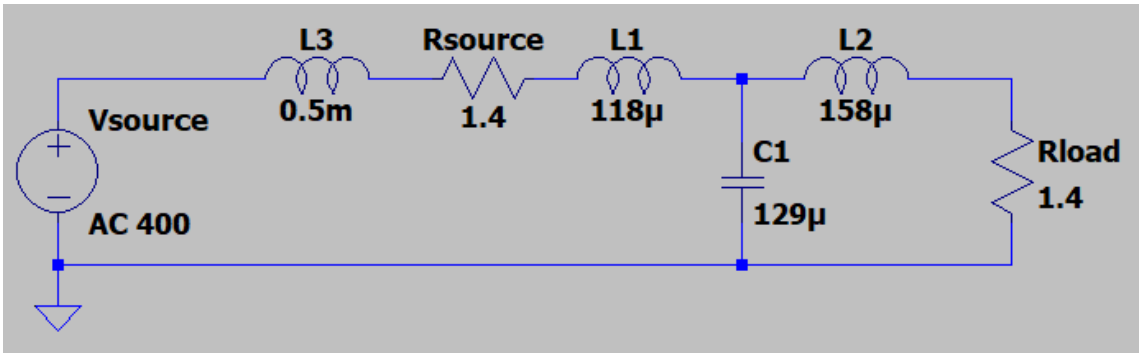

Figure 3.3: Simulation model for the LCL-filter.

3.2 Measurements

The next part was to conduct EMI-measurements at Epiroc's production facility in Örebro. The measurements were taken on the drill-rig since it was the most readily available at the time. The measurements were done on a number of different measuring points in the power-train. These points have been listed below, see Fig. 3.5. The measurement points were chosen while considering previous measurement data that had been gathered on another machine to make sure that the most important parts of the power-train were considered. As mentioned previously, there were only a total of eight oscilloscope channels available at the time of testing that could then feed this data into Matlab to be properly processed, so some measurement points could not be considered, such as the battery current.

A big part of the measurement was to set up the vehicle so all currents listed could be measured unshielded. This was not difficult for any of the measurements except for the traction motor measurements, since the measurements could be done inside of the distribution box for all others, where the cables are not shielded. For the motor however, the cables themselves are shielded, thus an extension cable had to be connected to the six motor cables. In these extension cables, the shielding was broken out of part of the cable and a loop was created from the shielding on each

cable as illustrated in Fig. 3.4 below.

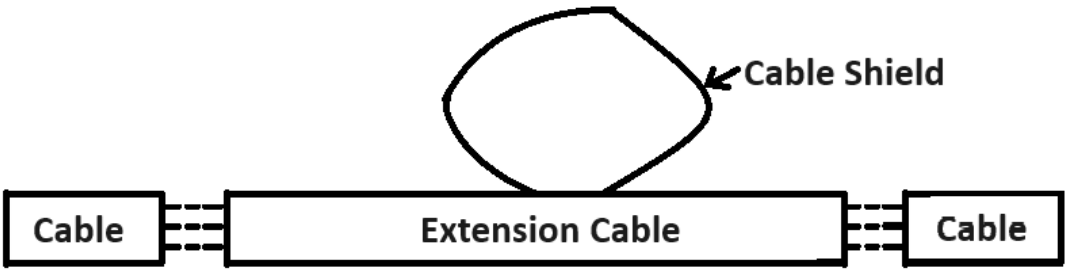

Figure 3.4: Cable shield broken out in the extension cable placed between motor and traction inverter.

The Rogowski coil was then placed on the extension cables, beneath the cable shield loops to measure unshielded current. As the line and neutral through the Rogowski coil were in the same direction, this meant that the addition of the current in the line and neutral, or in other words, the CM current was measured. All eight measurement points were connected to their own oscilloscope channel through the Rogowski coil. The points where the Rogowski coils were connected in the power train and what direction was assumed to be positive is illustrated in Fig. 3.5 below. The direction the arrows are pointing towards is considered positive current direction.

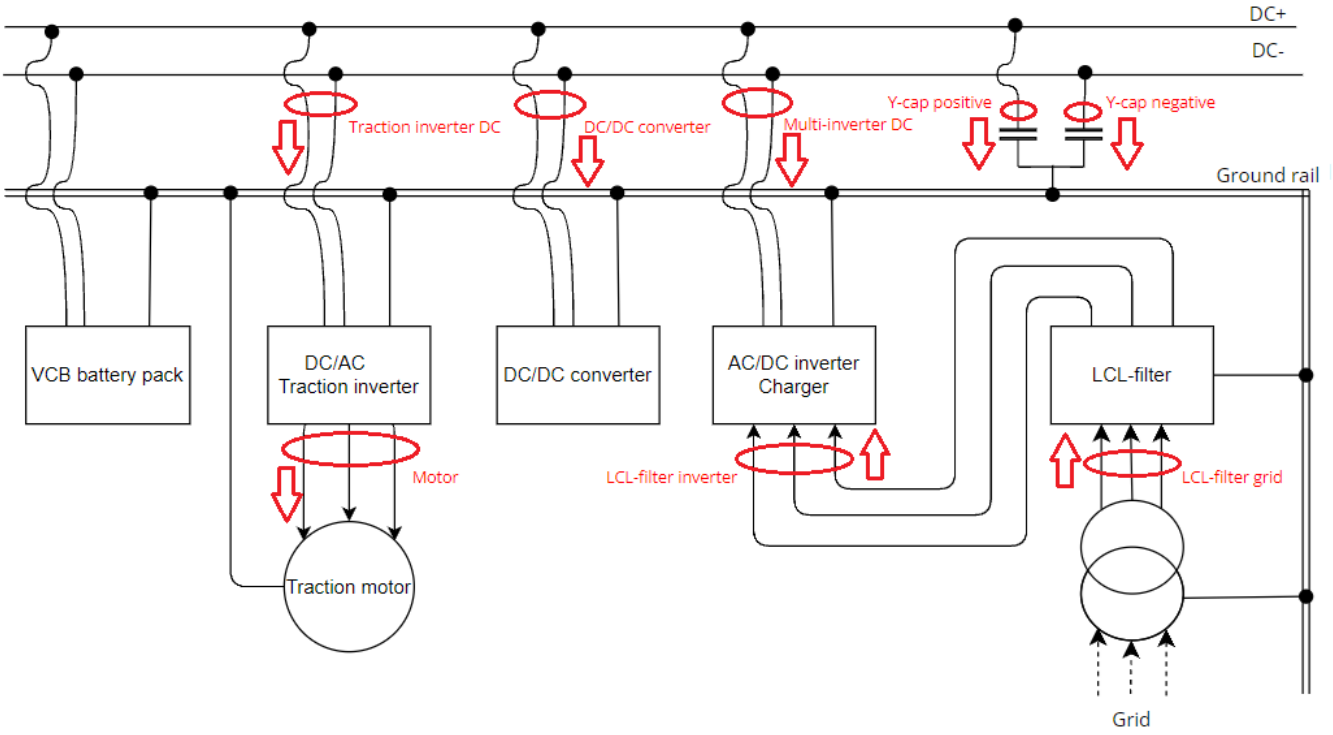

Figure 3.5: Power-train circuit with measuring point for rogowskicoils and its positive direction.

The next step was to make the actual measurements. The vehicle needed to be set up in charging mode, which means that the vehicle needed to be plugged in to the 1000 V grid outlet for most of the tests. Then it was simply a matter of conducting the test according to the following tables.

Table 3.1: no Y-cap filter

Charging	Motor off	Motor on
No charging	Test1	Test2
Charging 0 kW	Test3	Test4
Charging 50 kW	Test5	Test6
Charging 100 kW	Test7	Test8

Table 3.2: 47 nF Y-cap filter

Charging	Motor off	Motor on
No charging	Test1	Test2
Charging 0 kW	Test3	Test4
Charging 50 kW	Test5	Test6
Charging 100 kW	Test7	Test8

Table 3.3: 220 nF Y-cap filter

Charging	Motor off	Motor on
No charging	Test1	Test2
Charging 0 kW	Test3	Test4
Charging 50 kW	Test5	Test6
Charging 100 kW	Test7	Test8

Table 3.4: 330 nF Y-cap filter

Charging	Motor off	Motor on
No charging	Test1	Test2
Charging 0 kW	Test3	Test4
Charging 50 kW	Test5	Test6
Charging 100 kW	Test7	Test8

The motor parameter determines if the motor should be on or off, the different capacitance values are different Y-capacitor filter capacitances and the charging parameter determines how much power is taken from the grid and put towards charging the battery.

3.3 Data analysis

In order to analyse the measured data in Matlab, it first needed to be converted from Tiepie's own file format to .mat files. This could be done directly through Tiepie's own oscilloscope program. The raw data could then be ran through a Matlab script which was supplied by Epiroc and executable through the command prompt on any windows computer. The script transforms the raw data into various parameters for

each measurement point in excel. Only a handful of the parameters were used and are explained further in Ch. 4.

The next step was to interpret this data in order to determine what it meant and if it was useful in determining what happens in the Y-capacitor and LCL-filters. The best solution in this scenario was determined to be to plot all this data in Matlab, so any trends or aberrations could be picked up upon and, whether those aberrations were due to measurement errors or actual unusual behaviour in the power-train, further examined or dismissed. The Matlab script that was created simply plots the desired columns and rows of the excel sheet.

4

Results

4.1 Simulations

4.1.1 Y-capacitor filter

The first simulation was performed on the model in Fig. 3.1 with capacitor values of 330 nF and the results can be seen in Fig. 4.1, where the thick curve represents the gain/attenuation of the current through Rload and the dotted curve represents the phase shift of that current. The total attenuation of the signal is around 32 dB.

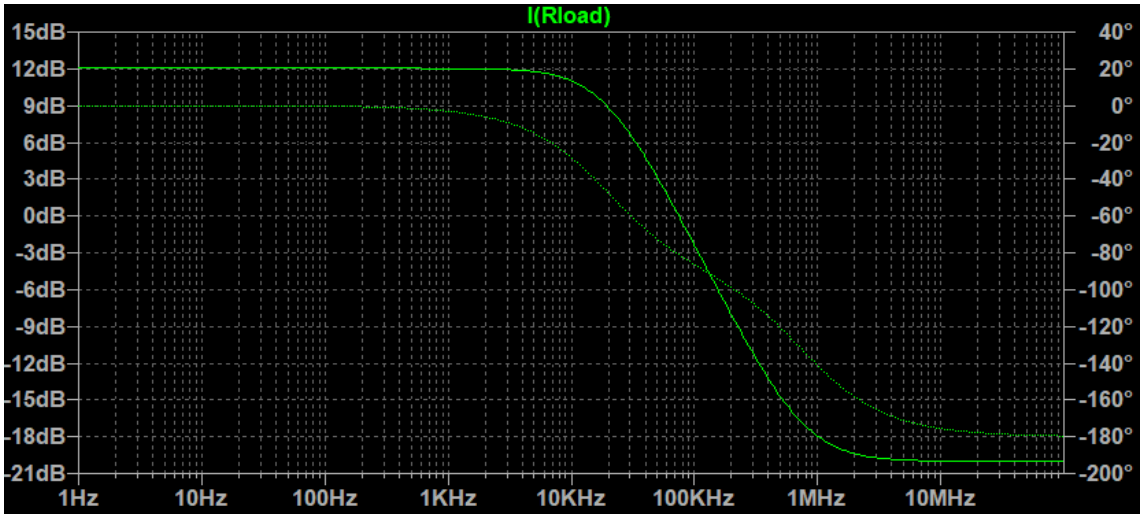

Figure 4.1: Attenuation of the current through Rload with a capacitor value of 330 nF.

When the capacitor values are switched to 47 nF each, the curve moves towards higher frequencies. This can be seen in Fig. 4.2. The attenuation of the signal remains at 32 dB. It seems that the curve moves towards higher frequencies when the capacitor values are lowered and towards lower frequencies when the capacitor values are increased. The attenuation does not seem to be affected by the change of the capacitor values. The increase of capacitor values to 1 μF also confirm these conclusions, see Fig. 4.3.

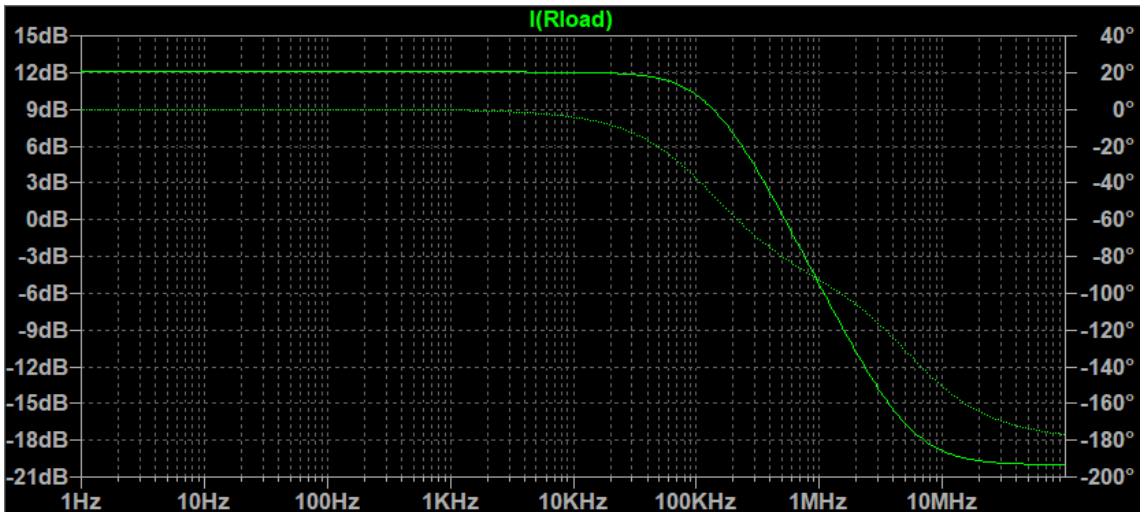

Figure 4.2: Attenuation of the current through R_{load} with a capacitor value of 47 nF.

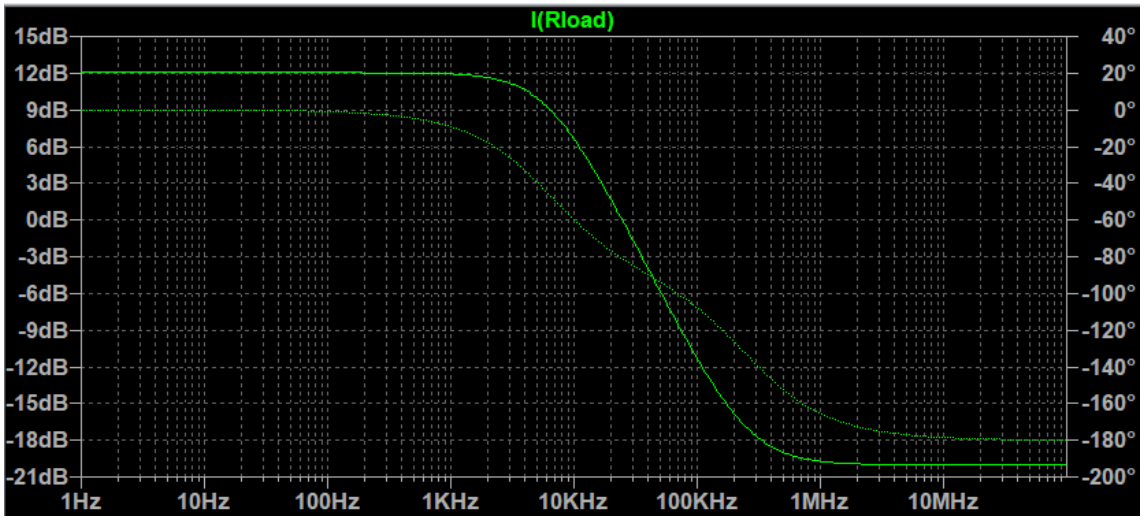

Figure 4.3: Attenuation of the current through R_{load} with a capacitor value of 1 μF.

4.1.2 Common mode choke

A possible component to add to the Y-capacitor filter is a CMC, which is why it was added to Y-capacitor simulation circuit. The filter will then become a multi-component filter, improving its attenuation of unwanted noise. Fig. 4.4 shows the clear improvement in the filters attenuation capabilities. There is also a prevalent resonance peak which is something to be aware of, but remember that this is not the real circuit being simulated.

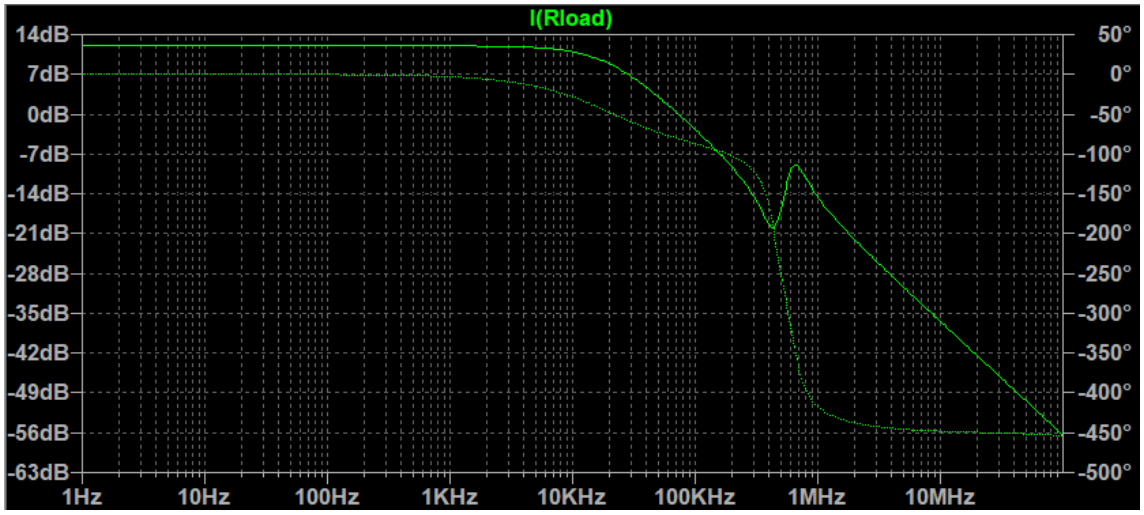

Figure 4.4: Attenuation of the current through Rload when a CMC has been added to the Y-capacitor filter. Capacitor value 330 nF.

4.1.3 LCL-filter

The result from the simulation on the model in Fig. 3.3 in Sec. 3.1.3 is shown in Fig. 4.5 below. Since the filter is used to suppress noise to and from the grid the result seems reasonable, starting to attenuate the signal at around 50 Hz.

Figure 4.5: Attenuation from the LCL-filter of the current through Rload

4.2 Measurements

In this section the measurement results will be presented and explanations for what they mean will be provided. Not all plots will be shown in this section as there are too many to not cause confusion. For this reason, it was decided that only the most relevant plots are to be shown in this section. If the plots are very similar for example, which is the case for many graphs, only one is shown. Similarly, if a graph has very low magnitudes close to zero for multiple different tests, one test will be shown and the rest omitted. All graphs will however be available in App. A for those interested. It should also be noted that the current magnitudes and THD levels are not shown, but rather explained in the text.

It is also important to note how the results are presented in the Matlab figures, as they are divided up in different frequency intervals. This can be seen in Fig. 4.6 below.

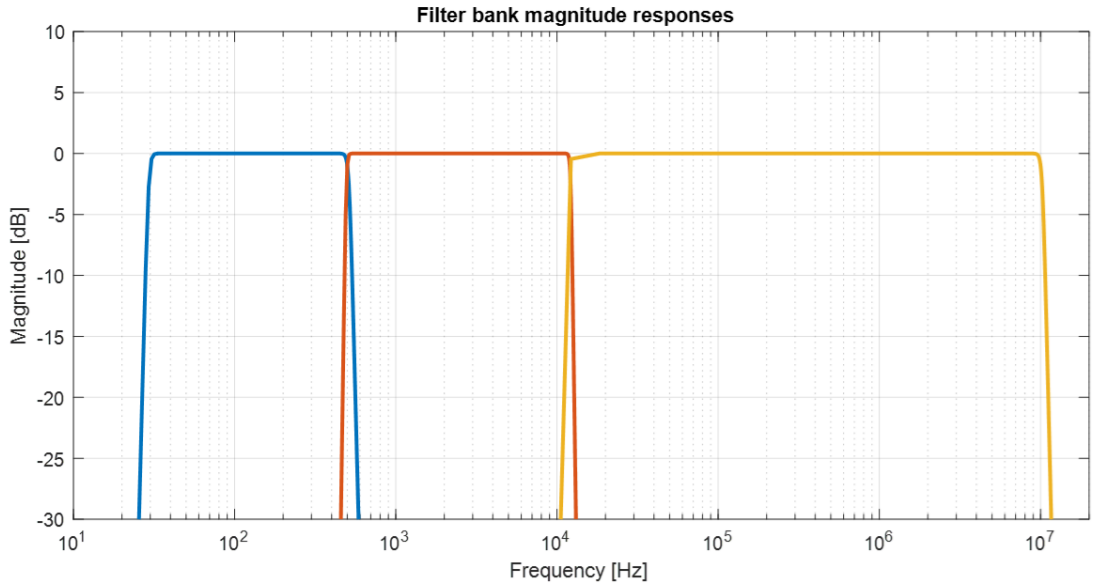

Figure 4.6: Frequency intervals.

As can be seen in the figure, there are three different frequency spectrum. The first is the blue spectrum which encapsulates the frequencies between around 25-550 Hz. This spectrum is supposed to represent the fundamental frequencies, currents that are close to the operating frequency of the vehicle. The second frequency range is the orange one, that encapsulates frequencies from the upper edge of the fundamental spectrum all the way to about 20000 Hz. This spectrum is supposed to represent the switching noise that is generated by power electronics in the power train. The last spectrum is the yellow one, which stretches from the upper edge of the switching spectrum to around 10 MHz. This spectrum is supposed to represent high frequency transients. There is not a specific reason that the cutoff is at 10 MHz specifically, however it was determined that this cutoff would encapsulate almost all signals of any relevance to the measurements.

In the plots these signals are represented slightly different. There are both peak-to-peak and RMS values plotted for all of the graphs. For the peak-to-peak values, the measurements are divided up into small time segments, so each peak is taken into account. The values are then averaged out and displayed as a peak-to-peak mean value. The legend of the plots are further explained in the table below.

Table 4.1: Explanation for legends in Matlab plots

$P2P\_1ms\_mean$	The mean of all peak-to-peak values representing the switching frequency range, with 1 ms time intervals.
$P2P\_5\mu s\_mean$	The mean of all peak-to-peak values representing the transient frequency range, with 5 μs time intervals.
RMS(1)	RMS value of the conducted noise in the fundamental spectrum.
RMS(2)	RMS value of the conducted noise in the switching spectrum.
RMS(3)	RMS value of the conducted noise in the transient spectrum.
RMS(AC)	Total RMS value of the conducted noise in the entire spectrum, minus the DC-component.

4.2.1 Common mode current in Y-capacitor and LCL-filters

The first thing to present is the CM current through both the Y-cap filters and the LCL-filters. In Fig. 4.7 the Y-capacitor filter current can be seen for the case of 100 kW charging with the traction motor turned on.

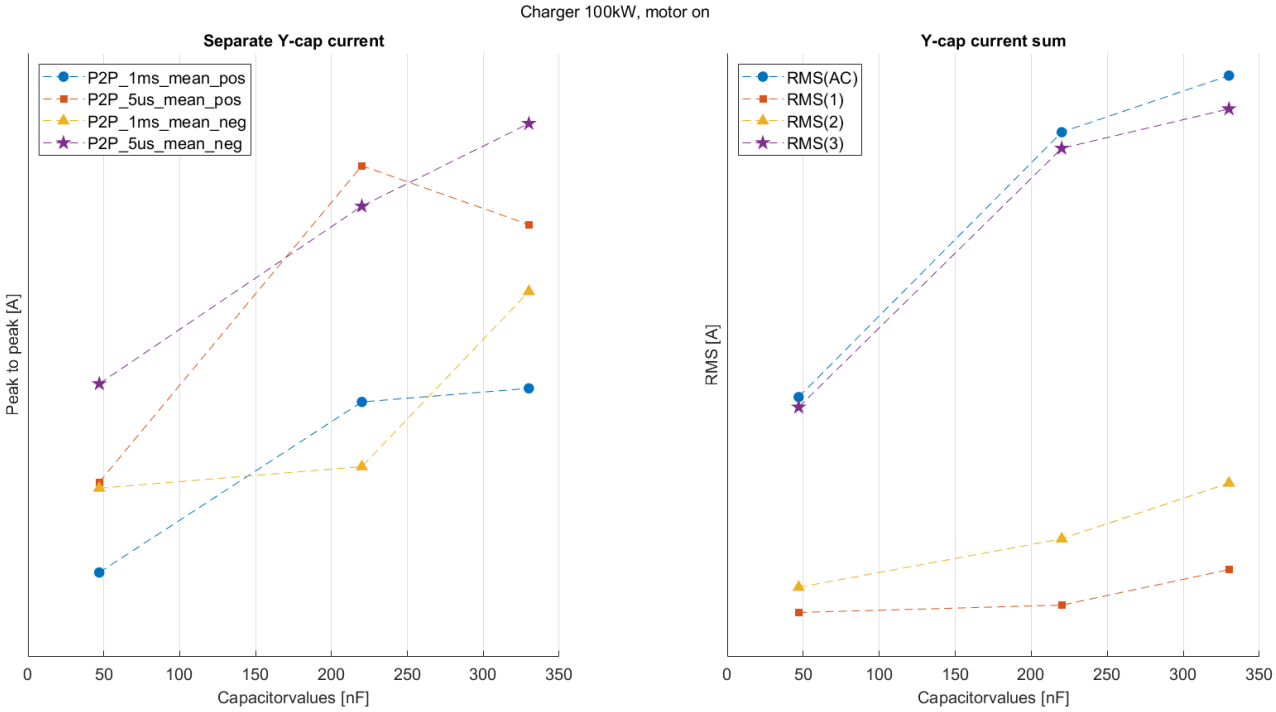

Figure 4.7: Y-capacitor filter current for 100kW charging, motor on.

For all capacitance values the Y-cap filter CM current increases with increasing capacitance. This makes sense due to how capacitors couple in the circuit, with increasing capacitance the impedance decreases which gives the current a lower and lower impedance path which of course means that more CM current will also flow through the filter. This was also seen in the simulations earlier. However, the overall filtered noise is quite low. Another thing to note regarding the Y-cap filters is that out of all the spectrum that the CM current is composed of, the largest is

the transient spectrum. This indicates that the Y-capacitor filter is doing what it is designed to do, filter these high frequency components. The magnitude of the currents is important too however, if it filters what it is supposed to but at too low of a magnitude it will hardly have any effect on the overall performance of the power-train.

The LCL-filter graphs were very similar for all tests, so only the 100 kW charging, motor off case is used. The graphs can be viewed in Fig. 4.8 below. Fig. 4.9 shows the difference in CM current between the inverter- and grid side of the LCL-filter when using the 220 nF Y-capacitor filter.

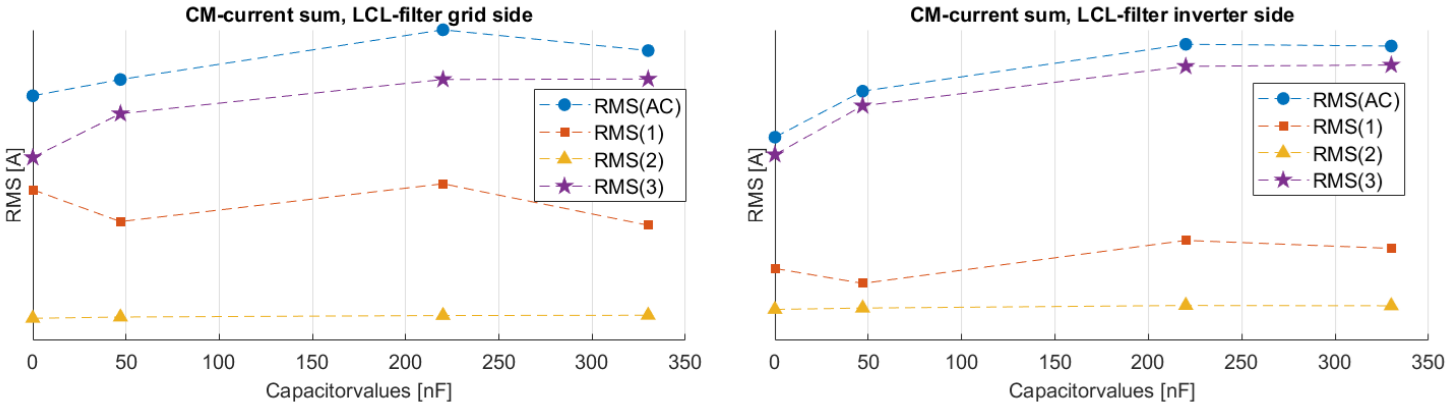

Figure 4.8: Common mode current on both sides of the LCL-filter. 100kW, motor off.

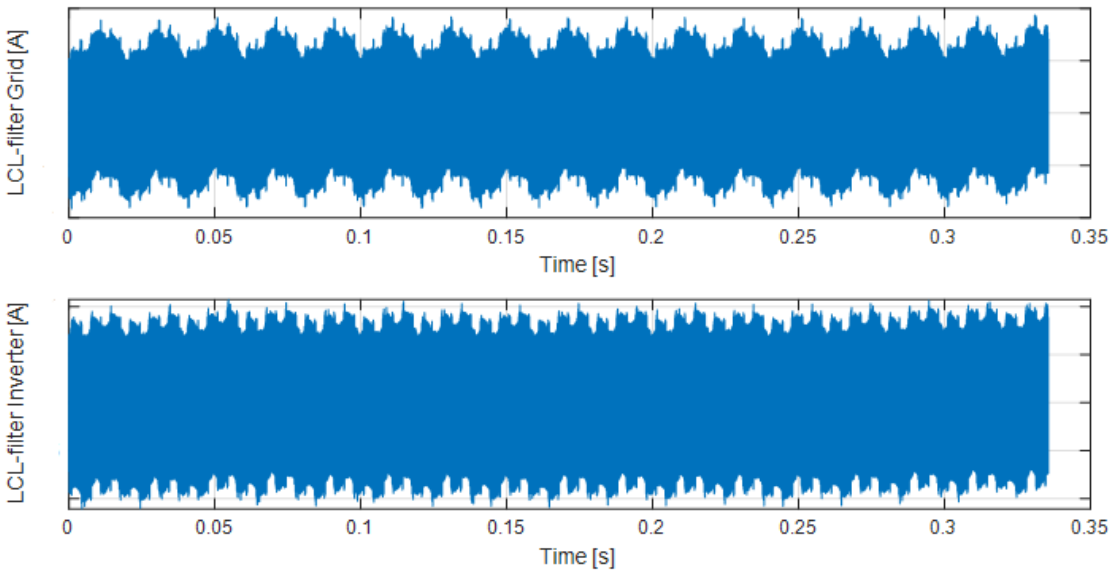

Figure 4.9: CM current on the inverter- and grid side of the LCL-filter when using the 220 nF Y-capacitor filter. 100 kW, motor on.

The graphs look very similar because the currents are not shown, but the LCL-filter

does reduce the CM noise out toward the grid slightly. The transient frequency spectrum is reduced by about 23 %. It also seems to have a lower frequency. The CM current from the switching frequency spectrum is negligible, likely due to the fact that any switching noise from the multi-inverter is transferred to the power train instead of back to the grid. Considering that the THD of the harmonics on the grid side of the LCL-filter should not exceed 8 % for a low voltage system, as mentioned in Sec. 2.2.3.2, it should be noted that changing Y-cap filter does change the THD. The lower capacitor values do tend to perform better in this regard, so increasing capacitance does bring the risk of the 8 % threshold being exceeded. Fig. 4.10 and Fig. 4.11 show the THD for both 47 nF and 220 nF in the 100 kW, motor on test. The values were almost the exact same for the motor off test so they were not plotted here.

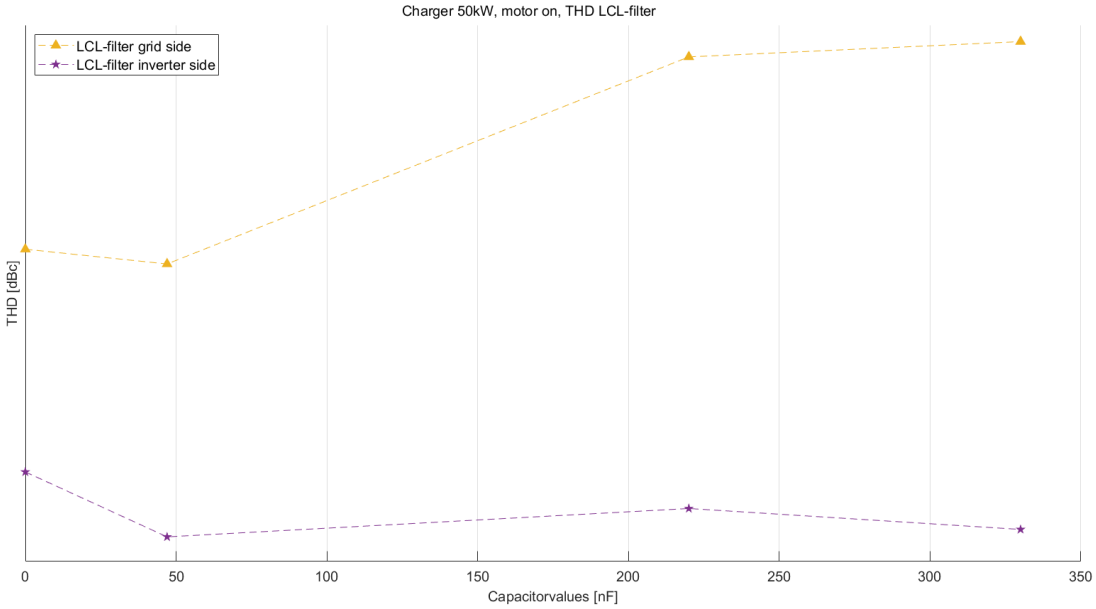

Figure 4.10: THD level before and after the LCL filter for 50 kW charging mode, motor on

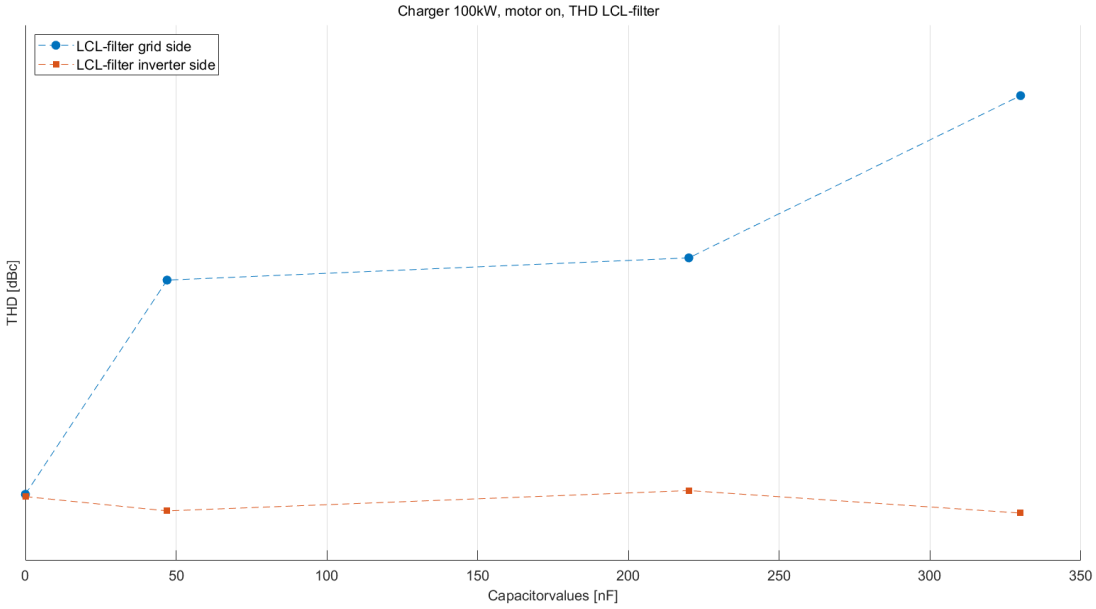

Figure 4.11: THD level before and after the LCL filter for 100 kW charging mode, motor on

4.2.2 Common mode noise in DC/DC-converter

The next thing that is directly obvious while viewing the graphs is that the DC/DC converter is almost completely unaffected by the noise introduced throughout the circuit in the measurements. The noise levels are very low. This is the case for every testing scenario. Increasing the charging power does increase the noise a little bit. The noise also fluctuates by a tiny amount when changing the capacitance, but these amounts are not significant. The motor does not contribute to any large difference either. The figure below shows the noise levels.

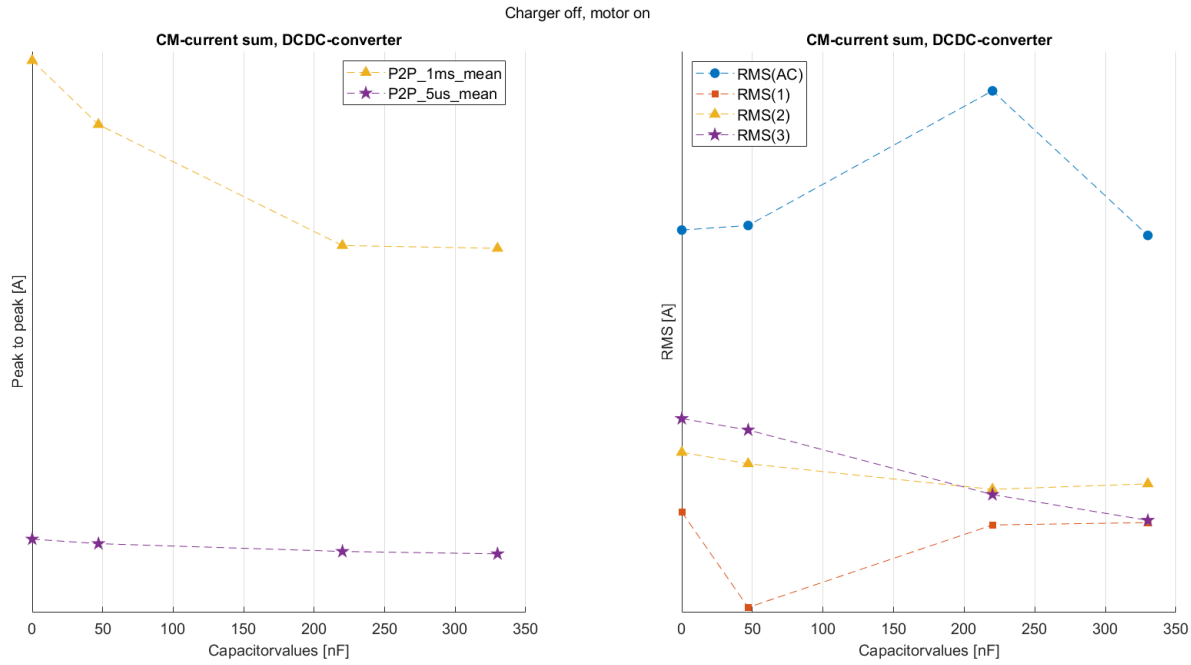

Figure 4.12: RMS and peak-to-peak for the CM-currents with varying Y-capacitor filter in the DC/DC-converter. Charger off, motor on.

All signals for the DC/DC converter are very low in magnitude to the point where they do not contribute to the overall noise issue. The reason for this could be the fact that this converter only works with DC current and that there is not much switching happening.

4.2.3 Inverters

The most eye catching plots are the multi-inverter plots. The plots for when the charger uses 100 kW, for both motor on and motor off, can be seen below in Fig. 4.18a and Fig. 4.18b respectively.

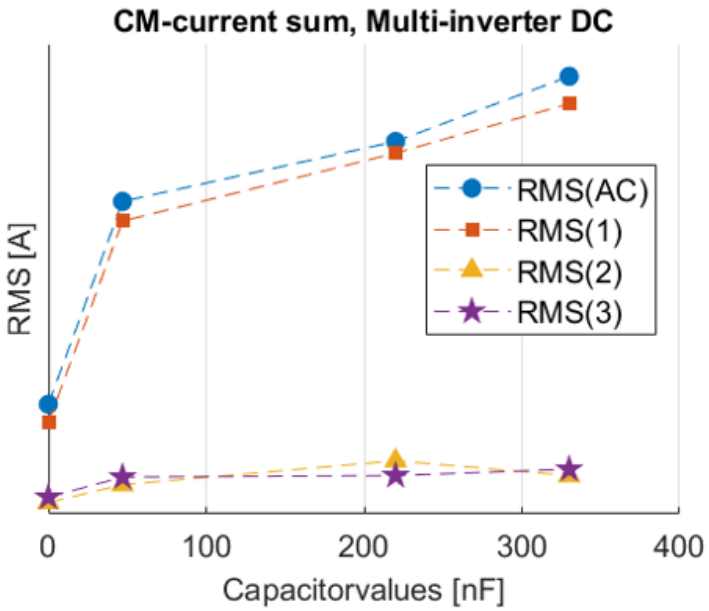

(a) RMS for the CM currents with varying Y-capacitor filter in the multi-inverter. 100 kW, motor on.

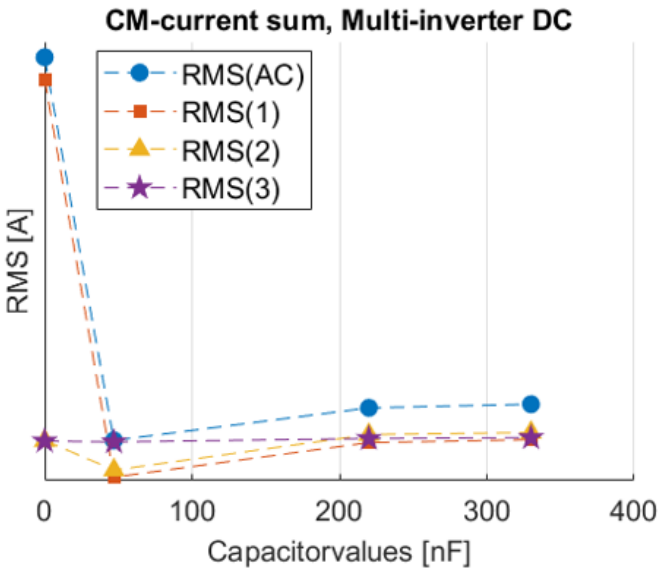

(b) RMS for the CM currents with varying Y-capacitor filter in the multi-inverter. 100 kW, motor off.

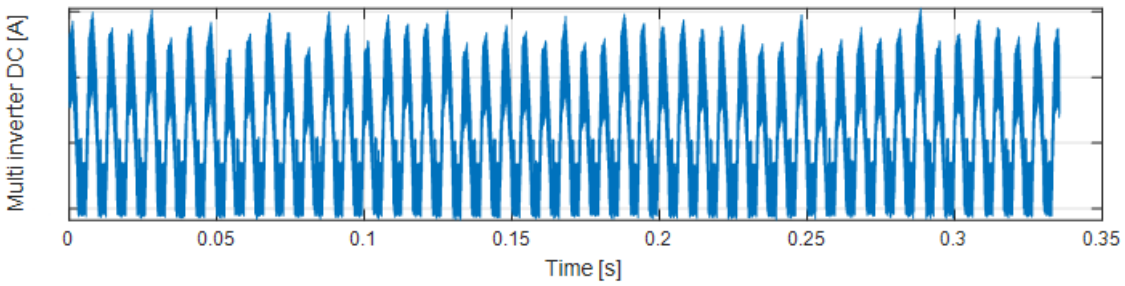

Figure 4.14: 150 Hz CM current in the multi-inverter when using the 220 nF Y-capacitor filter. 100 kW, motor on.

There is a clear difference in the two plots. When the motor is turned on, the CM current in the fundamental frequency spectrum increases in magnitude for the different Y-capacitor values. The fundamental frequency for these signals are 150 Hz, except for without the filter. Fig. 4.14 shows the 150 Hz CM current in the multi-inverter when using the 220 nF Y-capacitor filter. These peak-to-peak levels are quite large. Then when the motor is turned off, the CM current becomes insignificant, but without the filter the current also sees this same increase. This signal's fundamental frequency is also 150 Hz.

When the charger power is set to 50 kW the same thing happens. When the motor is on, the CM current increases and it decreases when the motor is turned off. See Fig. A.11 and Fig. A.16 in App. A. You can also see this happening to some degree when the charging power is set to 0 kW, but not to the same extent. When the charger is turned off, there is not enough current in order to draw any conclusions.

Looking at the plots for the traction-inverter, Fig. 4.15a is 100 kW motor on and Fig. 4.15b is 100 kW motor off. In general the CM current is not that high when the motor is on due to there being no load. But at 220 nF there is a large peak, mainly from the fundamental frequency spectrum, and the fundamental frequency for this point is 150 Hz. Fig. 4.17 shows the 150 Hz CM current over time in the traction-inverter when using the 220 nF Y-capacitor filter.

When the motor is turned off, there is not much CM current at all, which is reasonable since the traction-inverter also is turned off then. 50 kW motor on is shown in Fig. 4.16 and like for the 100 kW motor on case there are large peaks, this time for 220 nF and 330 nF. The fundamental frequency for these points are also 150 Hz. The peaks in these plots are not as high as for the multi-inverter, but they are still significant. For the rest of the plots there is not much to say, since the CM current is generally low, but they can be seen in App. A.

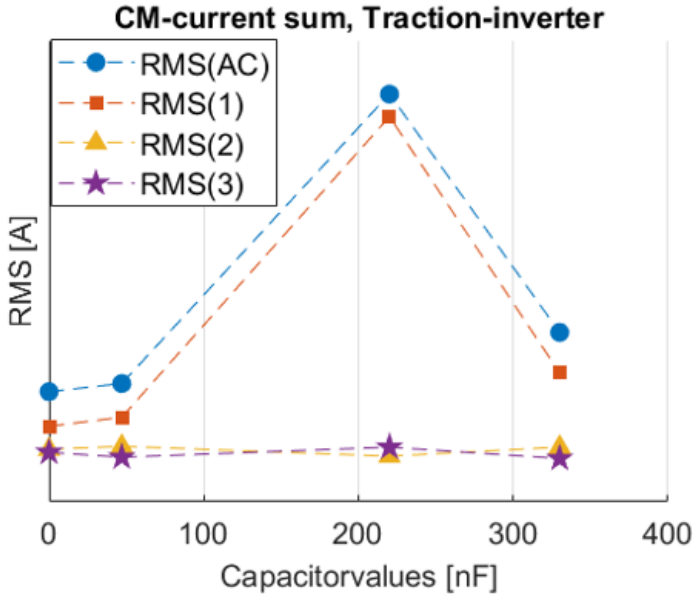

(a) RMS for the CM currents with varying Y-capacitor filter in the traction-inverter. 100 kW, motor on.

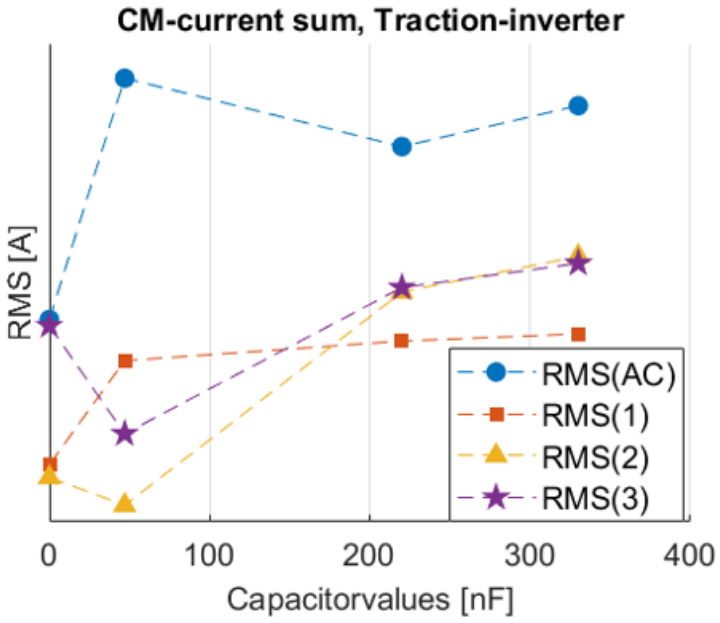

(b) RMS for the CM currents with varying Y-capacitor filter in the traction-inverter. 100 kW, motor off.

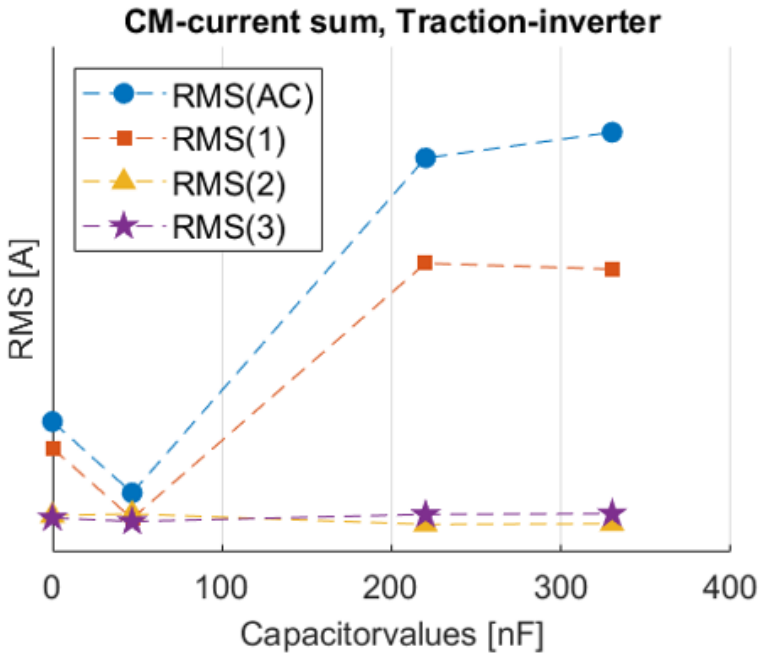

Figure 4.16: RMS for the CM currents with varying Y-capacitor filter in the traction-inverter. 50 kW, motor on.

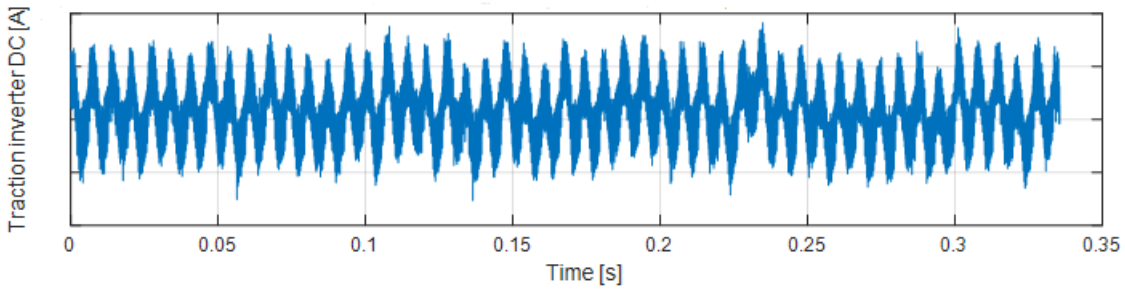

Figure 4.17: 150 Hz CM current in the traction-inverter when using the 220 nF Y-capacitor filter. 100 kW, motor on.

4.2.4 Traction motor

The currents when the motor was turned off were not plotted in this traction motor case as it unsurprisingly did not really have any significant or reliable noise. The 50 kW charging case was omitted because it was very similar to the 100 kW case. The 100 kW and 0 kW charging cases can be observed in Fig. 4.18.

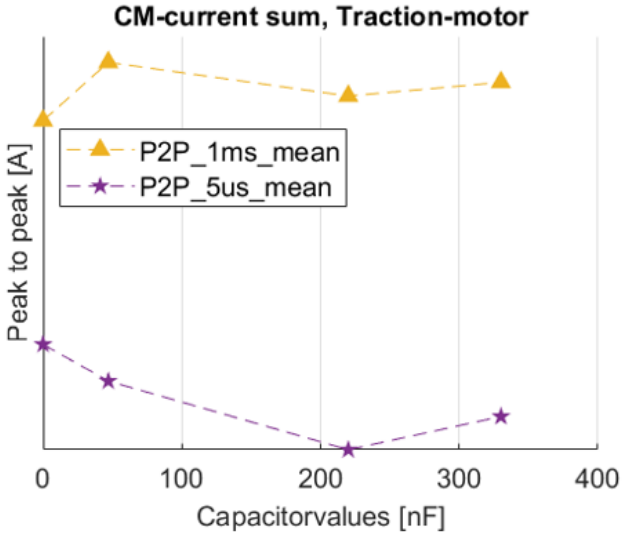

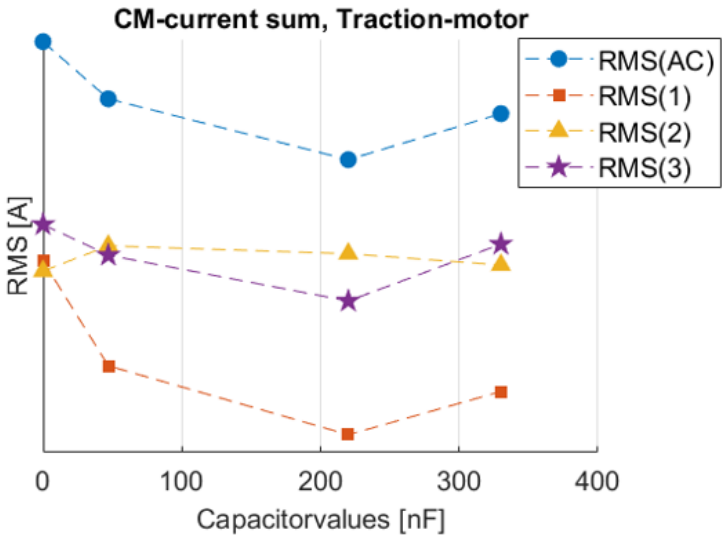

(a) RMS and peak-to-peak for the CM currents with varying Y-capacitor filter and measuring points. 100 kW, motor on.

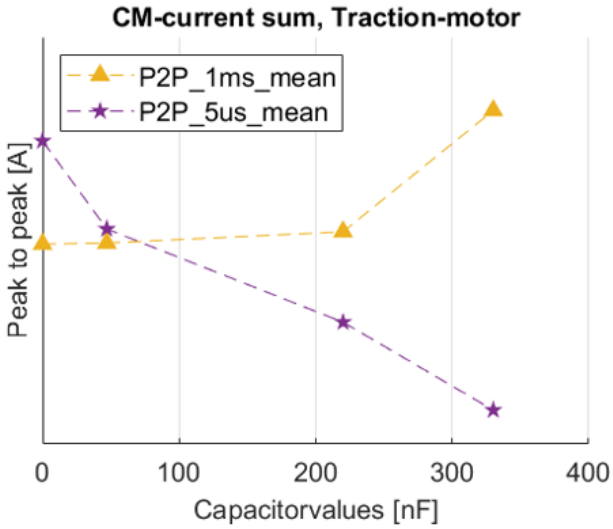

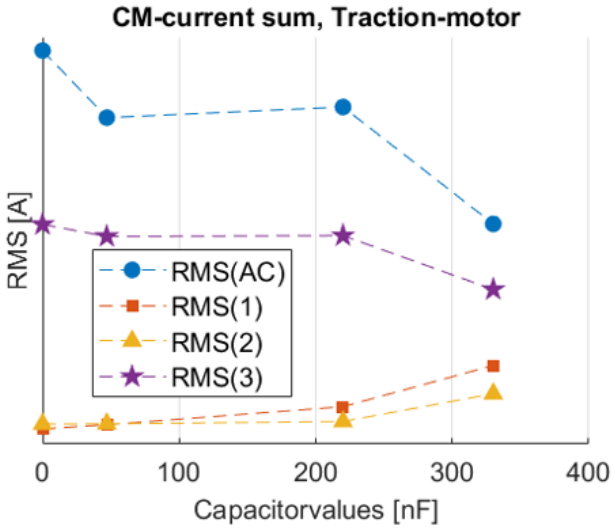

(b) RMS and peak-to-peak for the CM currents with varying Y-capacitor filter and measuring points. 0 kW, motor on.

Figure 4.18: 100 kW and 0 kW, motor on.

Overall however, the traction motor does not seem to be too affected by CM noise in the charging operation mode as the RMS values of the current do not seem to decrease or increase very much in any of the charging powers except for the 0 kW charging case, and even then, the currents are quite small overall.

5

Conclusion and discussion

5.1 Power-train noise

The inverters used in the power-train seem to be causing some problems when the motor is turned on, mainly the multi-inverter. When there is some charging power and the motor is turned on, the CM current sees a significant increase in RMS, mainly in multi-inverter and also some in the traction inverter. Fig. 4.14 shows the peak-to-peak for the CM current to be increasing when using the 220 nF Y-capacitor filter. Further testing and analyses need to be established in order to find the reason for these increasing currents. The fact that this current operates at 150 Hz should also be investigated so it can be determined that it does not disrupt desired signals.

The reason for these high CM currents is hard to determine and the fact that it mainly happens when the motor is turned on and using a Y-capacitor filter makes it even harder to understand. One thought is that there is some sort of resonance happening and that the 150 Hz signals are third order harmonics of the grid fundamental frequency. This would also explain why we do not really see this when there is no filter, because resonance happens when there is both capacitance and inductance in a circuit. Why it mainly happens when the motor is turned on though, is still a question to be answered.

The CM current is the largest in the multi-inverter, so it would be believable that it is created there. It is then likely transmitted to different parts of the vehicles through the various coupling mechanisms mentioned earlier.

Further measurements have to be made in other parts of the vehicle to be able to definitely determine whether the Y-cap filter can or should be improved upon and what path the CM current takes. However, generally speaking, the transient (20 kHz-10 MHz) and switching frequency spectrum (550 Hz-20 kHz) currents are quite low in magnitude outside of a few notable exceptions. This means that this noise should not pose a significant problem in the everyday charging operation of the vehicle. What can be said though is that it is not certain from these measurements that one filter value performs overall better than any of the other two values for the operation mode that was analysed. The advantages and disadvantages seem to depend on what parameters are used. The CM current that flows through the filter does increase with increased capacitance, which could be a good sign, however without seeing any significant decline in noise generated in the power-train it could

just be that it is noise from other parts of the vehicle.

Considering the LCL-filter, it does lower the magnitude of both the switching and transient spectrum. This means that the overall high-frequency noise is dampened to some extent. At the same time there is not large amounts of noise being thrown at this filter, so it is hard to conclude how well it performs.

As for the THD content, it can change quite significantly with an increase of capacitance in the Y-capacitor filter. In order to stay below the recommended 8 % as outlined in the Swedish standard, it is best to use lower capacitance values, as they perform overall better in terms of THD.

5.2 Possible improvements

5.2.1 Testing method

An improvement in testing method that could be made in order to conclusively understand what changes need to be done in the machine regarding EMI, is to measure all of the different operation modes of the machines instead of just charging mode, such as traction mode and energy dump mode. Additionally, all these tests would also have to be conducted on any machines that need an EMC-filter.

Another improvement on the testing method that could potentially be very significant in reducing overall noise in the vehicle is the use of proper EMC-testing, where not only the noise from inside the closed system of the power-train is considered, but also how well the vehicle can withstand degradation when exposed to significant electromagnetic radiation from the surroundings, or in other words, how good the vehicle's immunity is. This could give an overall better understanding of the produced noise, making it easier to construct countermeasures.

5.2.2 Y-capacitor filter

The Y-capacitor filter operates at quite high frequencies, filtering out mostly transient frequency noise. From the measurements conducted in this project, it can be seen that the increased CM current is created at 150 Hz, which is far from the operation range of the Y-capacitor filter, meaning that the noise is outside the effective operating frequency of the filter. An improvement to this would be to make the filter operate at lower frequencies, however probably not as low as 150 Hz, by adding other filter components. One such component could be the common mode choke. This would also make it a higher order filter, improving its attenuation ability.

5.3 Conclusion

The measurements have provided better understanding of the emitted noise in the power-train of the vehicle and how effective the filters are at suppressing it. The highest CM current is measured when the vehicle is charging and the motor is on. The likely source of the CM current is the multi-inverter. This may be due to resonance in the circuit, that this certain range of capacitors seems to make the circuit resonate and increase the current significantly. To determine why it happens, further testing needs to be conducted, but one idea would be to measure a significantly higher or significantly lower capacitor value, say in the pico or microfarad range and see if this resonance phenomenon can still be observed.

The Y-capacitor filter is successful in filtering transient noise. However there is no large amount of transient noise being transmitted, so it cannot be concluded if it would successfully filter any large amounts of noise. This is also the case for the LCL-filter. It does suppress the noise to the grid, but there is no large amounts of noise being conducted to see how effective the filter really is.

Introducing the Y-capacitor filter influences the THD towards the grid. The 47 nF filter seems to keep the THD the lowest throughout the different tests.

To increase the performance of the filters there are a few things to consider doing. Firstly, to get a better understanding of the noise, further testing need to be conducted. This could be done by doing measurements in other operation modes. Proper EMC-testing is also something to consider. Secondly, the filters could be improved by adding more filter components, further improving their suppression capabilities.

Bibliography

[1] G. Wright, "What is Electromagnetic Interference (EMI)," *TechTarget*. [Online]. Available: https://www.techtarget.com/searchmobilecomputing/definition/electromagnetic-interference (accessed on: 2024-04-21).

[2] B. Odhiambo, "EMI: Understanding the Causes in Power Electronics,"*EEPower*.[Online]. Nov. 2023. Available: https://eepower.com/technical-articles/emi-understanding-the-causes-in-power-electronics/ (accessed on: 2024-04-21).

[3] Y. Tang, "High Power Inverter EMI characterization and Improvement Using Auxiliary Re-sonant Snubber Inverter," MSc thesis, Virginia Polytechnic Institute and State University, Blacksburg, VA, USA, 1998. [Online]. Available: https://vtechworks.lib.vt.edu/server/api/core/bitstreams/de5970b7-4c21-4db2-b431-d0056a154c0f/content.

[4] R. B. Keller, "Noise Coupling," in *Design for Electromagnetic Compatibility-In a Nutshell: Theory and Practice*, Ed. Cham, Switzerland: Springer Nature Switzerland AG, 2022, ch. 12 , pp. 189-209. [Online]. Available: https://doi.org/10.1007/978-3-031-14186-7, Accessed on: 2024-03-10.

[5] "EMC Question of the Week: August 24, 2020," *LearnEMC*. [Online]. Available: https://learnemc.com/qotw-200824 (accessed on: 2024-05-03).

[6] Sunpower Electronics, "Differential Mode Noise," [Online]. Available: https://www.sunpower-uk.com/glossary/what-is-differential-mode-noise/ (accessed on: 2024-04-21).

[7] *Basics of EMI Filters*, Kyoto, Japan: Murata Manufacturing, 1998. [Online]. Available: https://datasheet.datasheetarchive.com/originals/library/Datasheets-UEA1/DSAFRAZ008703.pdf, Accessed on: 2024-04-21.

[8] J. Gaboian, "A Survey of Common-Mode Noise," Texas Instruments, Dallas, TX, USA, 2002. [Online]. Available: https://www.ti.com/lit/pdf/slla057 Accessed on: 2024-04-21.

[9] T. Williams, "Chapter 10 - interference coupling mechanisms," in EMC for Product Designers (Fourth Edition), fourth ed., T. Williams, Ed. Oxford, United Kingdom: Newnes, 2007, ch. 10, pp. 222–257. [Online]. Available: https://doi.org/10.1016/B978-075068170-4/50010-4, Accessed on: 2024-03-23.

[10] "6.2: Electric Flux," *LibreTexts*. [Online]. Available: https://phys.libretexts.org/Bookshelves/University_Physics/University_Physics_(OpenStax)/Book%3A_University_Physics_II_-_Thermodynamics_Electricity_and_Magnetism_(OpenStax)/06%3A_Gauss%27s_Law/6.02%3A_Electric_Flux(accessed on: 2024-05-15).

[11] S. Ling; W. Moebs and J. Sanny, "Mutual Inductance," in *University Physics Volume 2*, Ed. Houston, TX, USA: OpenStax, 2016, ch. 14.1 , pp. 612-615. [Online]. Available: https://openstax.org/details/books/university-physics-volume-2?Book%20details, Accessed on: 2024-03-10.

[12] R. B. Keller, "Cable Shields," in *Design for Electromagnetic Compatibility-In a Nutshell: Theory and Practice*, Ed. Cham, Switzerland: Springer Nature Switzerland AG, 2022, ch. 13.7 , pp. 189-209. [Online]. Available: doi:10.1007/978-3-031-14186-7.

[13] Y. Zhao, W. Yan, J. Sun, M. Zhou and Z. Meng, "Electrical engineering," in *Electromagnetic Compatibility*, Ed., Singapore: Springer Nature Singapore Pte Ltd., 2021, ch. 3.1, pp. 35-40. [Online]. Available: https://link.springer.com/book/10.1007/978-981-16-6452-6, Accessed on: 2024-05-14.

[14] N. Nguyen and F. Blanchette, "Application of y-cap on noise attenuation in low power part of power converter," in *2017 IEEE International Conference on Industrial Technology (ICIT)*, Toronto, ON, Canada, 2017, pp. 48–53. [Online]. Available: https://ieeexplore.ieee.org/document/7913057 Accessed on: 2024-05-14.

[15] H. Hizarci, U. Pekperlak and U. Arifoglu, "Conducted Emission Suppression Using an EMI Filter for Grid-Tied Three-Phase/Level T-Type Solar Inverter," *IEEE Access*, vol. 9, pp. 67417 – 67431, Jan. 2021, doi:10.1109/ACCESS.2021.3077380.

[16] F. Hubert, P. Dorsch, D. Kuebrich, T. Duerbaum and S. J. Rupitsch, "Piezoelectric EMI Filter for Switched-Mode Power Supplies," in *IEEE Transactions on Power Electronics*, vol. 36, no. 6, pp. 6624-6643, Jun. 2021, doi: 10.1109/TPEL.2020.3043091.

[17] D. Wiest, "How does it Work? Common Mode Chokes," *Pulse Electronics*. [Online]. 2021. Available: https://www.pulseelectronics.com/wp-

content/uploads/2021/03/CMC-How-Does-it-Work.pdf (accessed on: 2024-05-13).

[18] S. Gulur, V. M. Iyer, S. Bhattacharya,"A CM Filter Configuration for Grid-Tied Voltage Source Converters" in *IEEE Transactions on Industrial Electronics*, pp. 1-1, Nov. 2019, doi: 10.1109/TIE.2019.2949530.

[19] D. A. Ward and J. La T. Exon, "Using Rogowski coils for transient current measurements" in *ENGINEERING SCIENCE AND EDUCATION JOURNAL*, Jun. 1993. [Online]. Available: https://web.archive.org/web/20160304102532/http://homepage.ntlworld.com/rocoil/Pr7o.pdf.

[20] M. M. Ishaya et al., "Single-tuned passive filter (STPF) for mitigating harmonics in a 3-phase power system," *Sci Rep*, vol. 13, no. 1, Nov. 2023, doi:10.1038/s41598-023-47614-7.

[21] D. Shmilovitz, "On the definition of total harmonic distortion and its effect on measurement interpretation," *IEEE Transactions on Power Delivery*, vol. 20, no. 1, pp. 526-528, Jan. 2005, doi:10.1109/TPWRD.2004.839744.

[22] *Voltage characteristics of electricity supplied by public electricity networks*, SS-EN 50160, UTG 5:2023, Swedish Institute for Standards, Stockholm, Sweden, 2023. Available: https://www-sis-se.eu1.proxy.openathens.net/en/produkter/electrical-engineering/electrical-engineering-in-general/ss-en-50160-utg-52023/?$_{ti}d$ = $PW4ct3FRTCWJGm0gdHQGfw_{tq}$ = $SS-EN+50160_{th}it.id$ = $SIS_se_site_Features_Product_Catalogs_StandardProduct/CatalogContent_57b402ae-99cc-49f7-b68b-5b59a05fdea6_en_{th}it.pos$ = $2_{tt}ags$ = $andquerymatch, language : en, siteid : 326c3465-4f01-4d81-93c2-166392ce4789$.

A

Appendix - Matlab plots of measured data

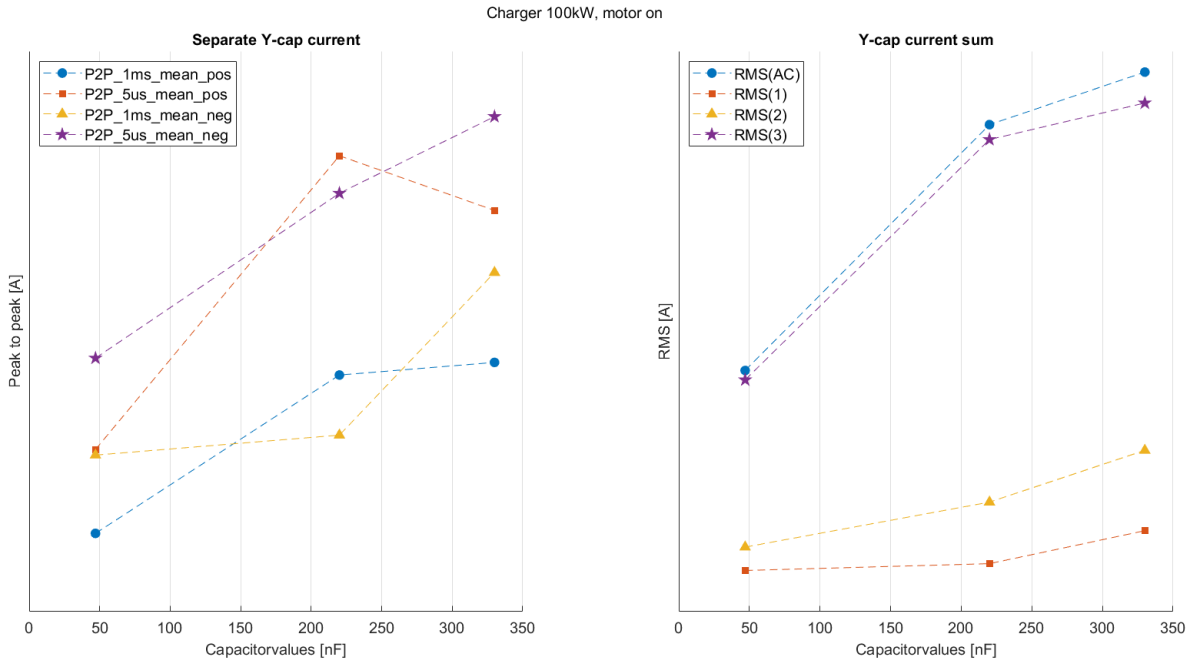

Figure A.1: RMS and peak-to-peak for the filtered Y-capacitor CM-current. 100kW, motor on.

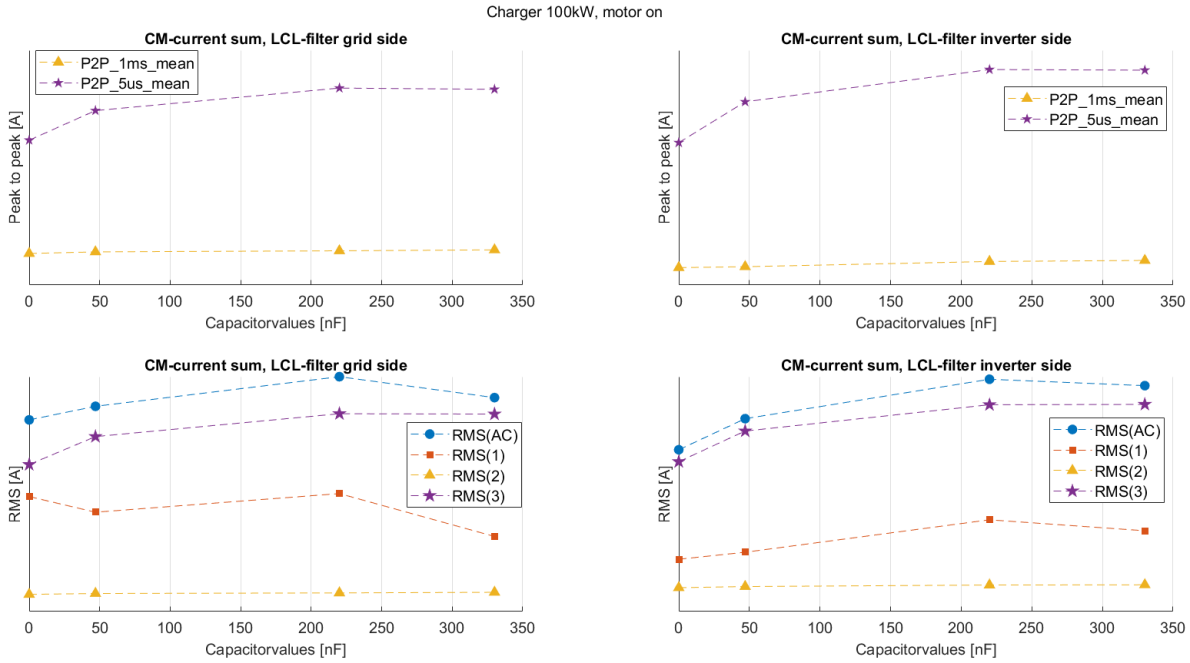

Figure A.2: RMS and peak-to-peak for the CM-currents with varying Y-capacitor filter before and after the LCL-filter. 100kW, motor on.

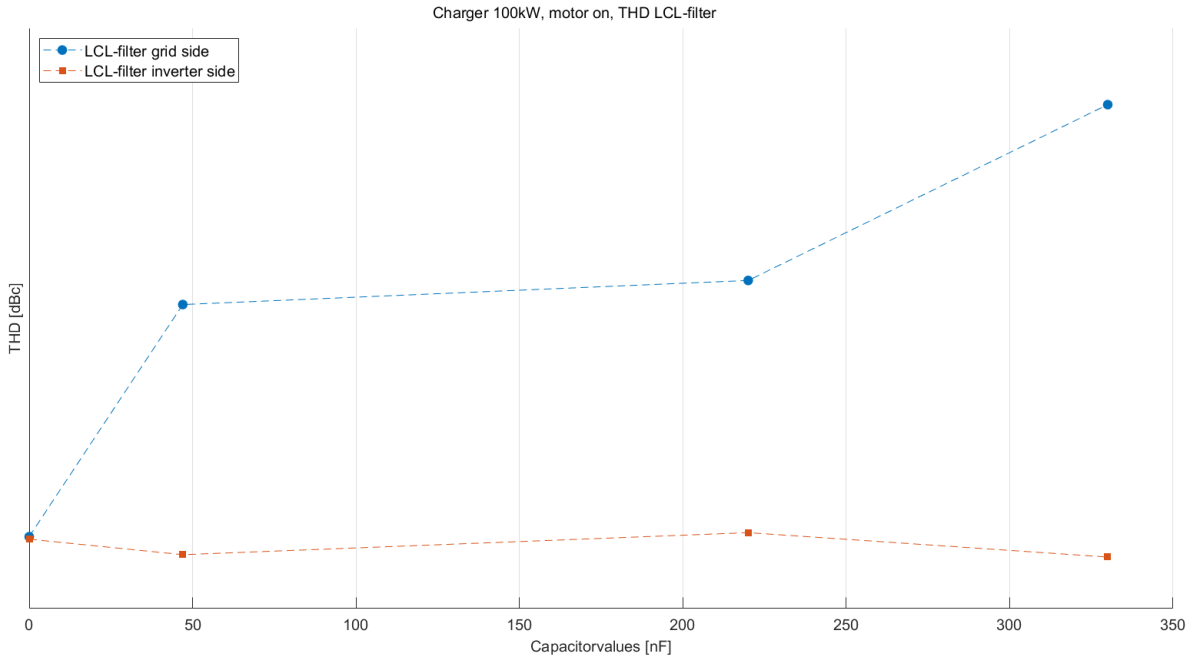

Figure A.3: THD before and after the LCL-filter, with varying Y-capacitor values. 100kW, motor on.

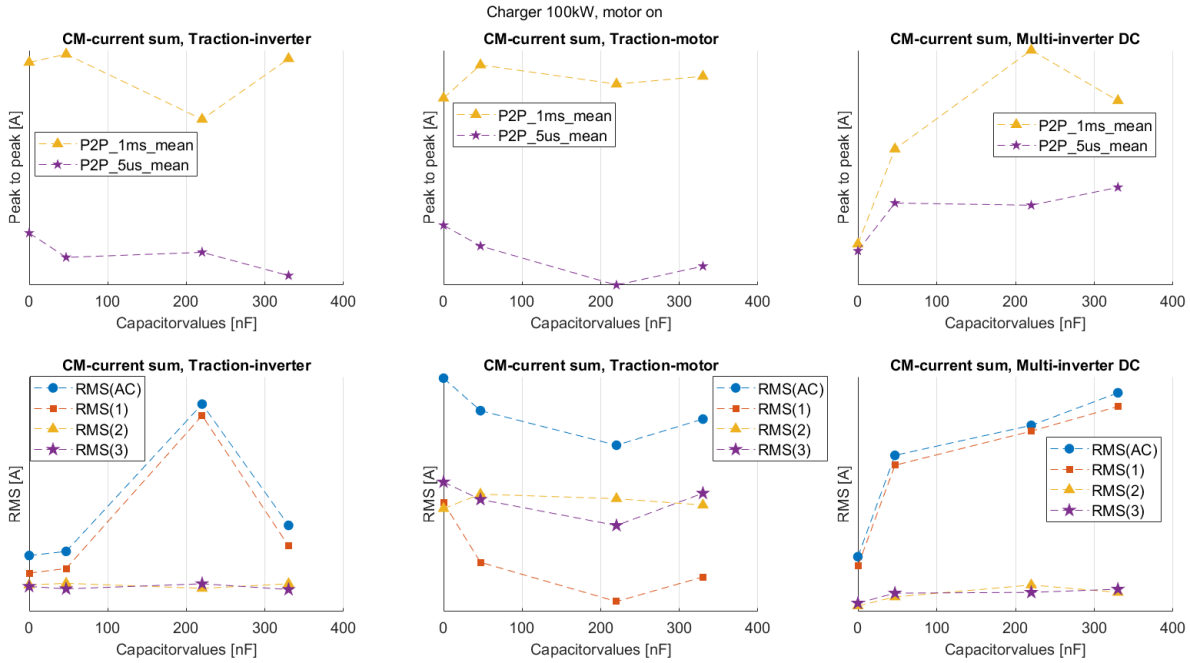

Figure A.4: RMS and peak-to-peak for the CM-currents with varying Y-capacitor filter and measuring points. 100kW, motor on.

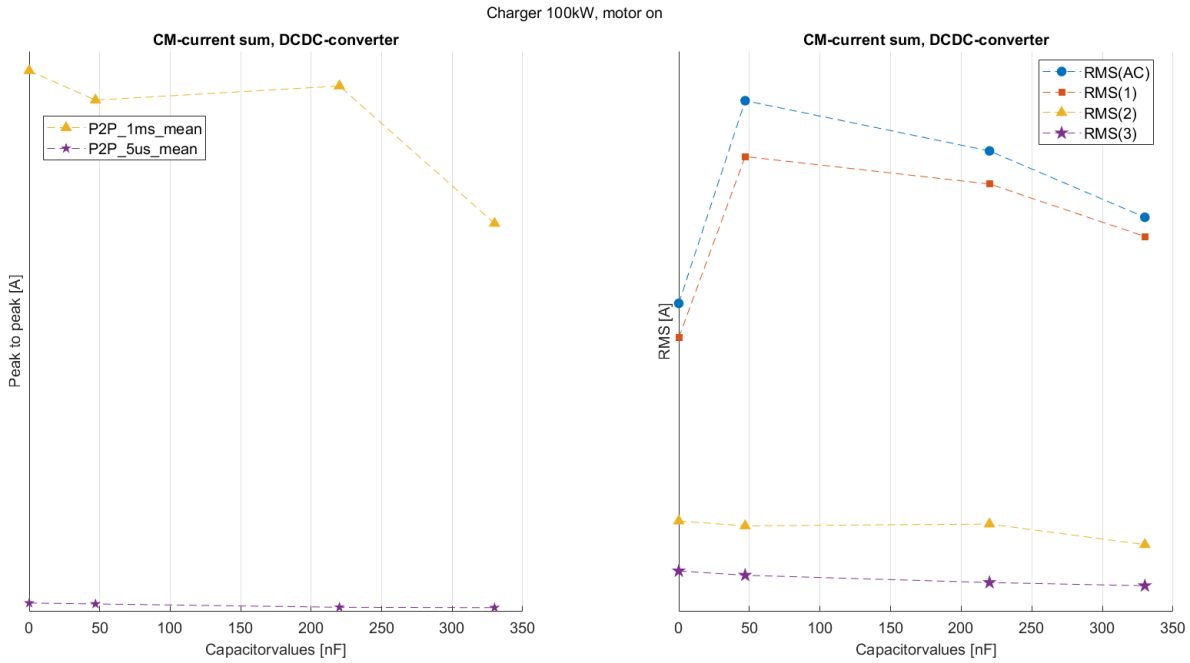

Figure A.5: RMS and peak-to-peak for the CM-currents in the DC/DC-converter with varying Y-capacitor filter. 100kW, motor on.

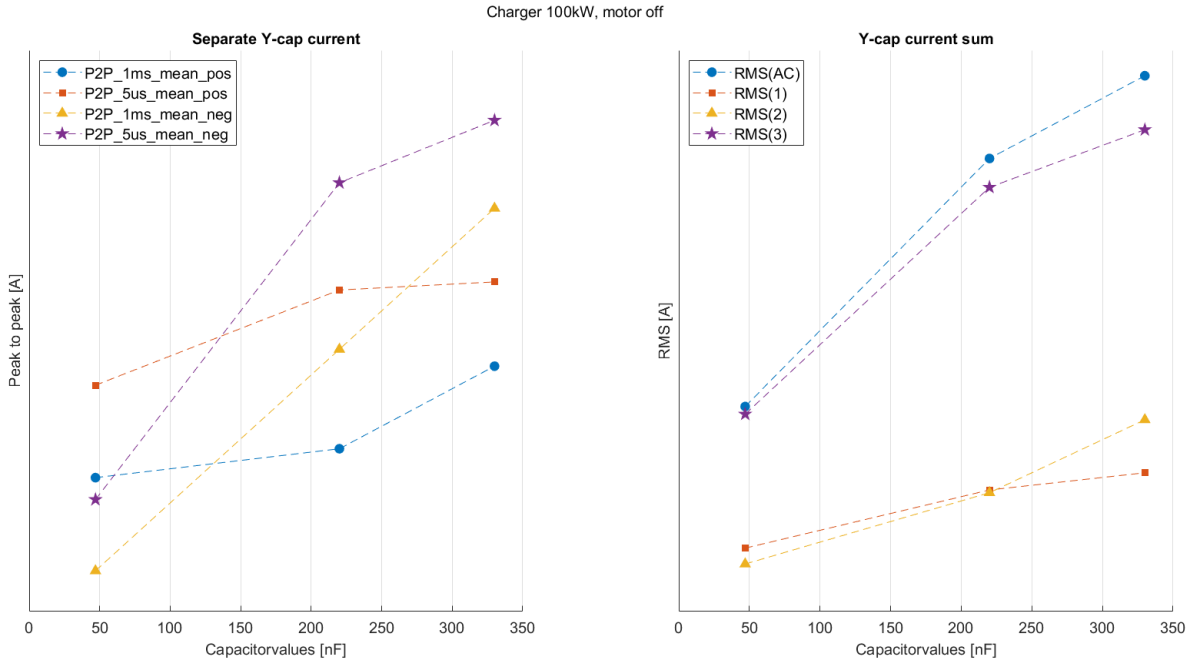

Figure A.6: RMS and peak-to-peak for the filtered Y-capacitor CM-current. 100kW, motor off.

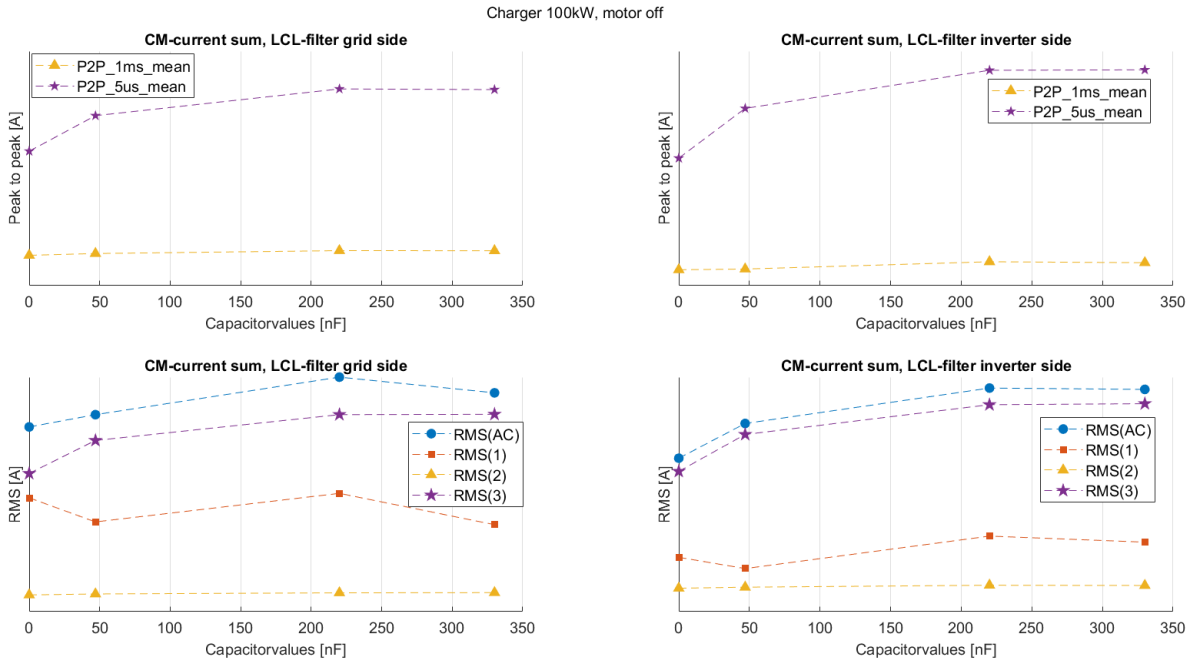

Figure A.7: RMS and peak-to-peak for the CM-currents with varying Y-capacitor filter before and after the LCL-filter. 100kW, motor off.

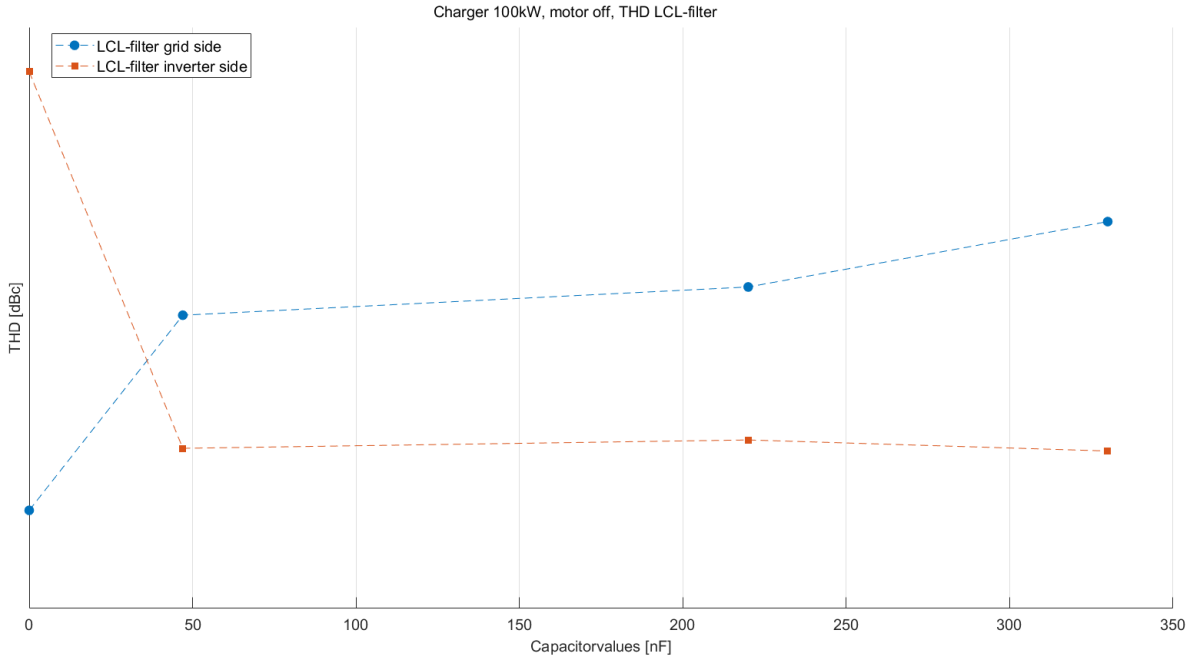

Figure A.8: THD before and after the LCL-filter, with varying Y-capacitor values. 100kW, motor off.

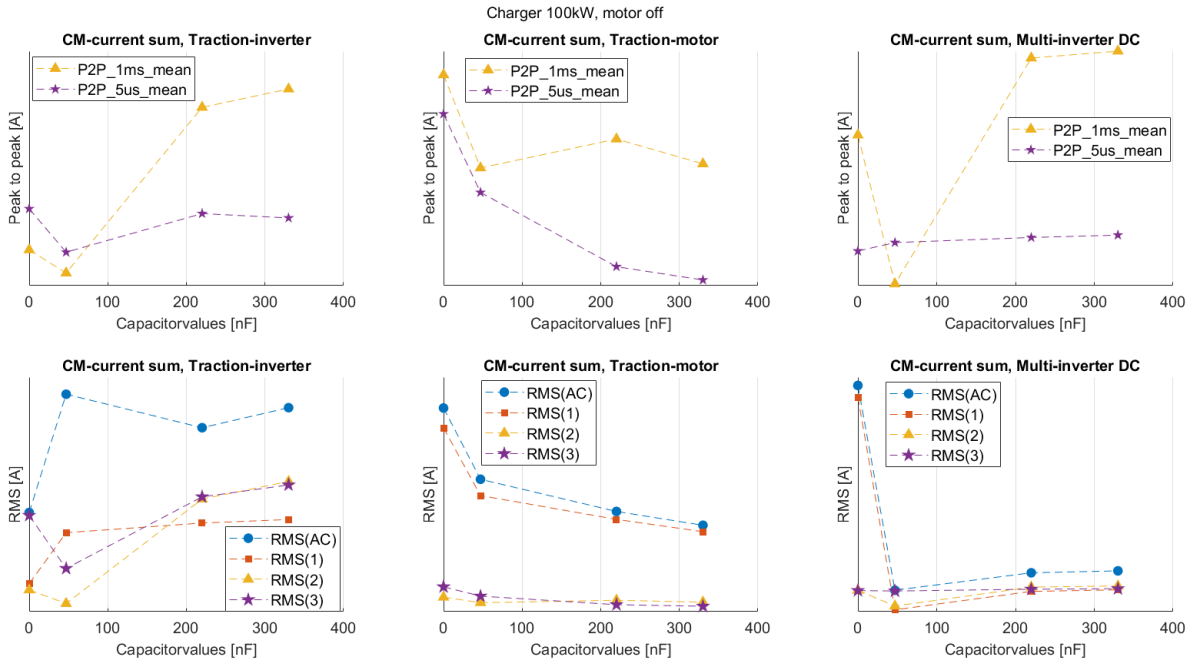

Figure A.9: RMS and peak-to-peak for the CM-currents with varying Y-capacitor filter and measuring points. 100kW, motor off.

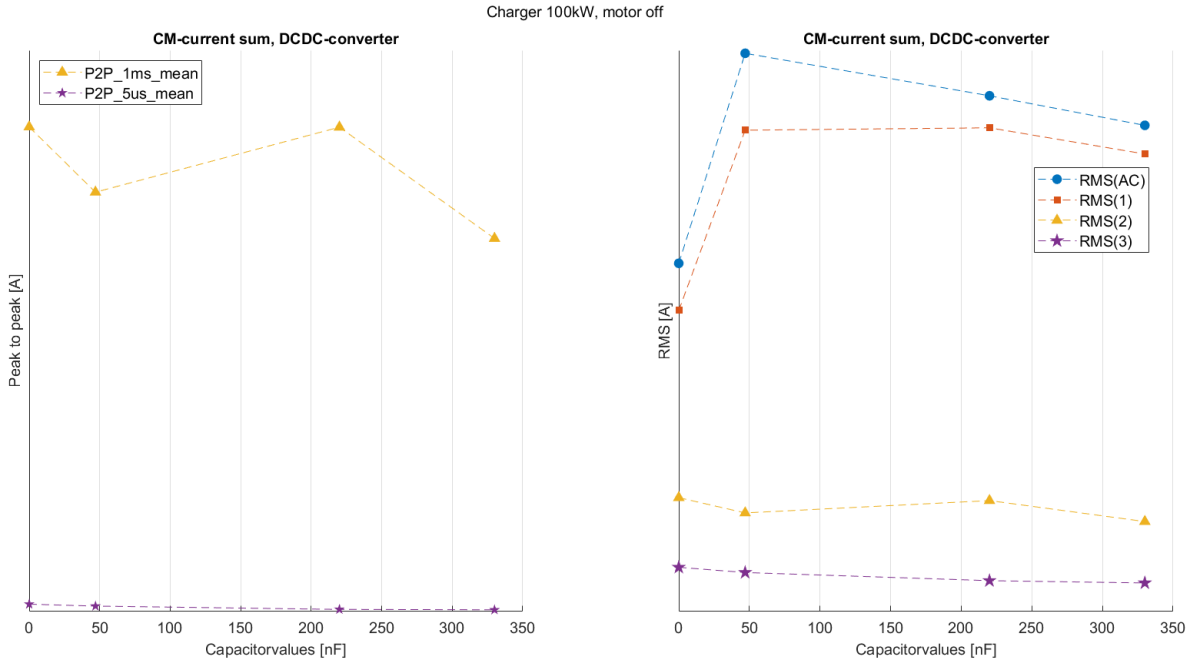

Figure A.10: RMS and peak-to-peak for the CM-currents in the DC/DC-converter with varying Y-capacitor filter. 100kW, motor off.

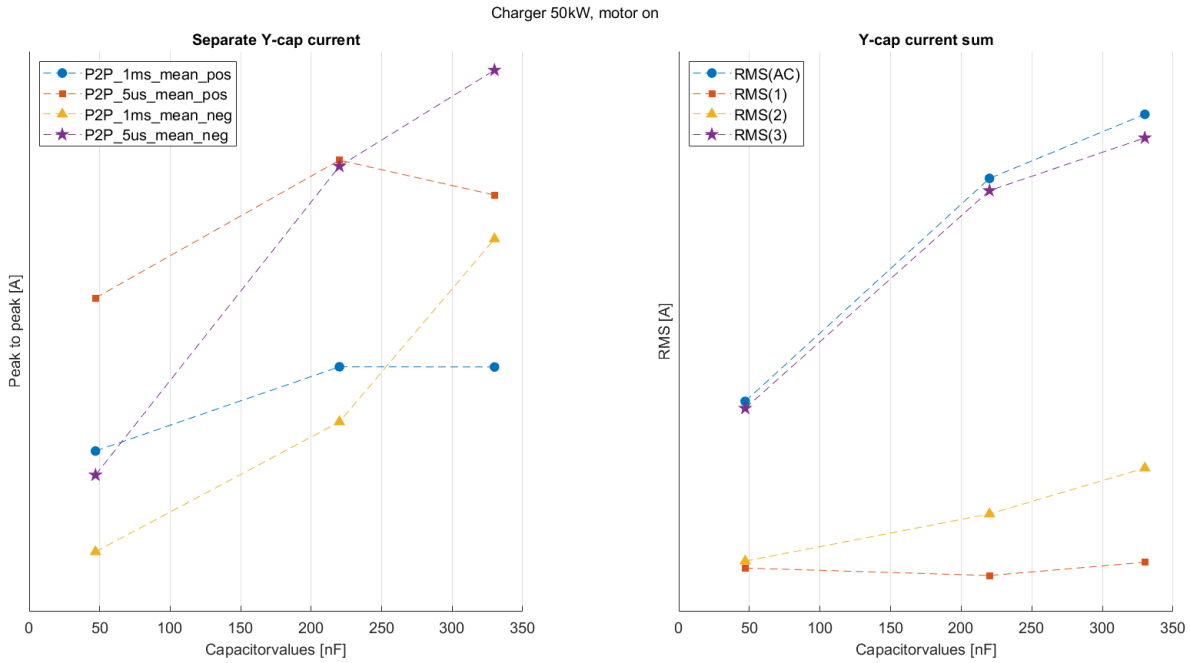

Figure A.11: RMS and peak-to-peak for the filtered Y-capacitor CM-current. 50kW, motor on.

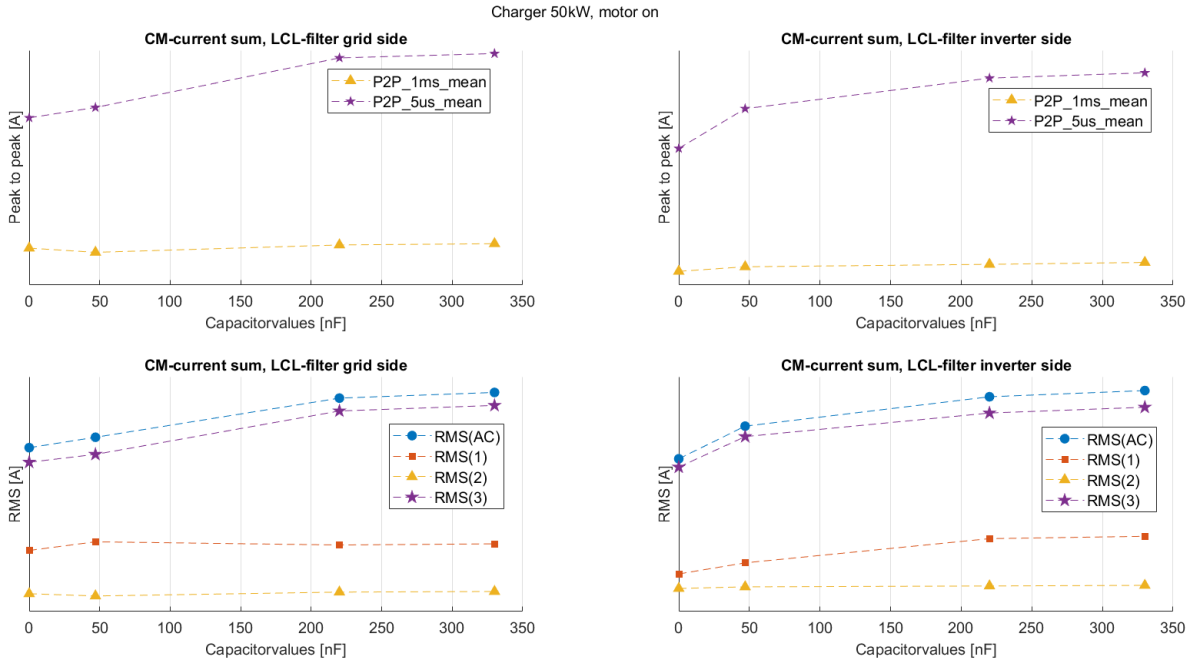

Figure A.12: RMS and peak-to-peak for the CM-currents with varying Y-capacitor filter before and after the LCL-filter. 50kW, motor on.

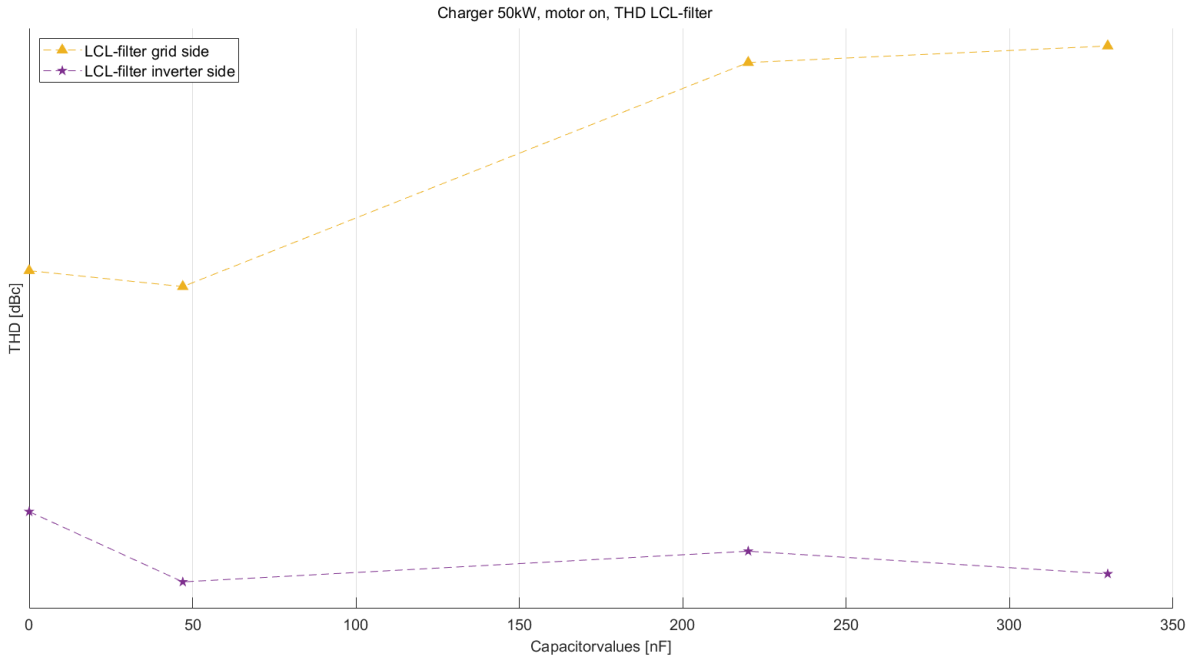

Figure A.13: THD before and after the LCL-filter, with varying Y-capacitor values. 50kW, motor on.

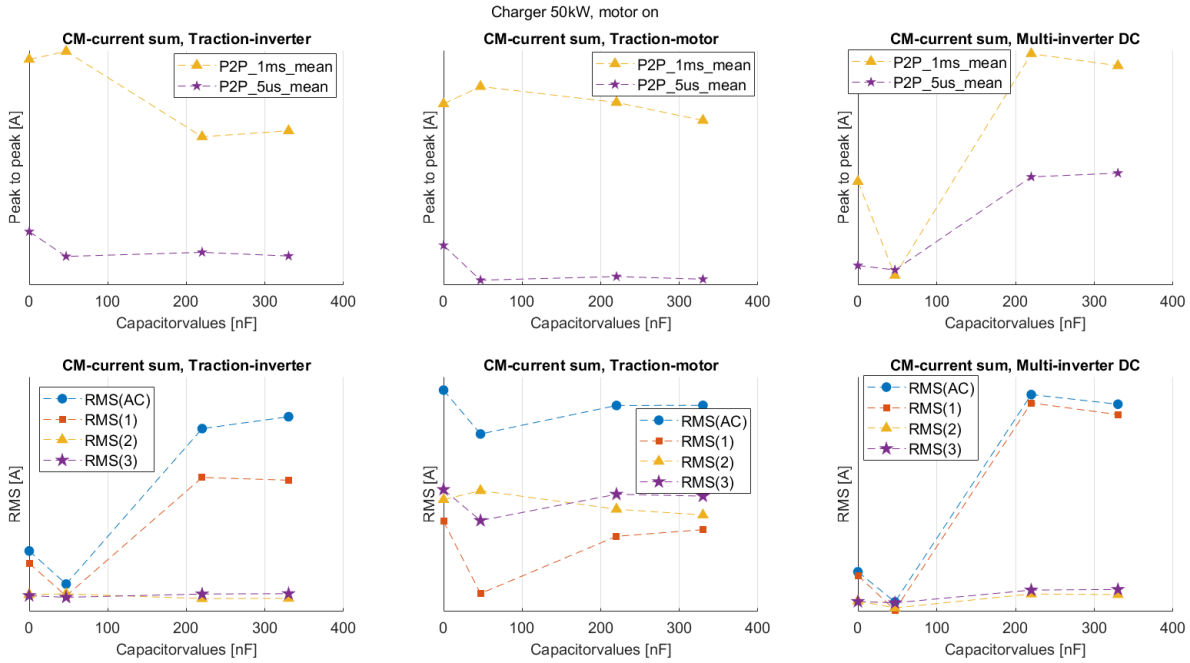

Figure A.14: RMS and peak-to-peak for the CM-currents with varying Y-capacitor filter and measuring points. 50kW, motor on.

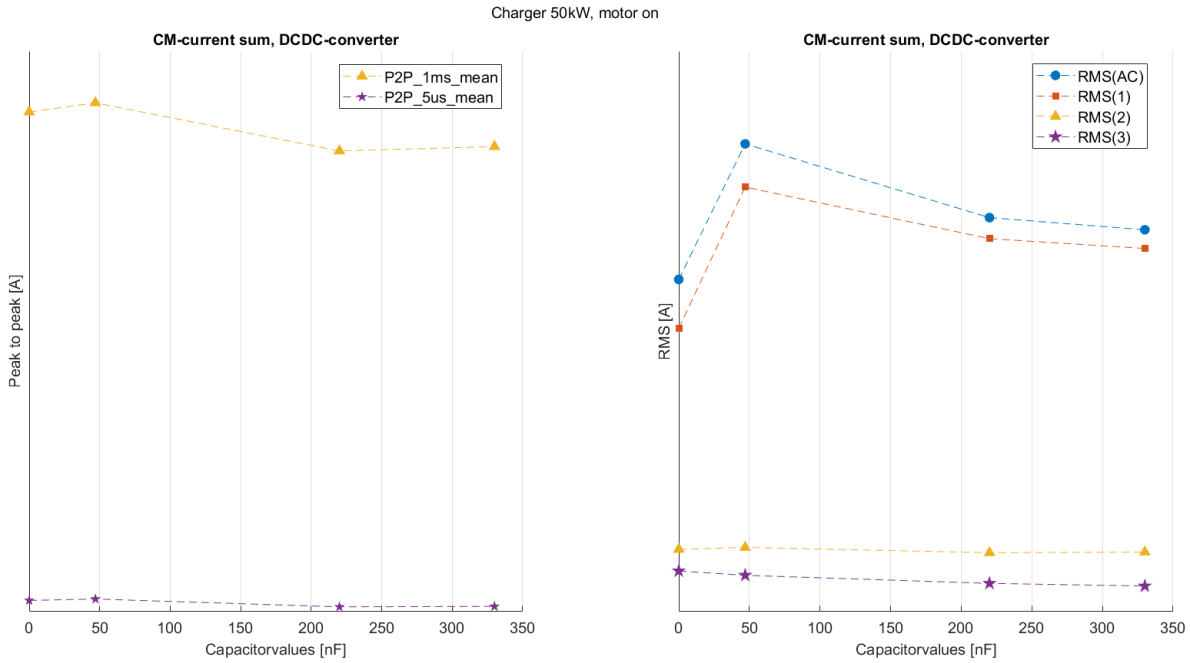

Figure A.15: RMS and peak-to-peak for the CM-currents in the DC/DC-converter with varying Y-capacitor filter. 50kW, motor on.

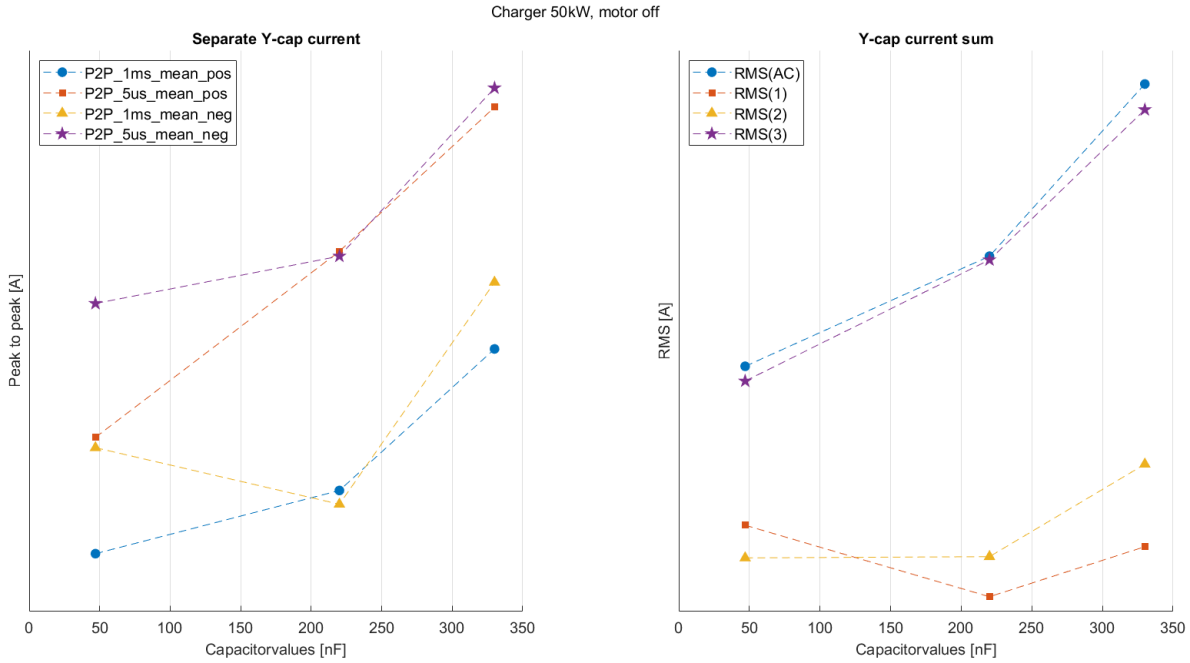

Figure A.16: RMS and peak-to-peak for the filtered Y-capacitor CM-current. 50kW, motor off.

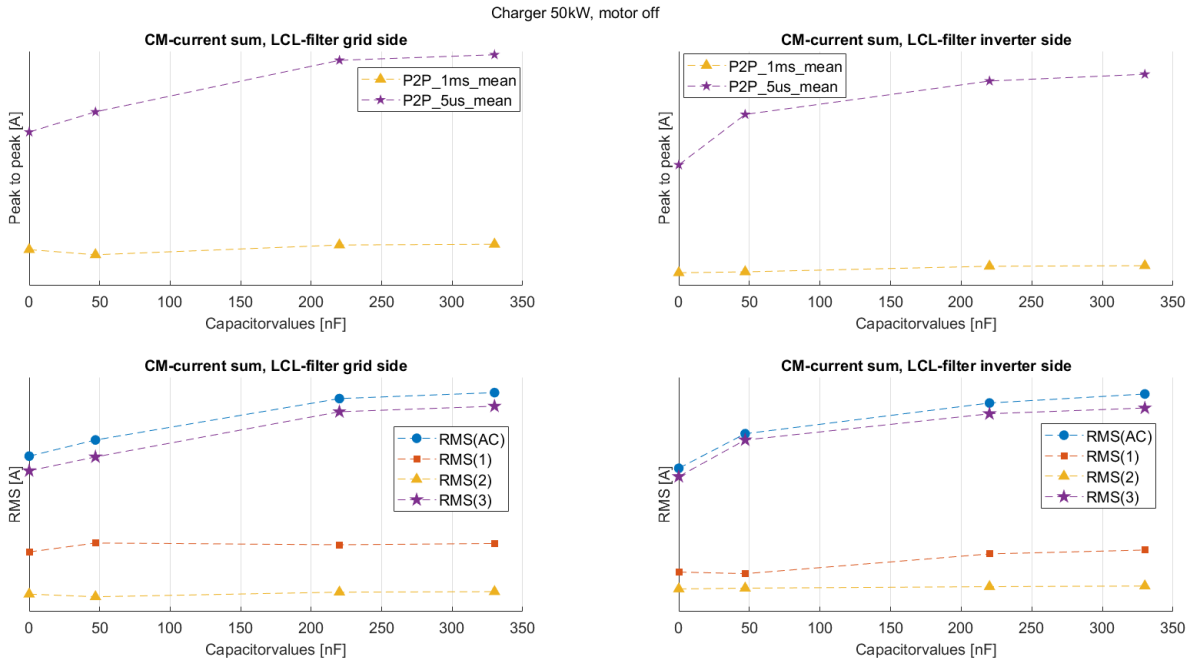

Figure A.17: RMS and peak-to-peak for the CM-currents with varying Y-capacitor filter before and after the LCL-filter. 50kW, motor off.

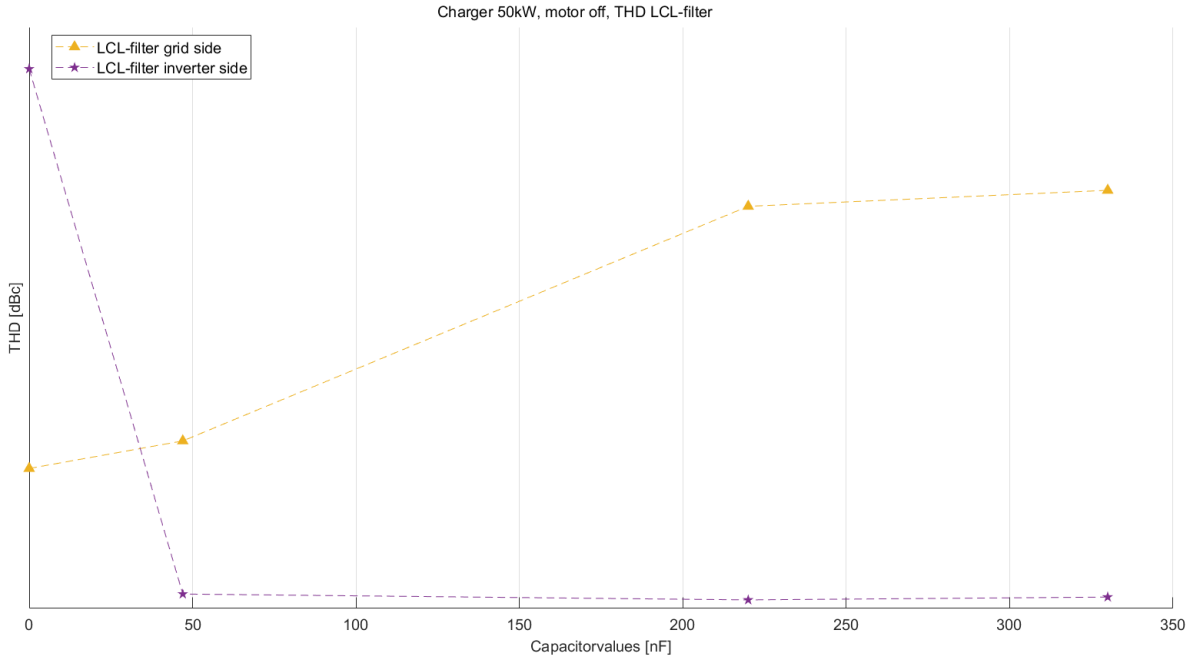

Figure A.18: THD before and after the LCL-filter, with varying Y-capacitor values. 50kW, motor off.

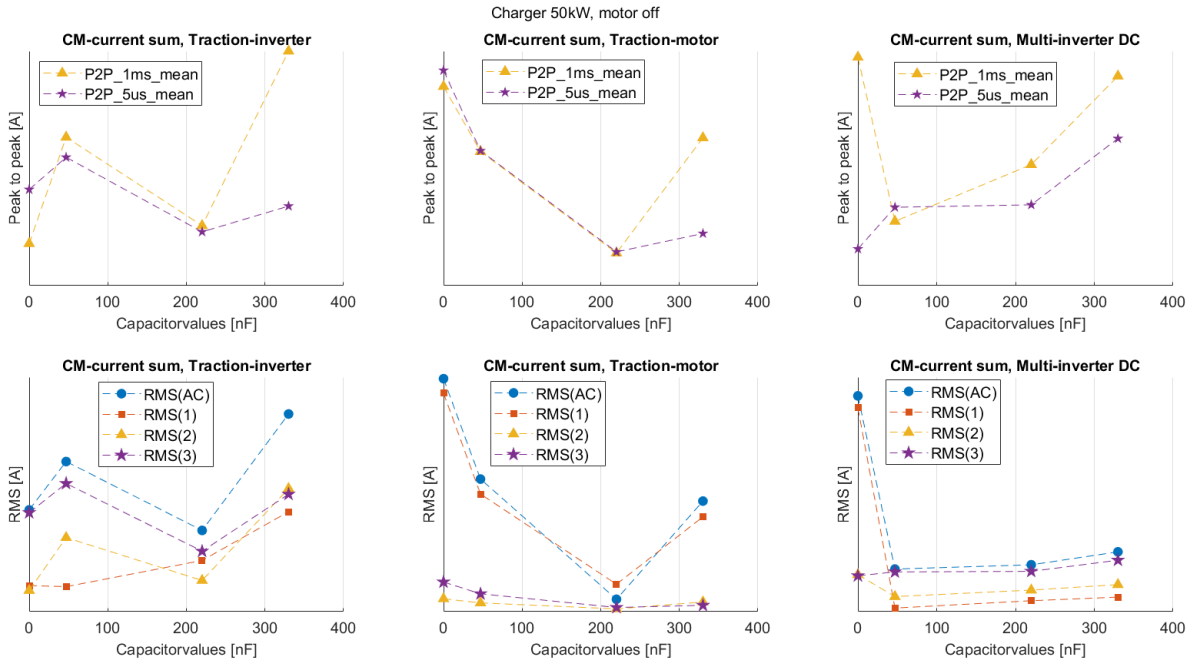

Figure A.19: RMS and peak-to-peak for the CM-currents with varying Y-capacitor filter and measuring points. 50kW, motor off.

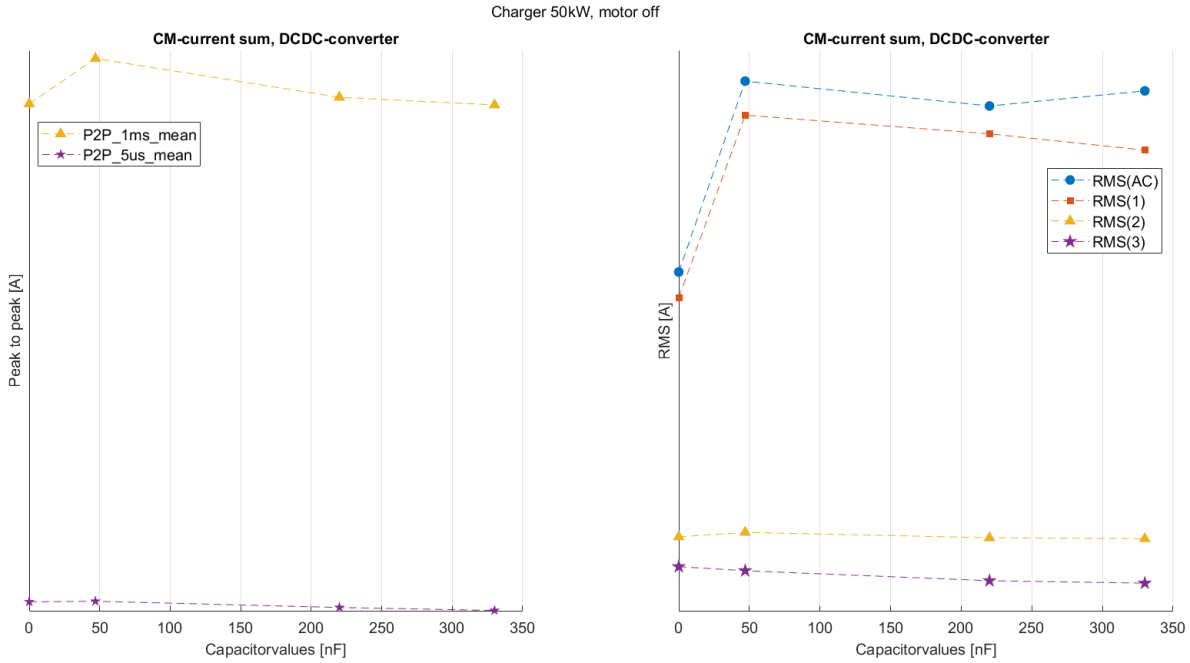

Figure A.20: RMS and peak-to-peak for the CM-currents in the DC/DC-converter with varying Y-capacitor filter. 50kW, motor off.

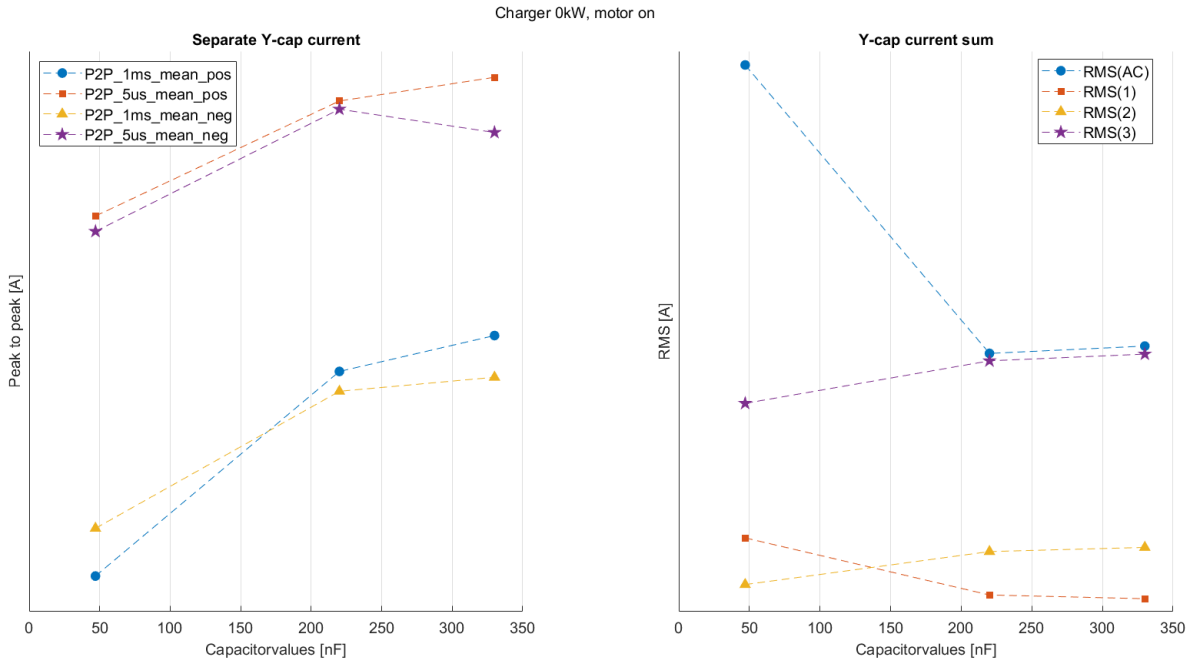

Figure A.21: RMS and peak-to-peak for the filtered Y-capacitor CM-current. 0kW, motor on.

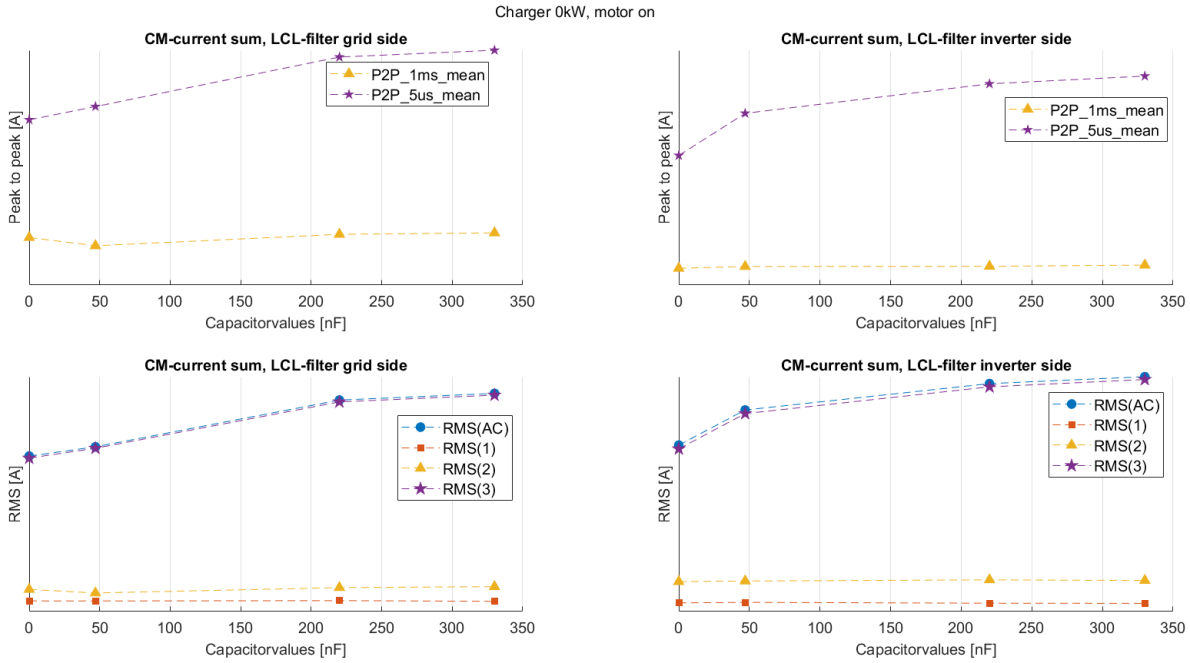

Figure A.22: RMS and peak-to-peak for the CM-currents with varying Y-capacitor filter before and after the LCL-filter. 0kW, motor on.

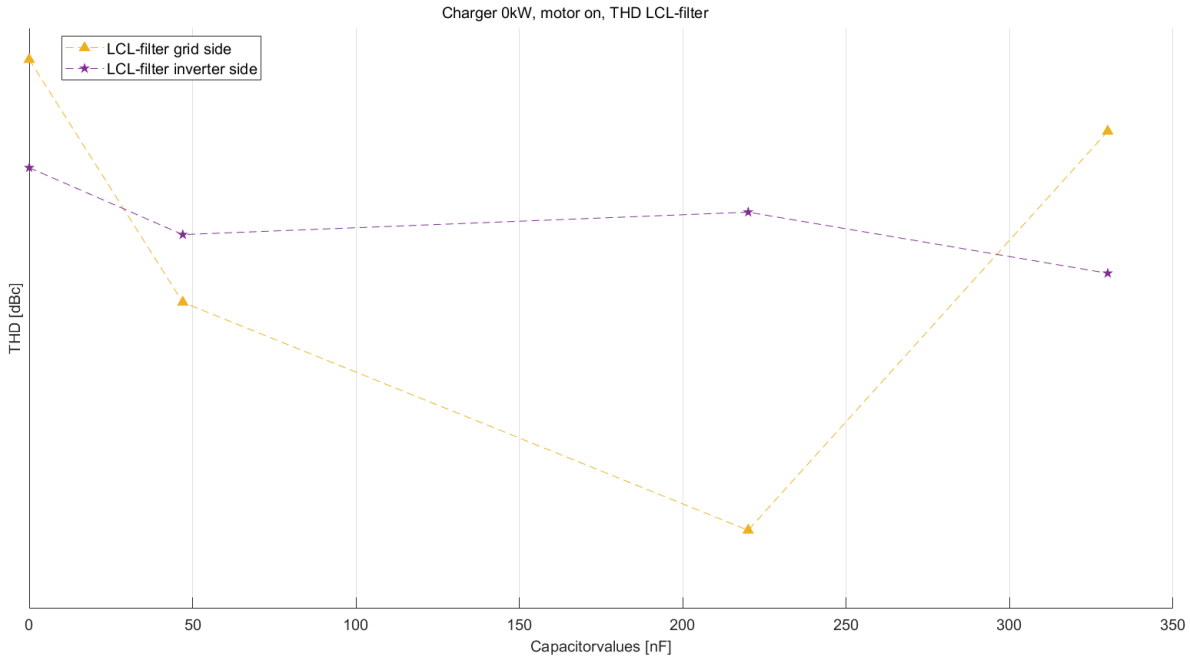

Figure A.23: THD before and after the LCL-filter, with varying Y-capacitor values. 0kW, motor on.

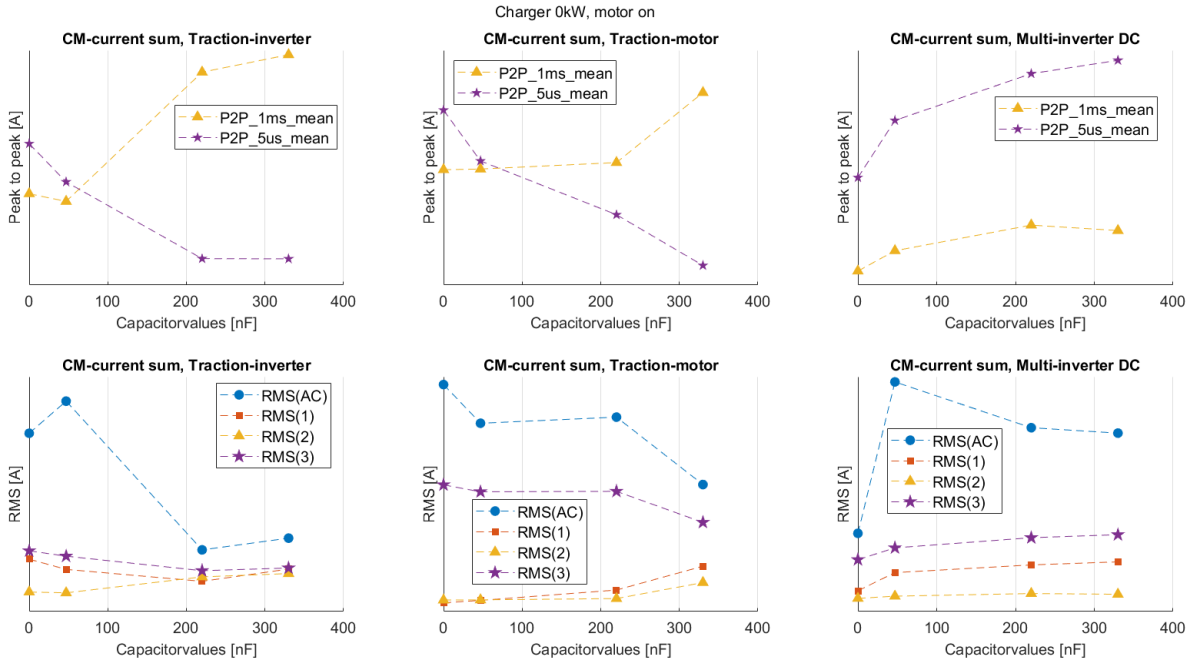

Figure A.24: RMS and peak-to-peak for the CM-currents with varying Y-capacitor filter and measuring points. 0kW, motor on.

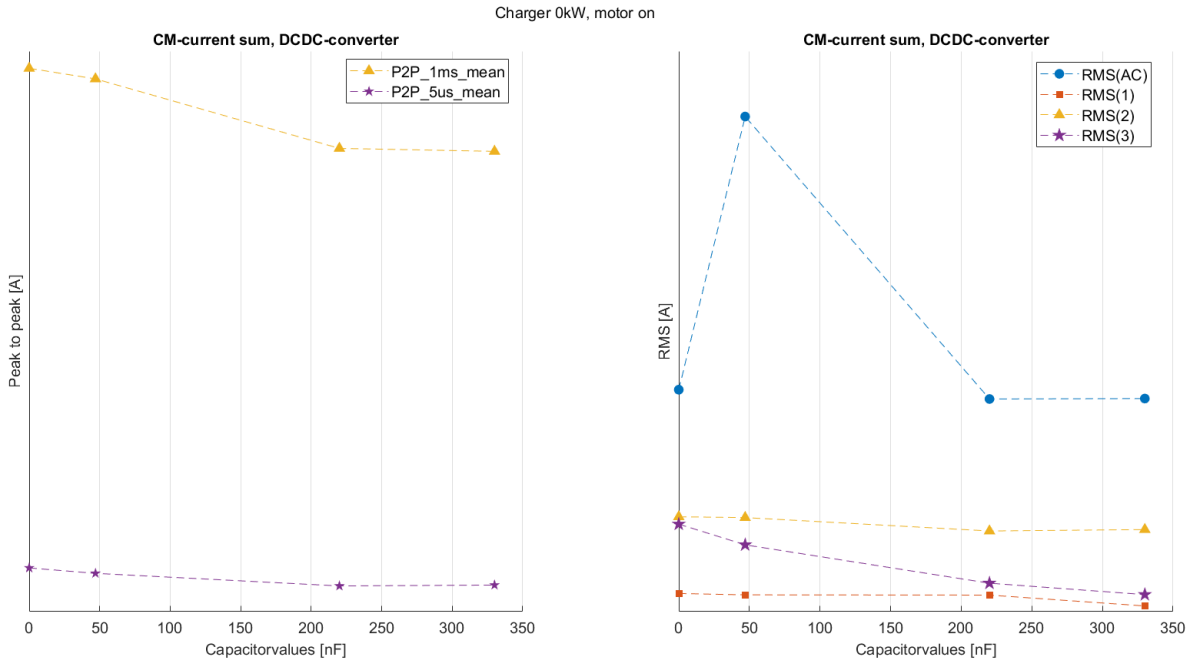

Figure A.25: RMS and peak-to-peak for the CM-currents in the DC/DC-converter with varying Y-capacitor filter. 0kW, motor on.

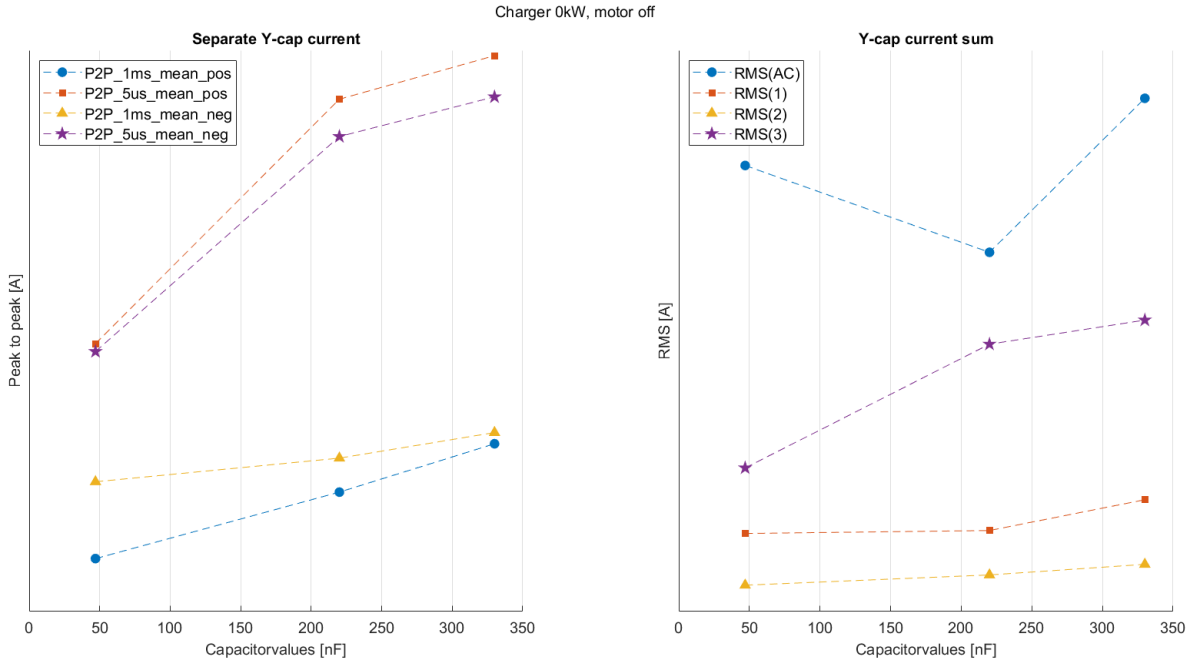

Figure A.26: RMS and peak-to-peak for the filtered Y-capacitor CM-current. 0kW, motor off.

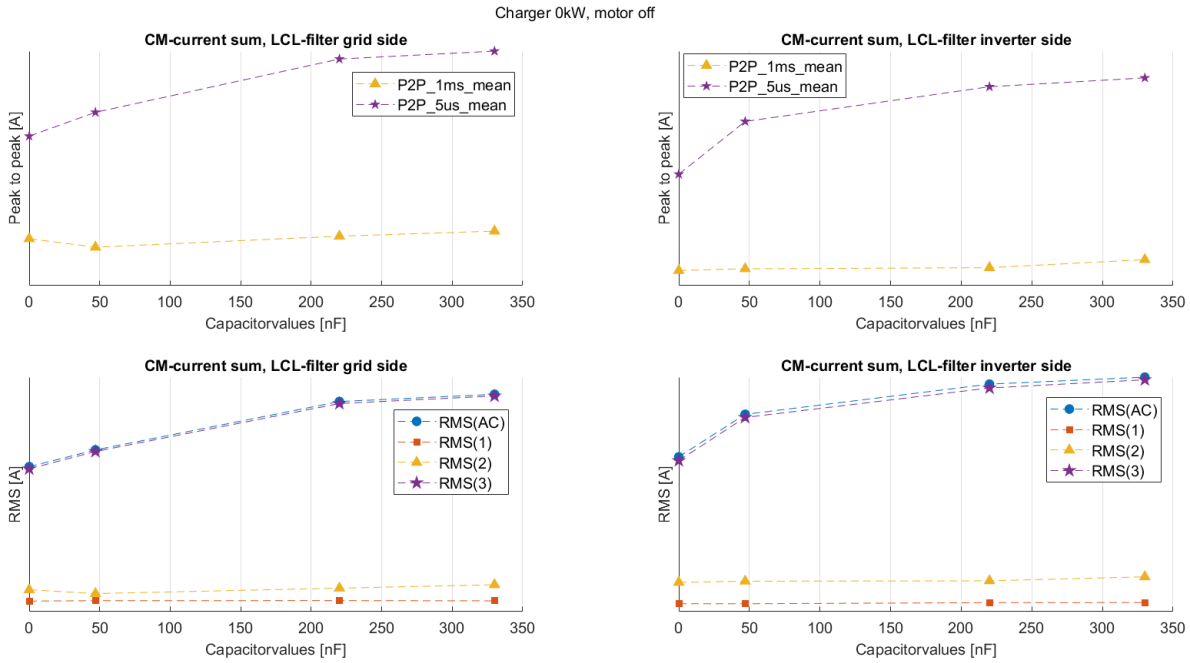

Figure A.27: RMS and peak-to-peak for the CM-currents with varying Y-capacitor filter before and after the LCL-filter. 0kW, motor off.

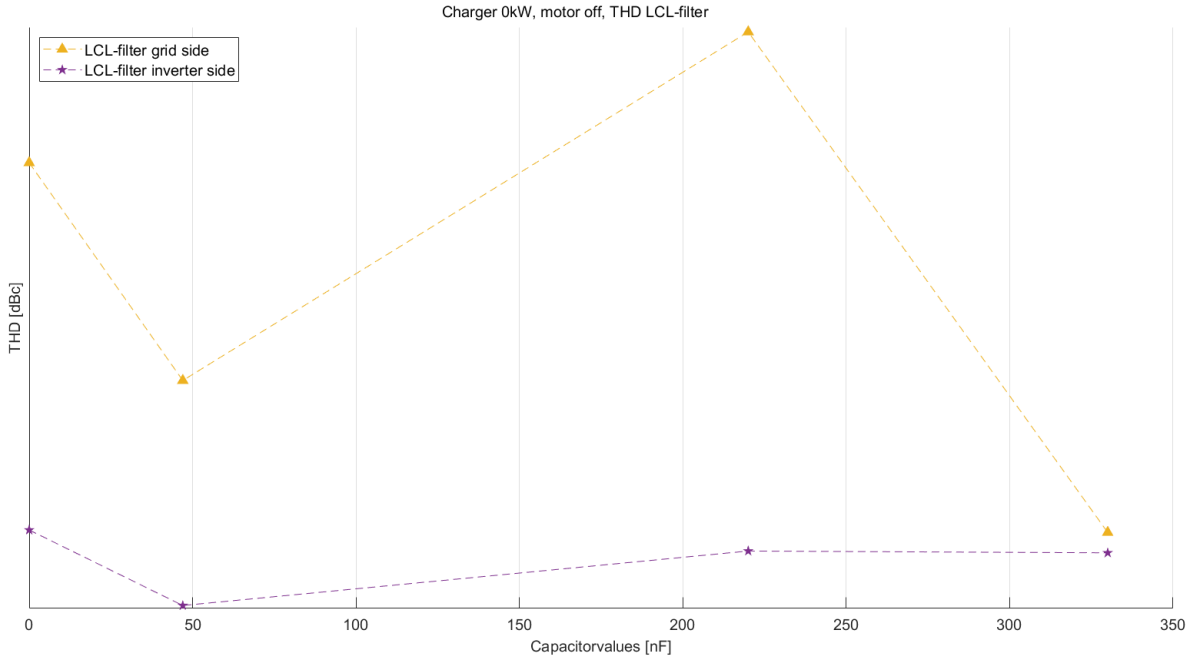

Figure A.28: THD before and after the LCL-filter, with varying Y-capacitor values. 0kW, motor off.

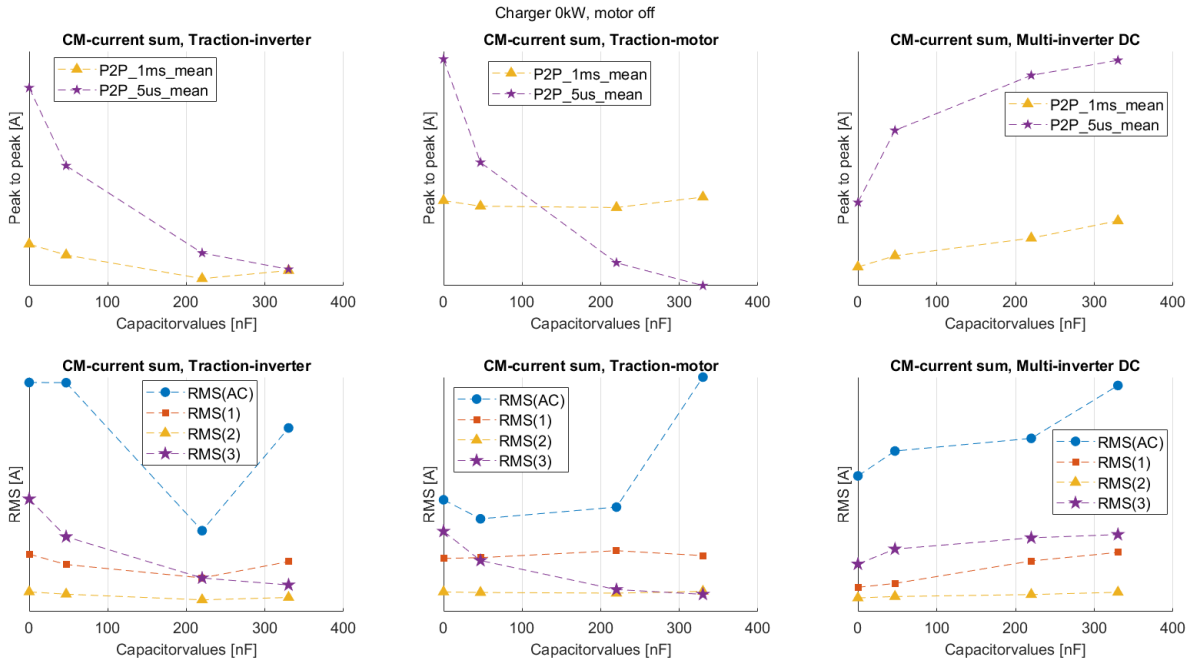

Figure A.29: RMS and peak-to-peak for the CM-currents with varying Y-capacitor filter and measuring points. 0kW, motor off.

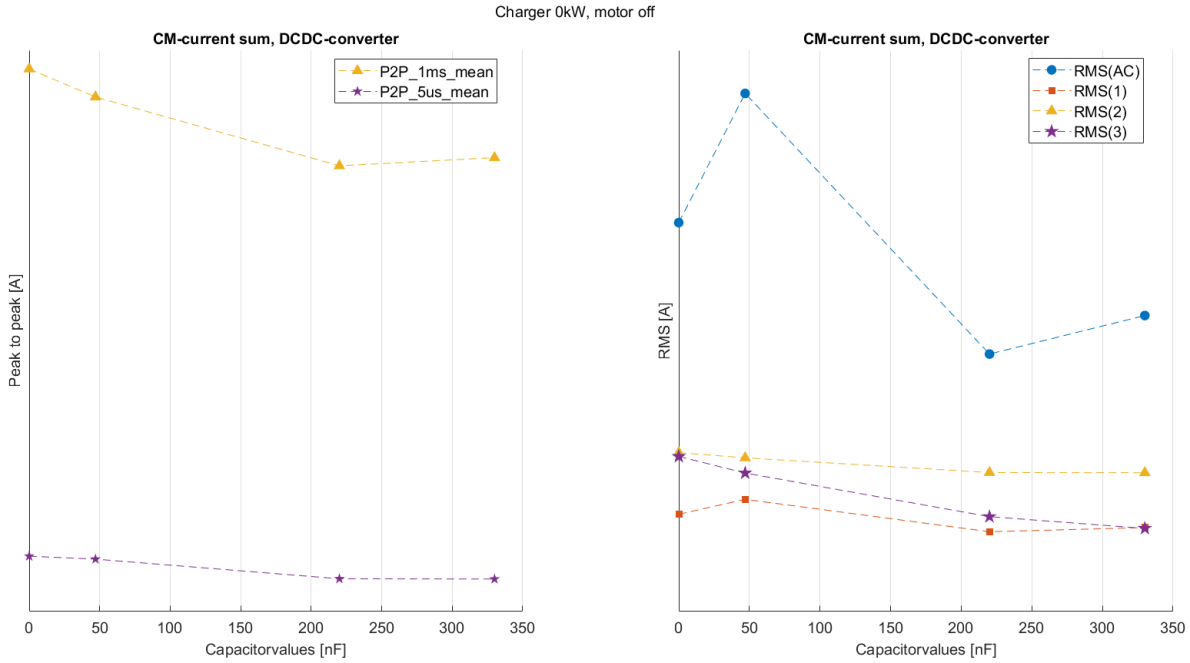

Figure A.30: RMS and peak-to-peak for the CM-currents in the DC/DC-converter with varying Y-capacitor filter. 0kW, motor off.

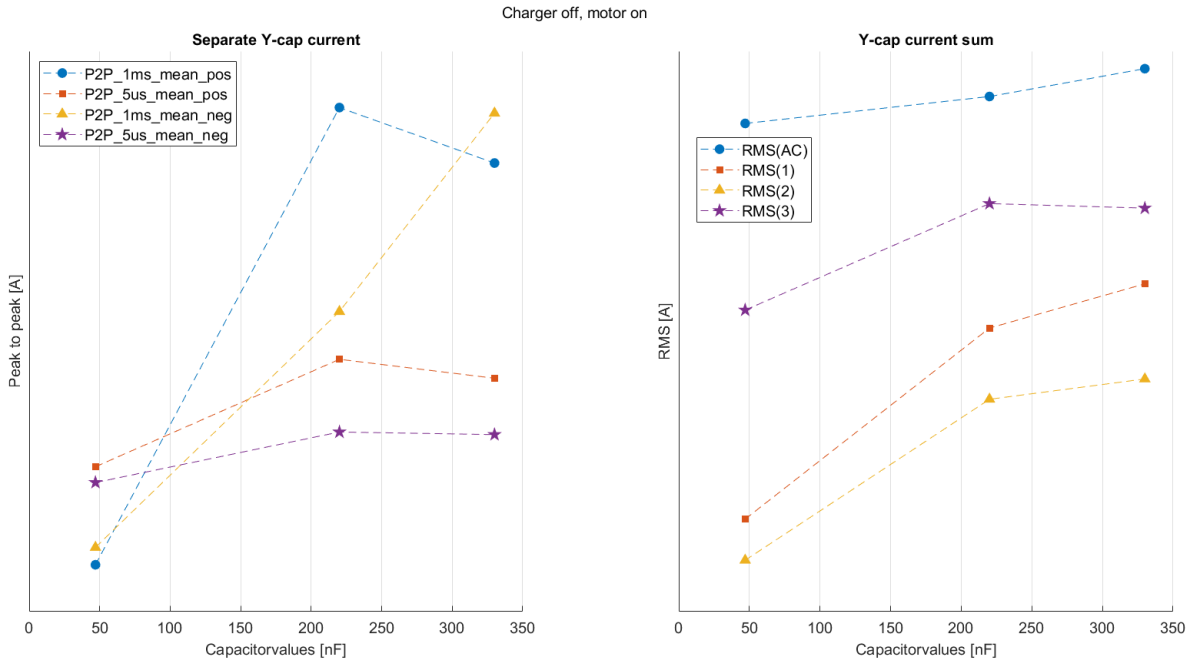

Figure A.31: RMS and peak-to-peak for the filtered Y-capacitor CM-current. off, motor on.

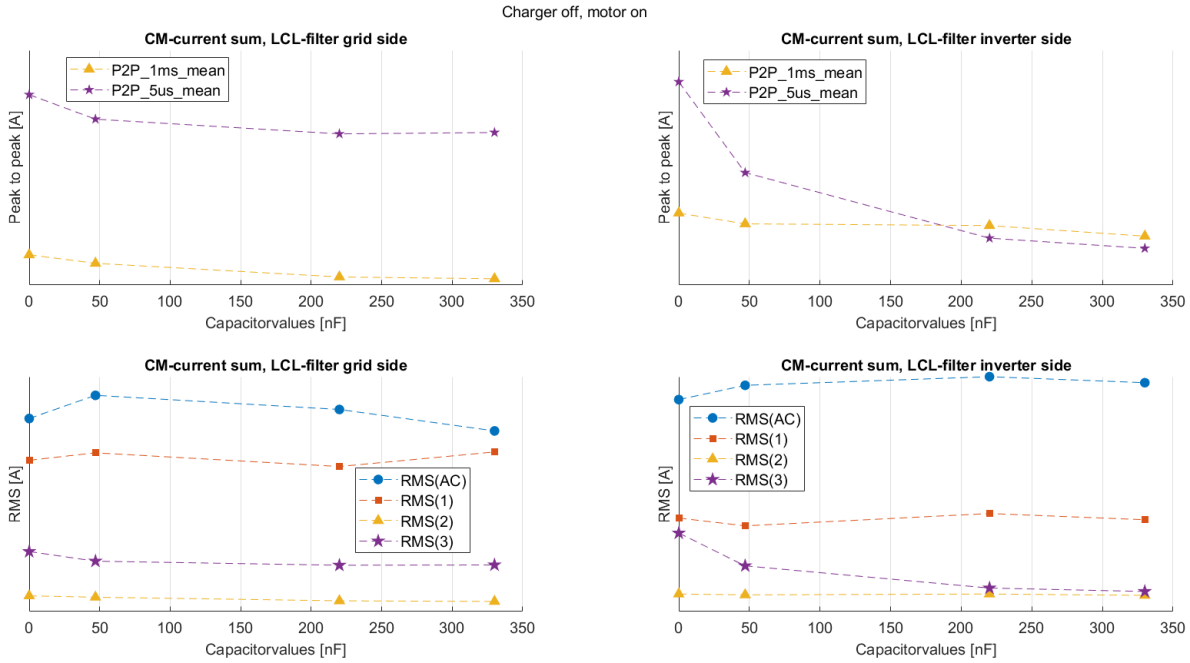

Figure A.32: RMS and peak-to-peak for the CM-currents with varying Y-capacitor filter before and after the LCL-filter. off, motor on.

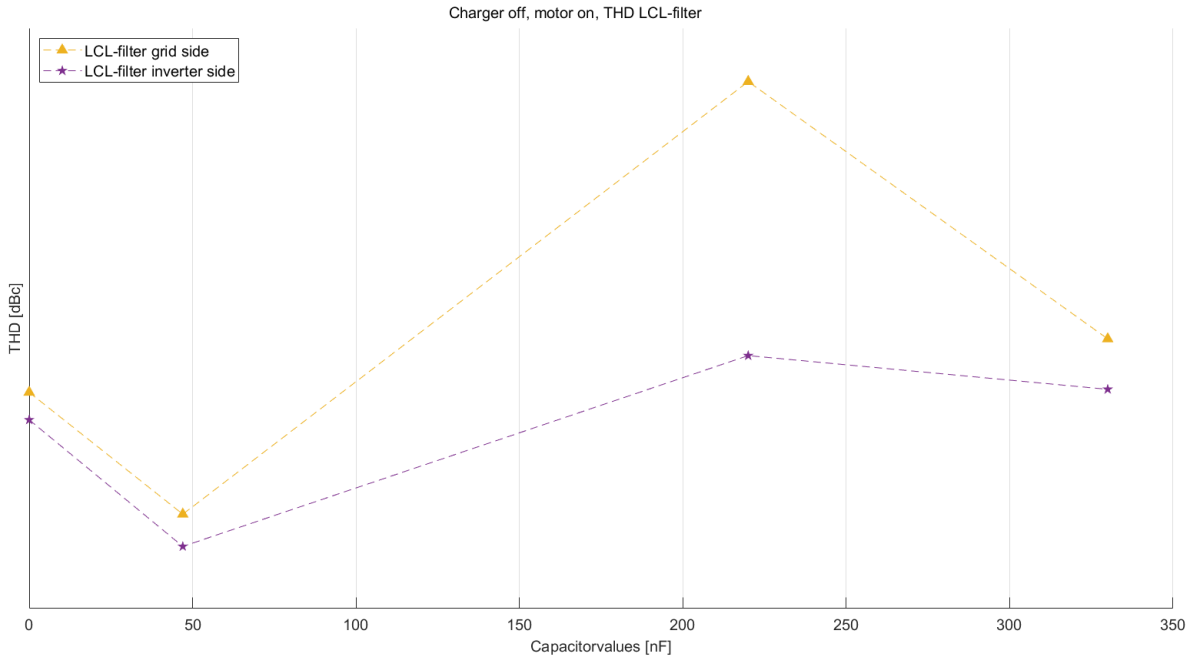

Figure A.33: THD before and after the LCL-filter, with varying Y-capacitor values. off, motor on.

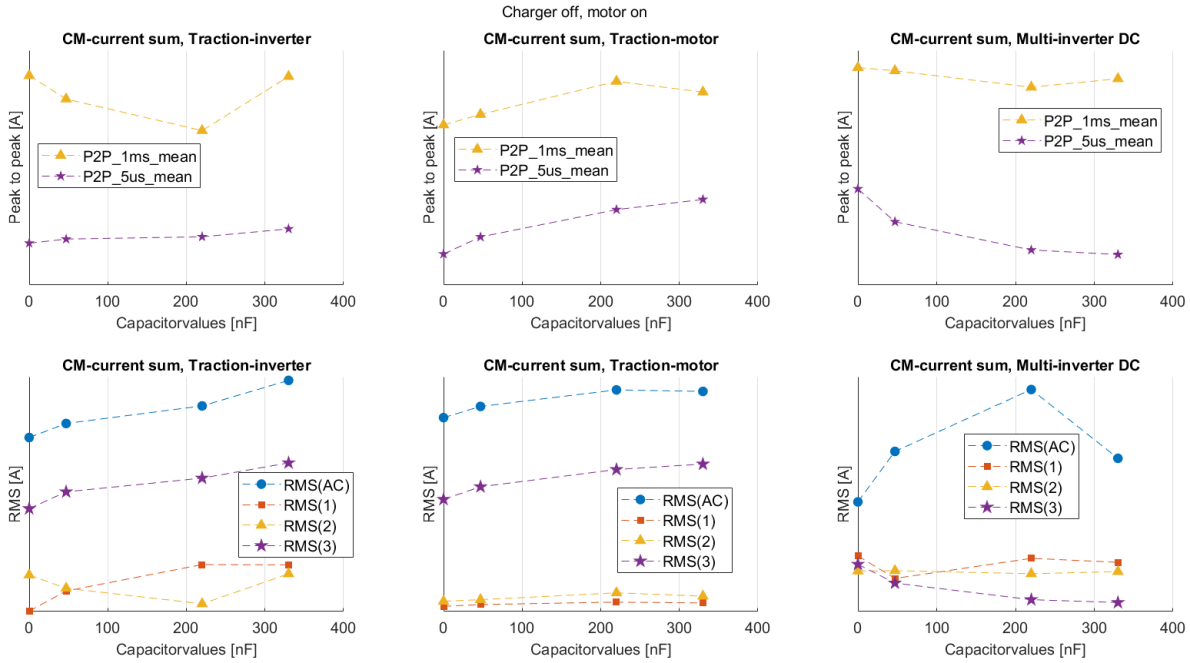

Figure A.34: RMS and peak-to-peak for the CM-currents with varying Y-capacitor filter and measuring points. off, motor on.

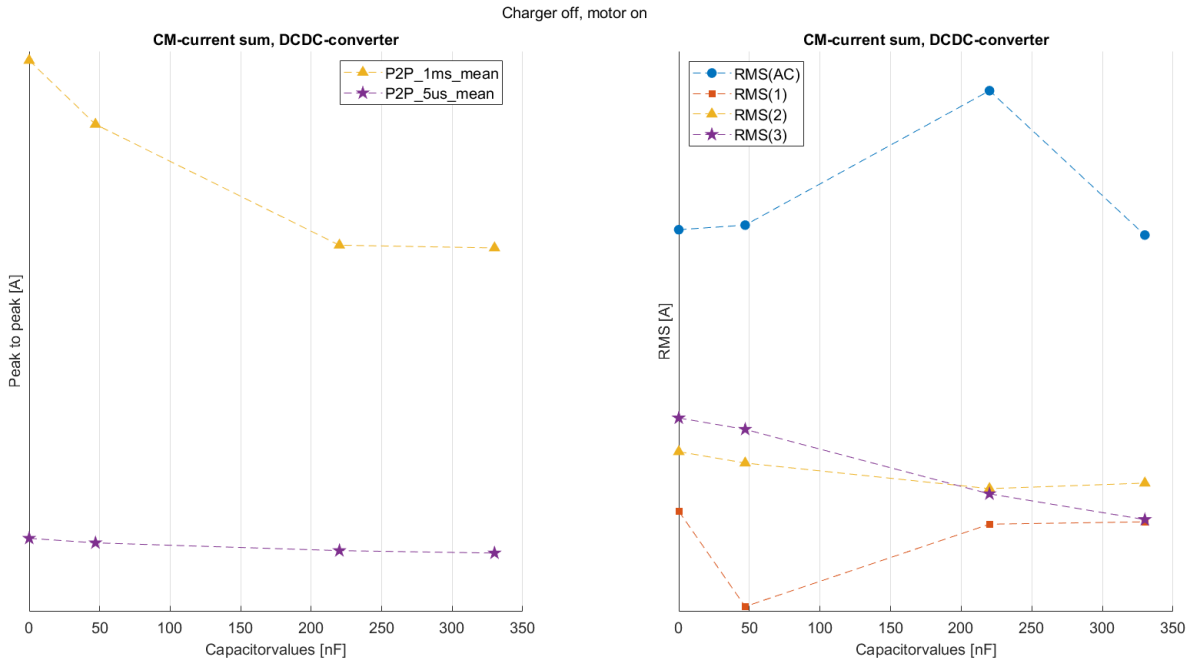

Figure A.35: RMS and peak-to-peak for the CM-currents in the DC/DC-converter with varying Y-capacitor filter. off, motor on.

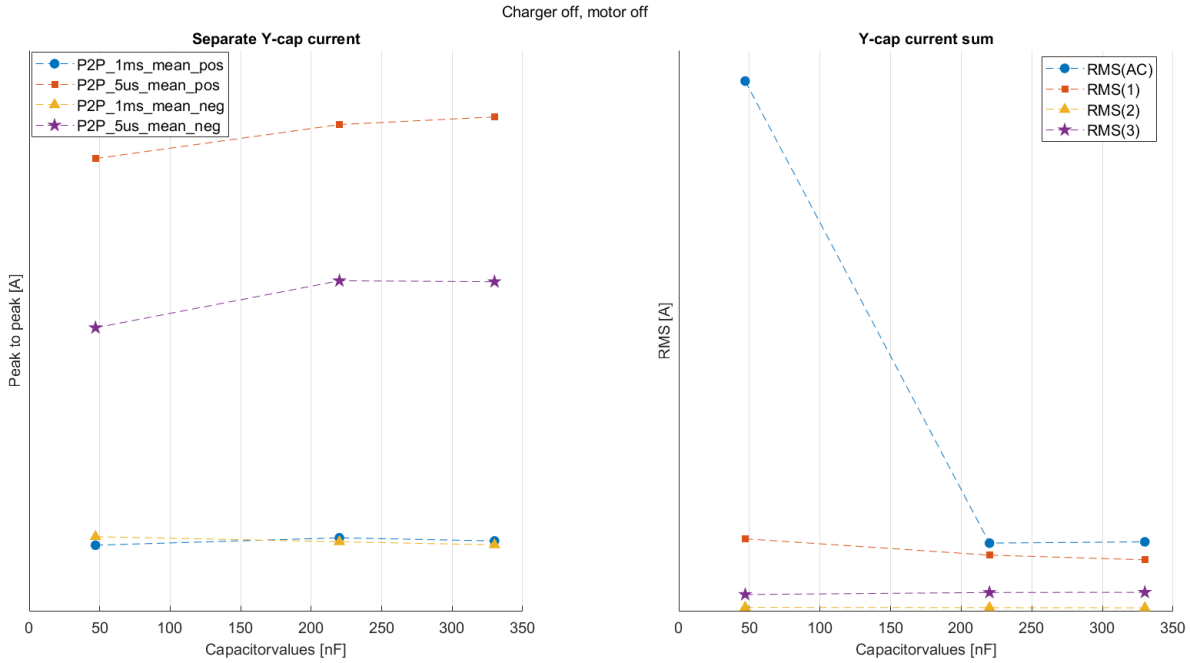

Figure A.36: RMS and peak-to-peak for the filtered Y-capacitor CM-current. off, motor off.

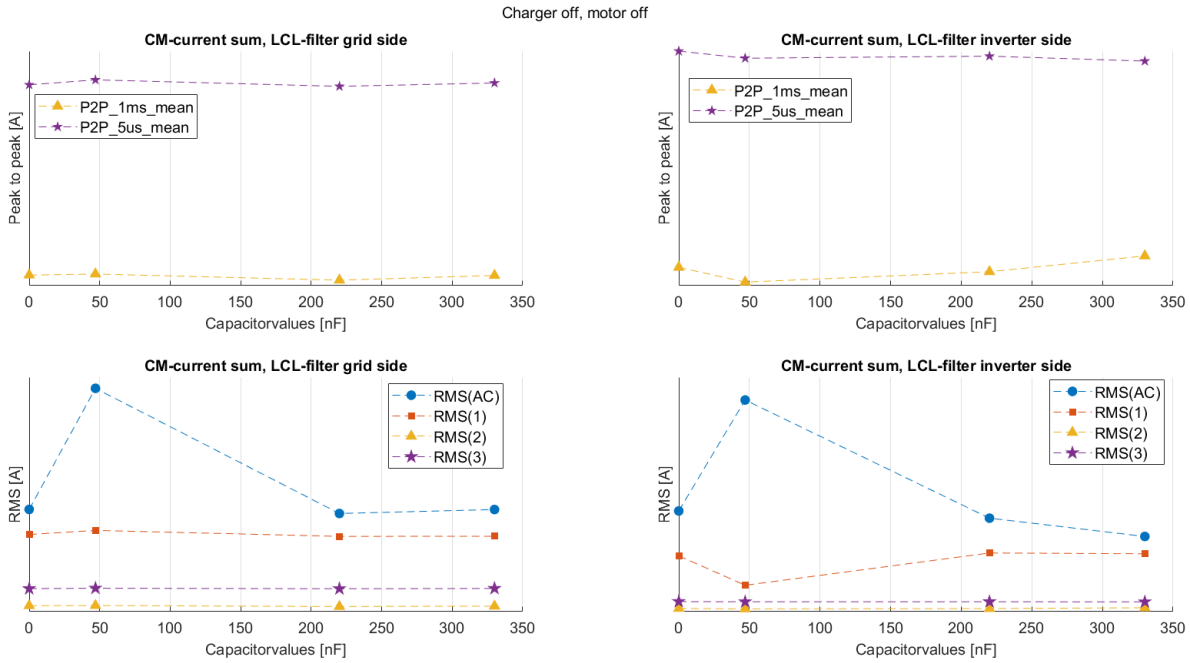

Figure A.37: RMS and peak-to-peak for the CM-currents with varying Y-capacitor filter before and after the LCL-filter. off, motor off.

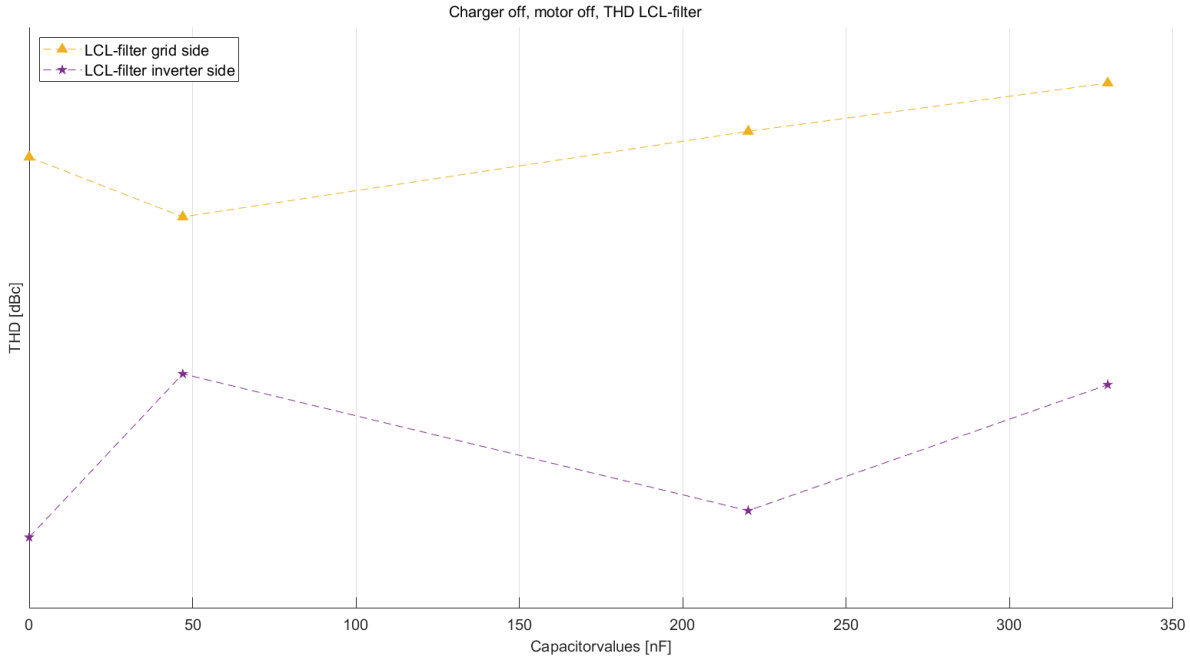

Figure A.38: THD before and after the LCL-filter, with varying Y-capacitor values. off, motor off.

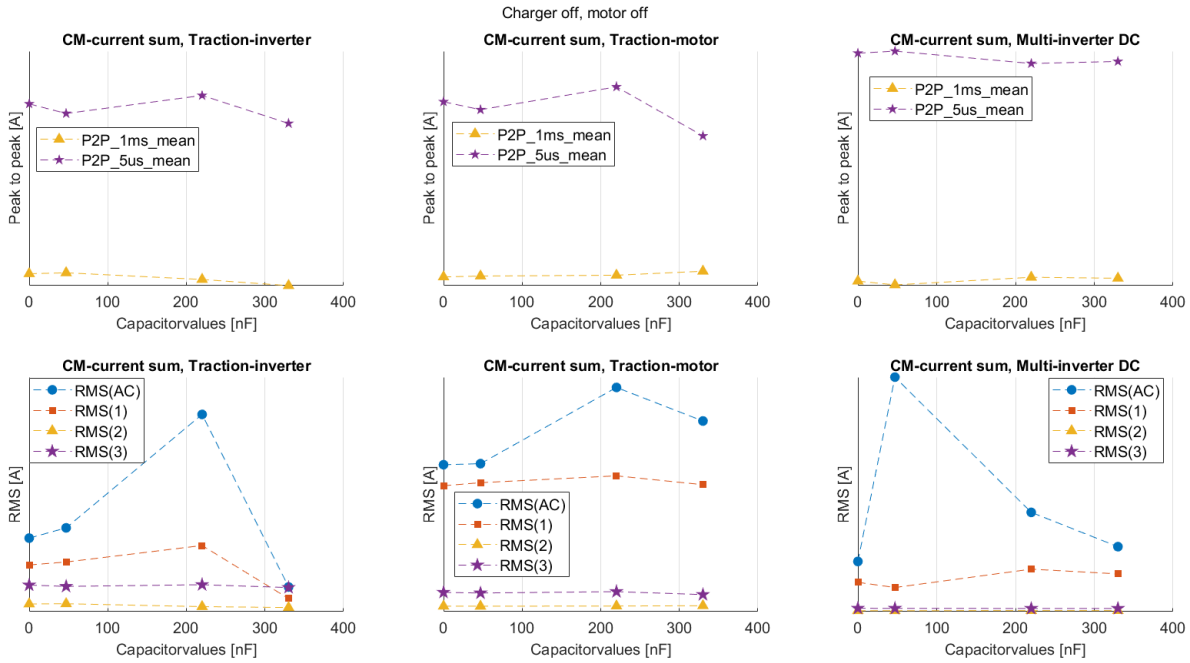

Figure A.39: RMS and peak-to-peak for the CM-currents with varying Y-capacitor filter and measuring points. off, motor off.

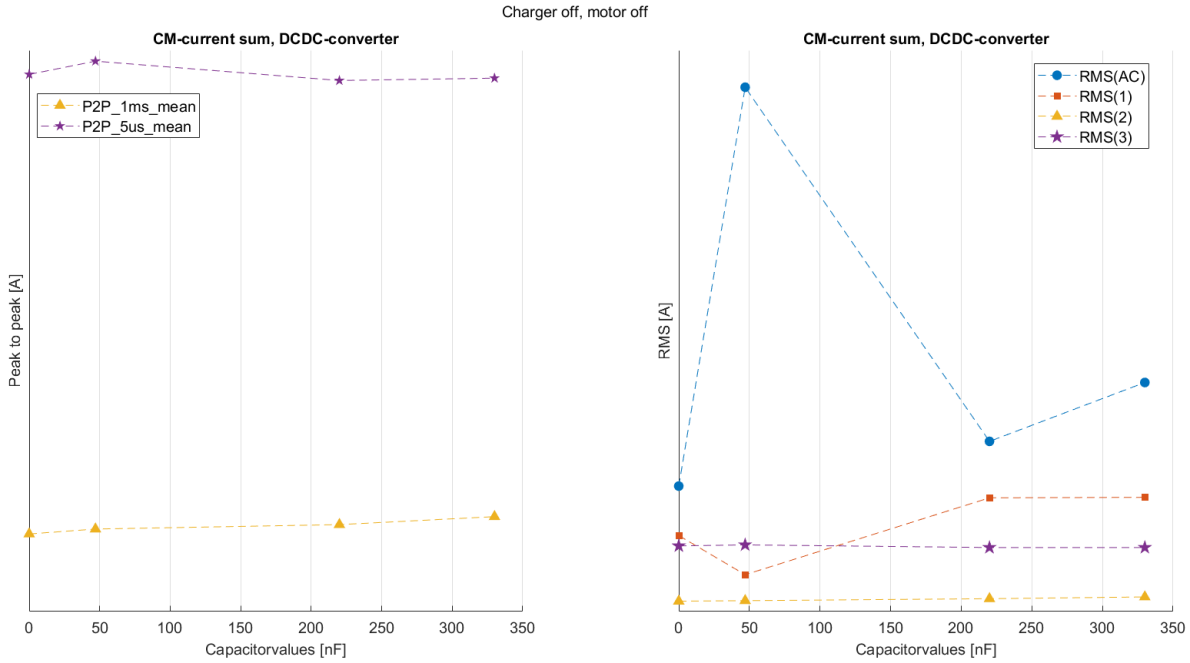

Figure A.40: RMS and peak-to-peak for the CM-currents in the DC/DC-converter with varying Y-capacitor filter. off, motor off.

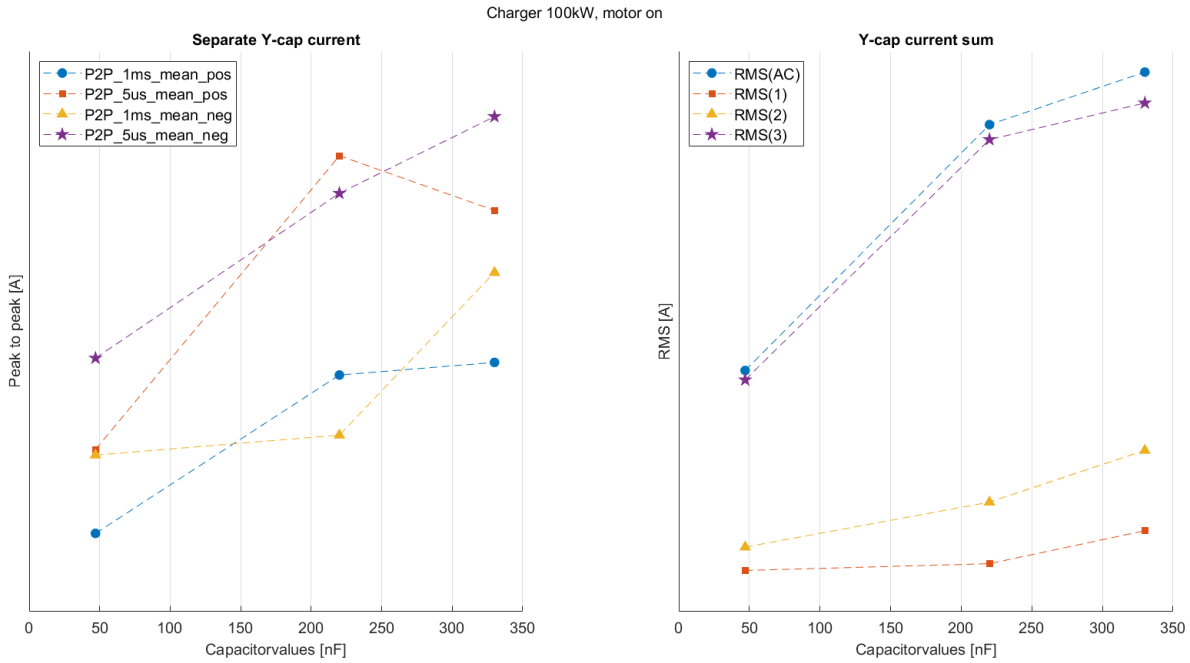

Figure A.41: RMS and peak-to-peak for the filtered Y-capacitor CM-current. 100kW, motor on.

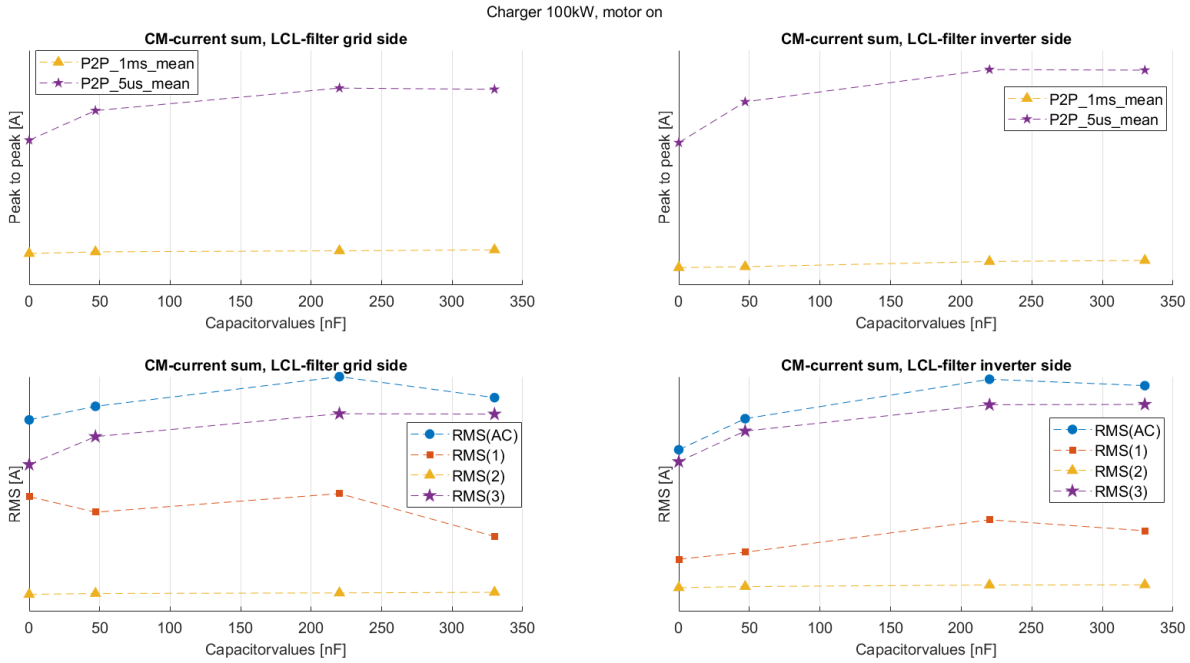

Figure A.42: RMS and peak-to-peak for the CM-currents with varying Y-capacitor filter before and after the LCL-filter. 100kW, motor on.

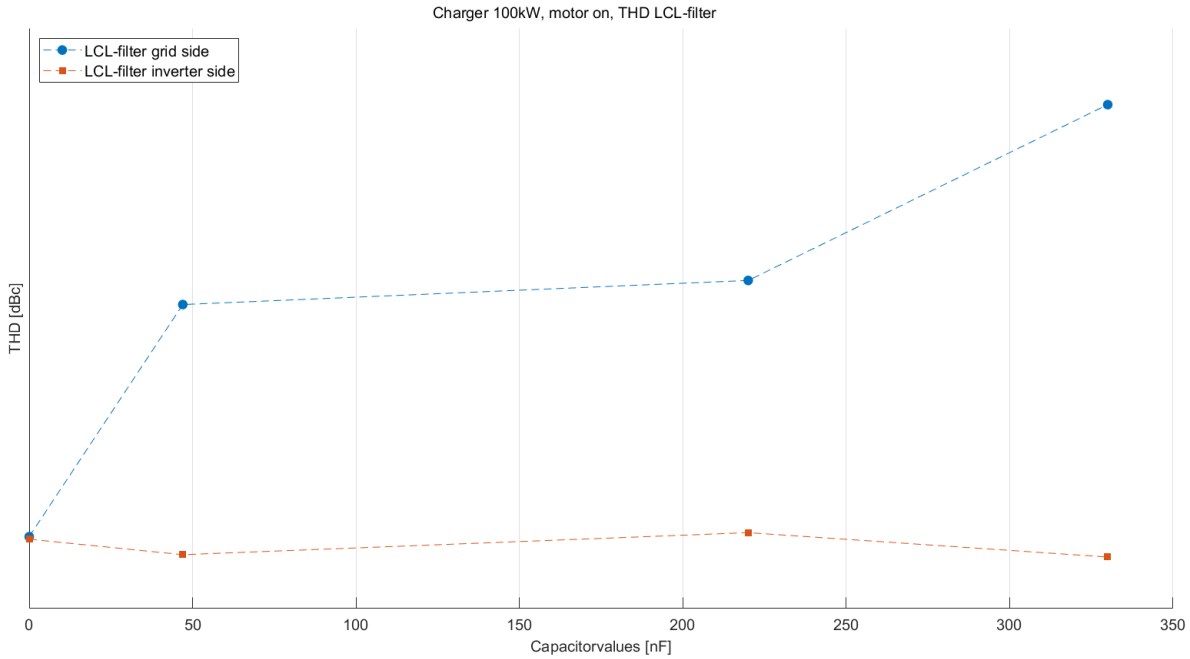

Figure A.43: THD before and after the LCL-filter, with varying Y-capacitor values. 100kW, motor on.

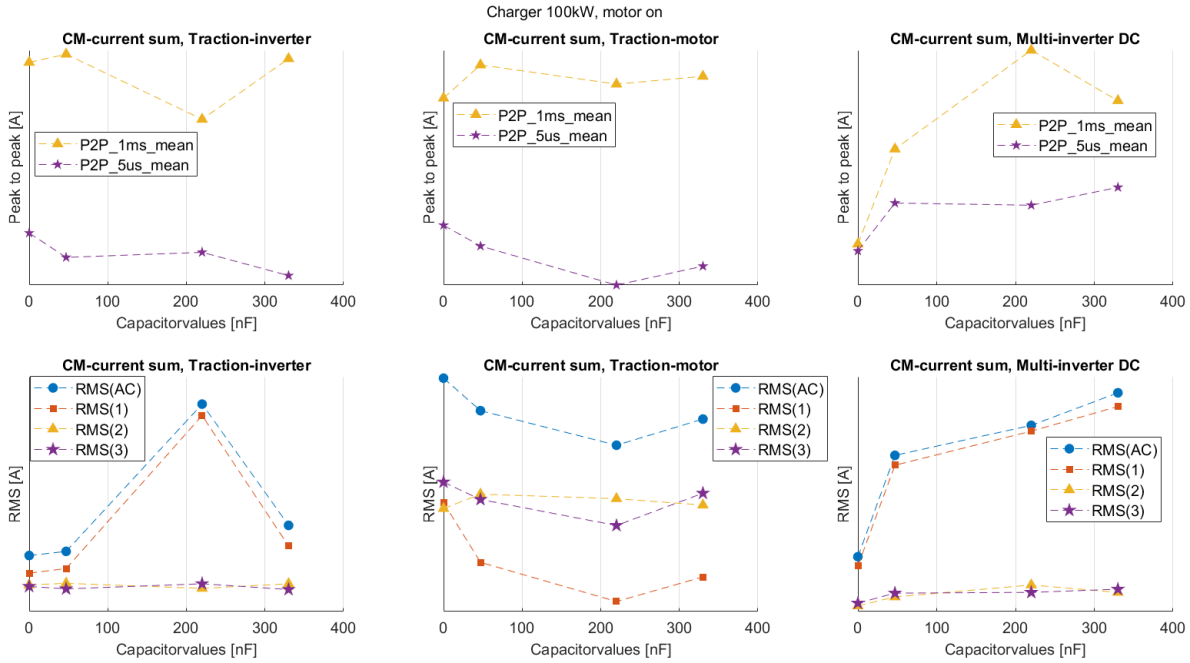

Figure A.44: RMS and peak-to-peak for the CM-currents with varying Y-capacitor filter and measuring points. 100kW, motor on.

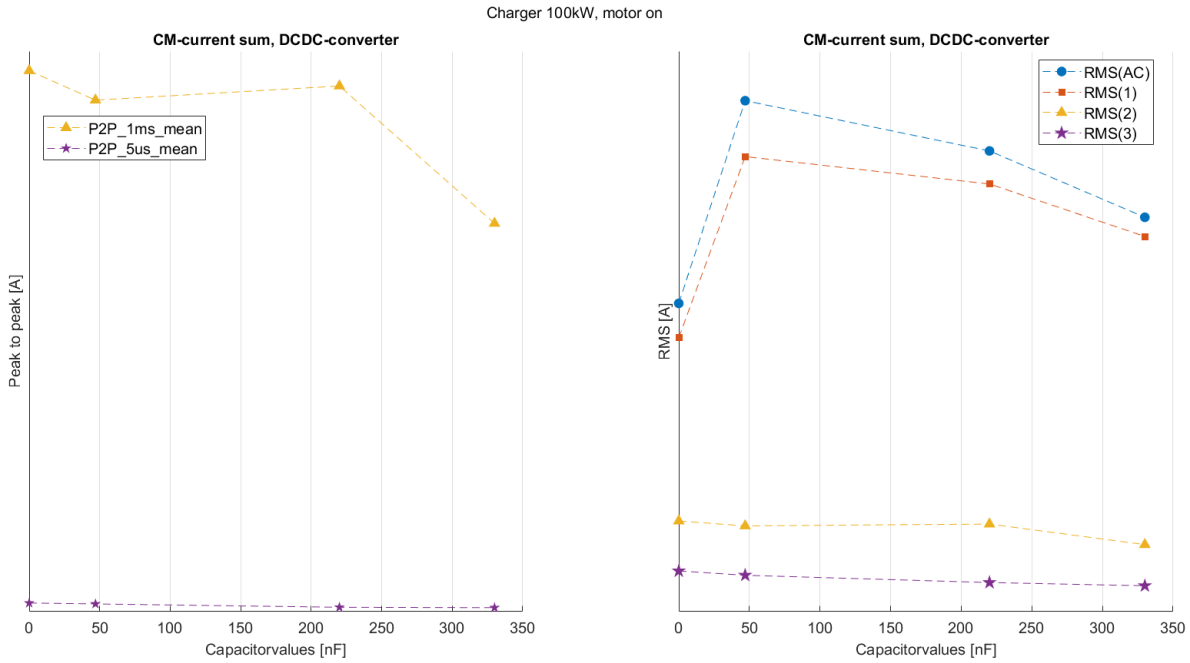

Figure A.45: RMS and peak-to-peak for the CM-currents in the DC/DC-converter with varying Y-capacitor filter. 100kW, motor on.

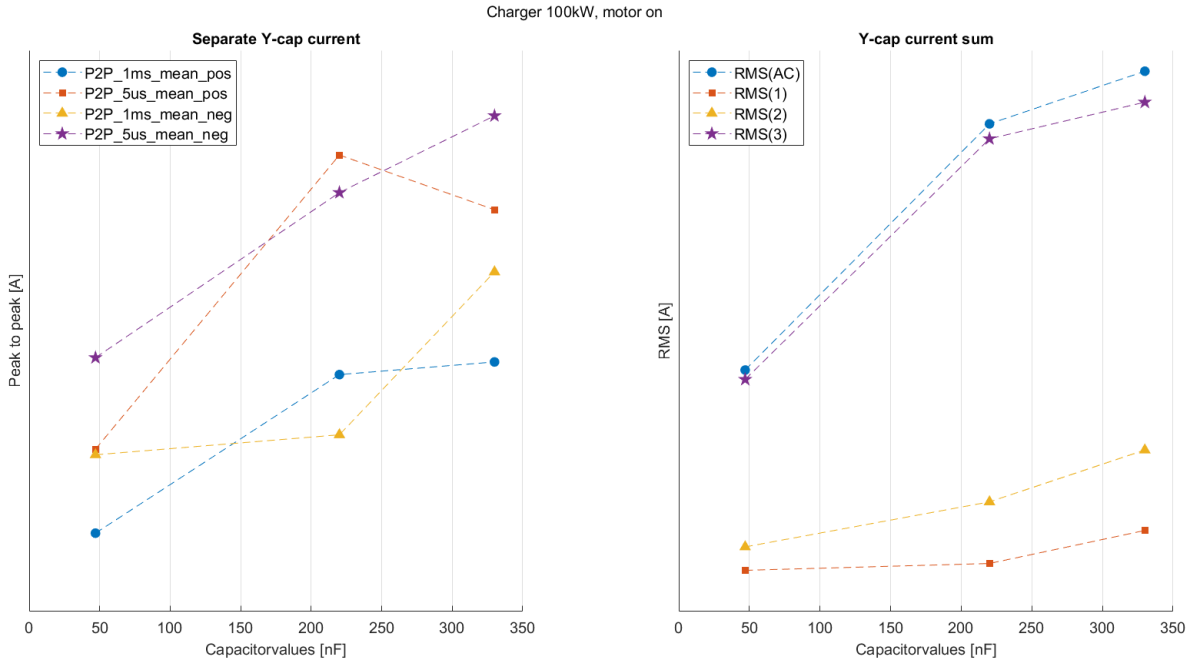

Figure A.46: RMS and peak-to-peak for the filtered Y-capacitor CM-current. 100kW, motor on.

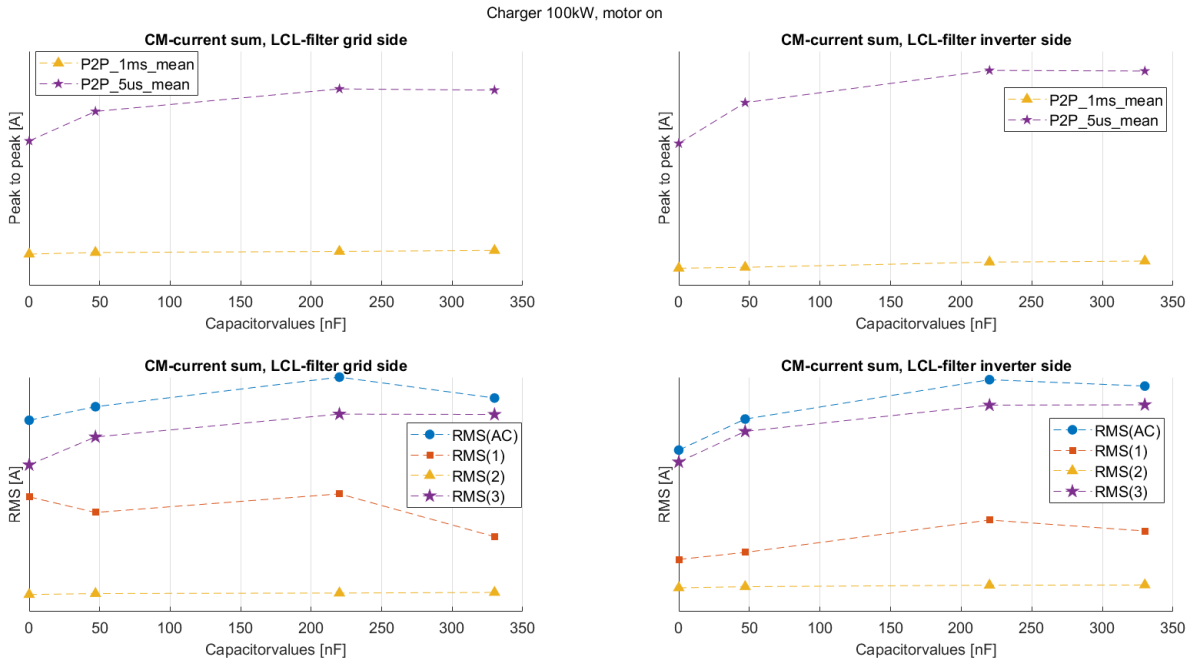

Figure A.47: RMS and peak-to-peak for the CM-currents with varying Y-capacitor filter before and after the LCL-filter. 100kW, motor on.

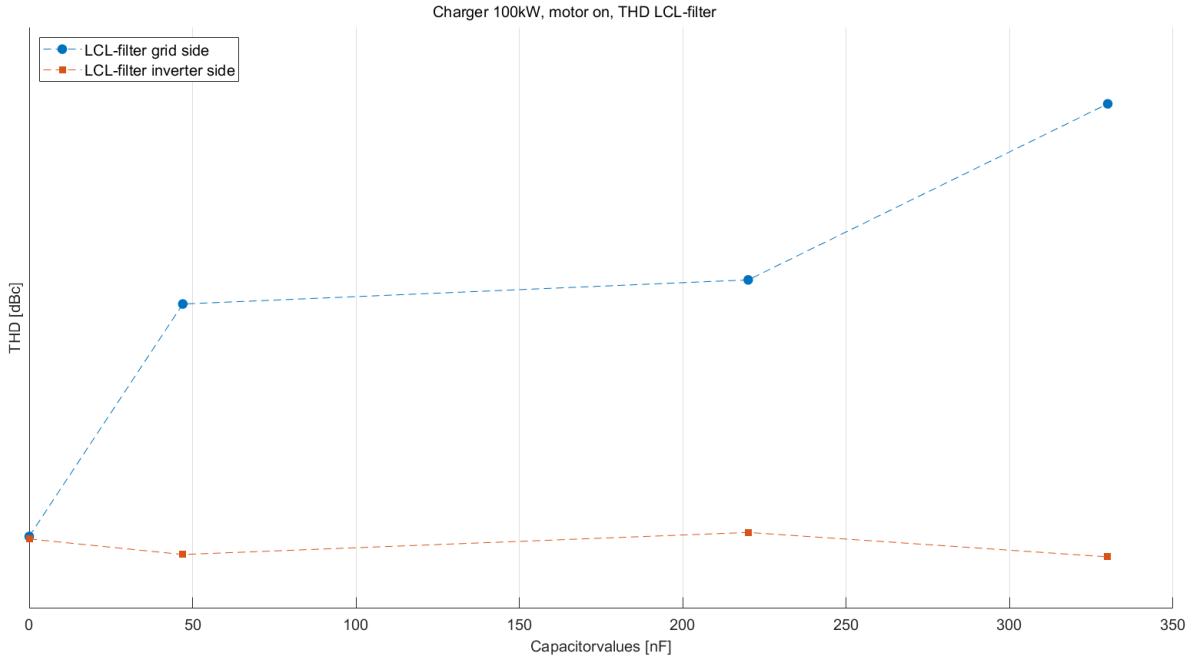

Figure A.48: THD before and after the LCL-filter, with varying Y-capacitor values. 100kW, motor on.

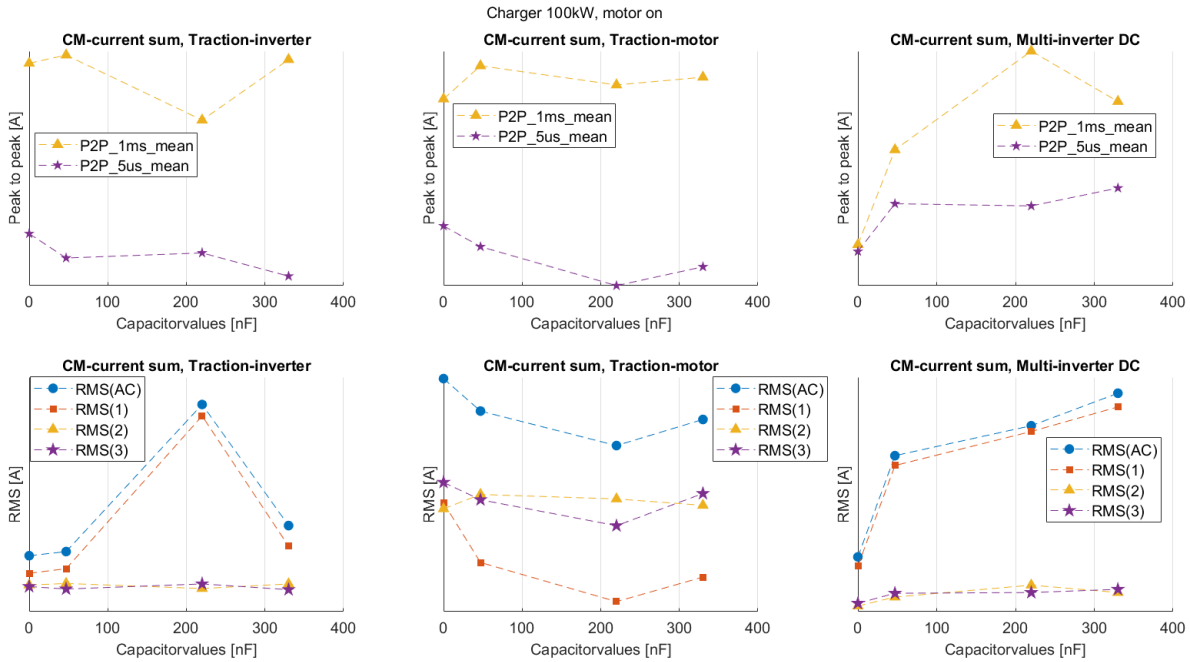

Figure A.49: RMS and peak-to-peak for the CM-currents with varying Y-capacitor filter and measuring points. 100kW, motor on.

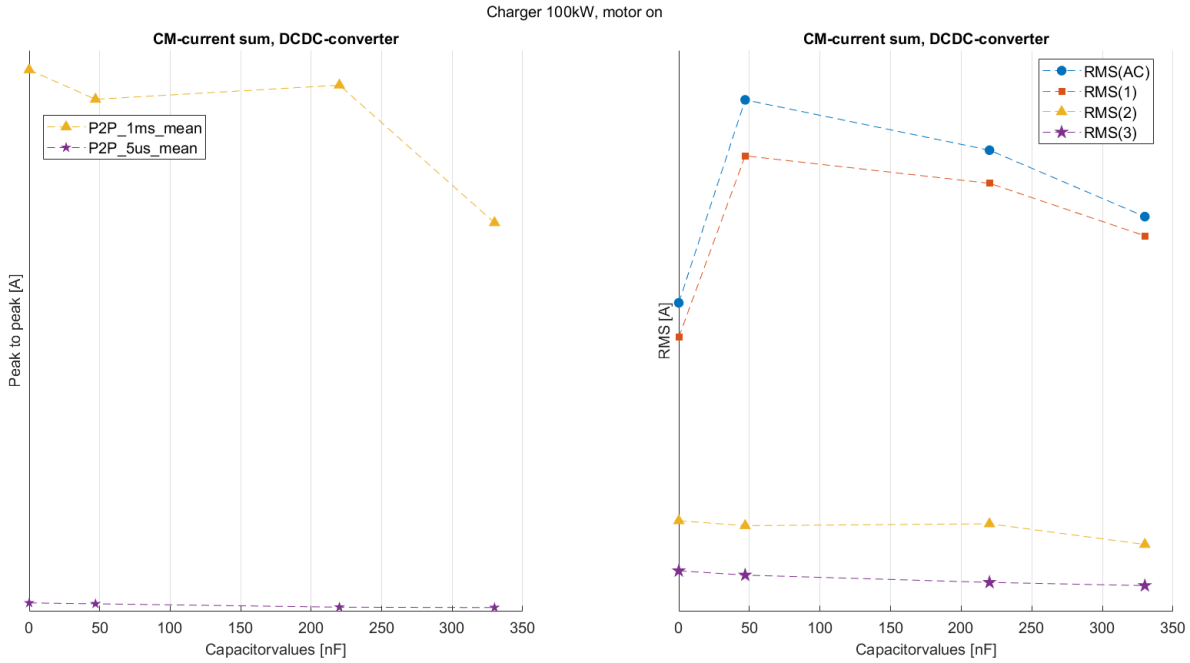

Figure A.50: RMS and peak-to-peak for the CM-currents in the DC/DC-converter with varying Y-capacitor filter. 100kW, motor on.

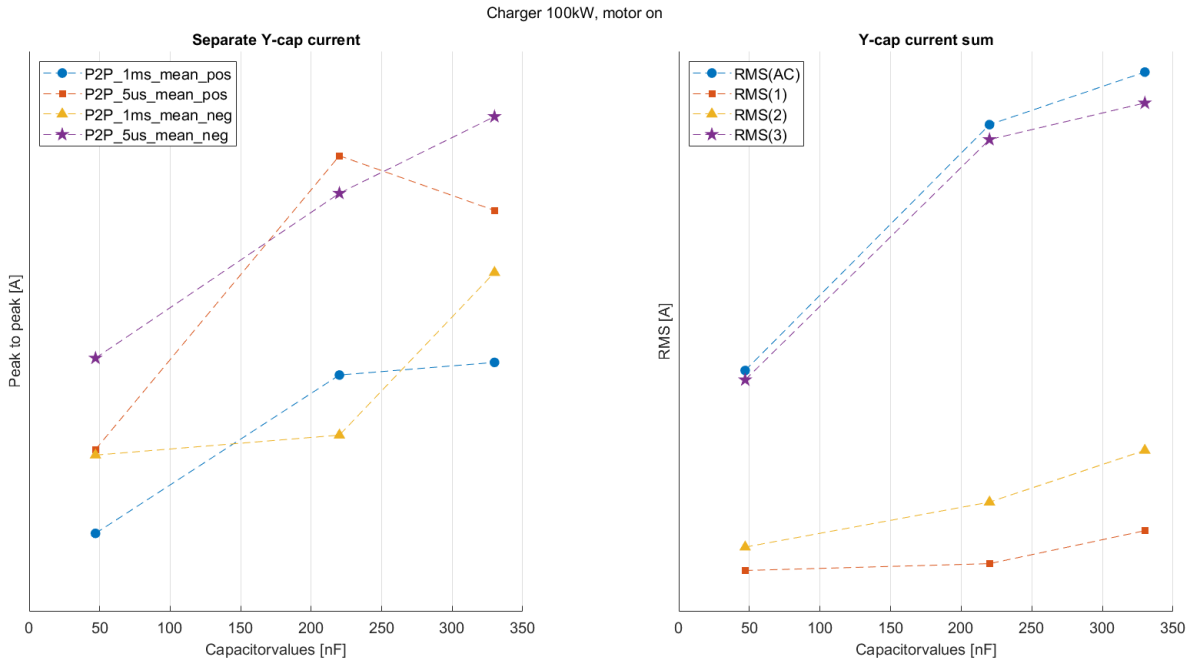

Figure A.51: RMS and peak-to-peak for the filtered Y-capacitor CM-current. 100kW, motor on.

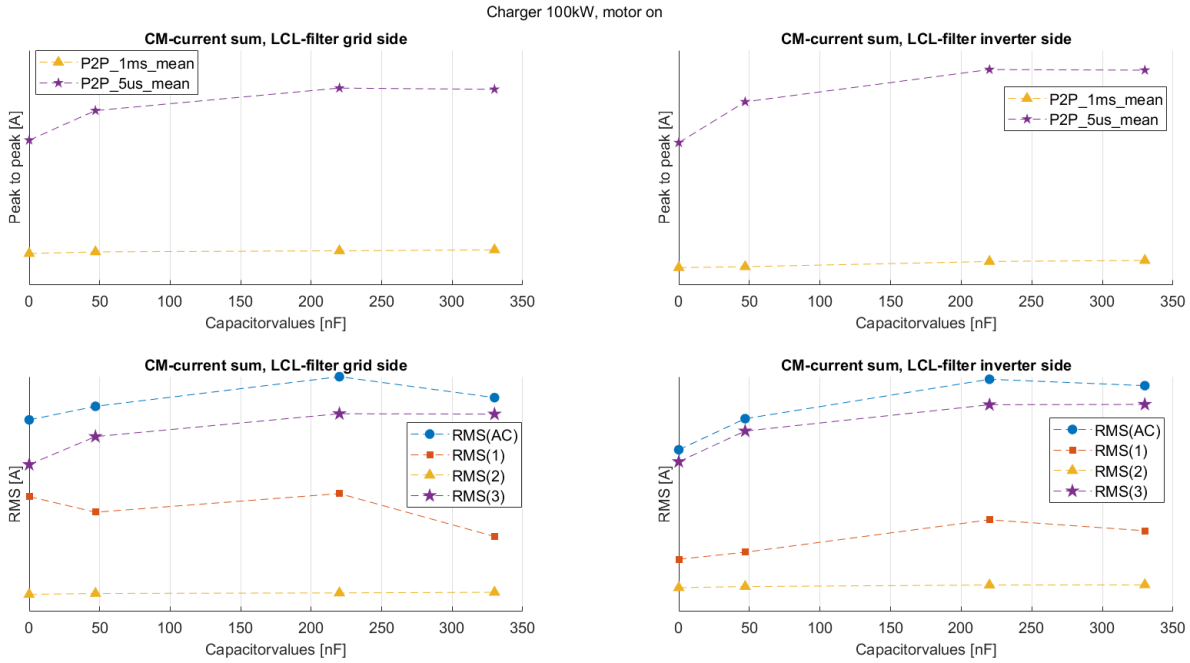

Figure A.52: RMS and peak-to-peak for the CM-currents with varying Y-capacitor filter before and after the LCL-filter. 100kW, motor on.

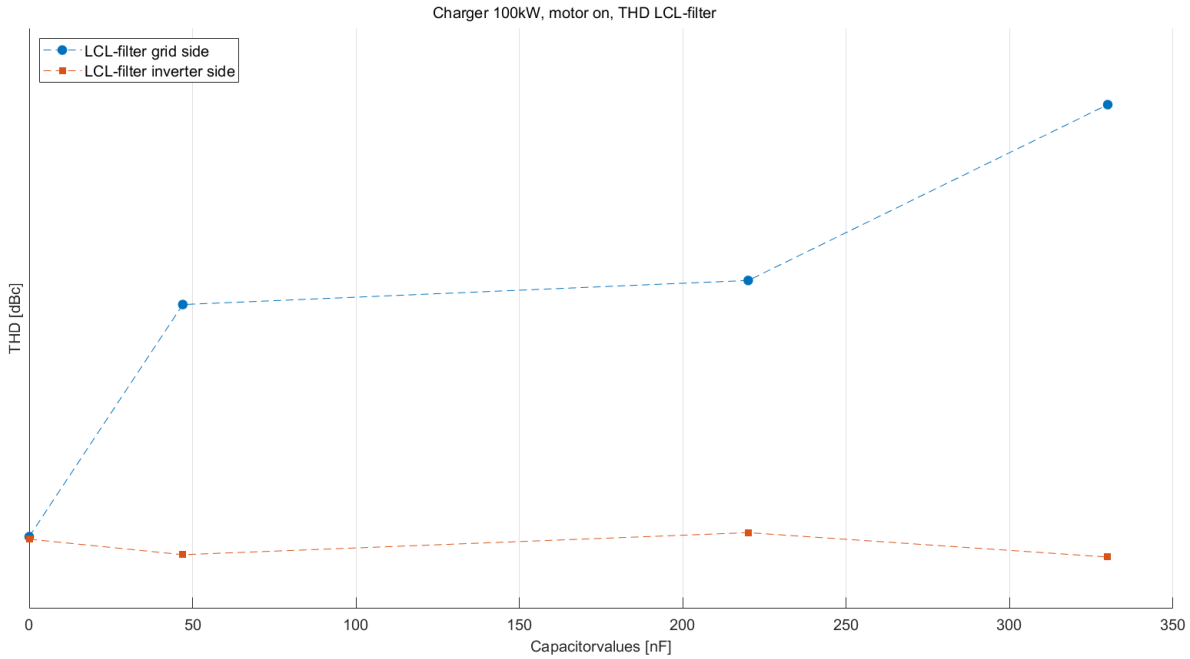

Figure A.53: THD before and after the LCL-filter, with varying Y-capacitor values. 100kW, motor on.

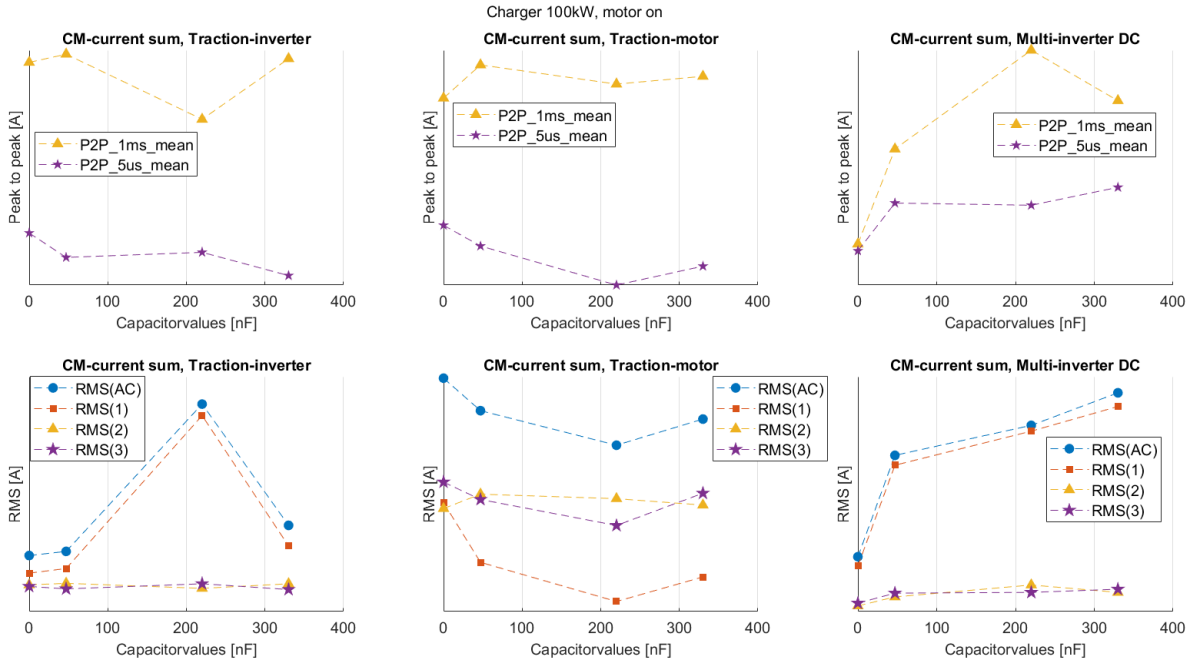

Figure A.54: RMS and peak-to-peak for the CM-currents with varying Y-capacitor filter and measuring points. 100kW, motor on.

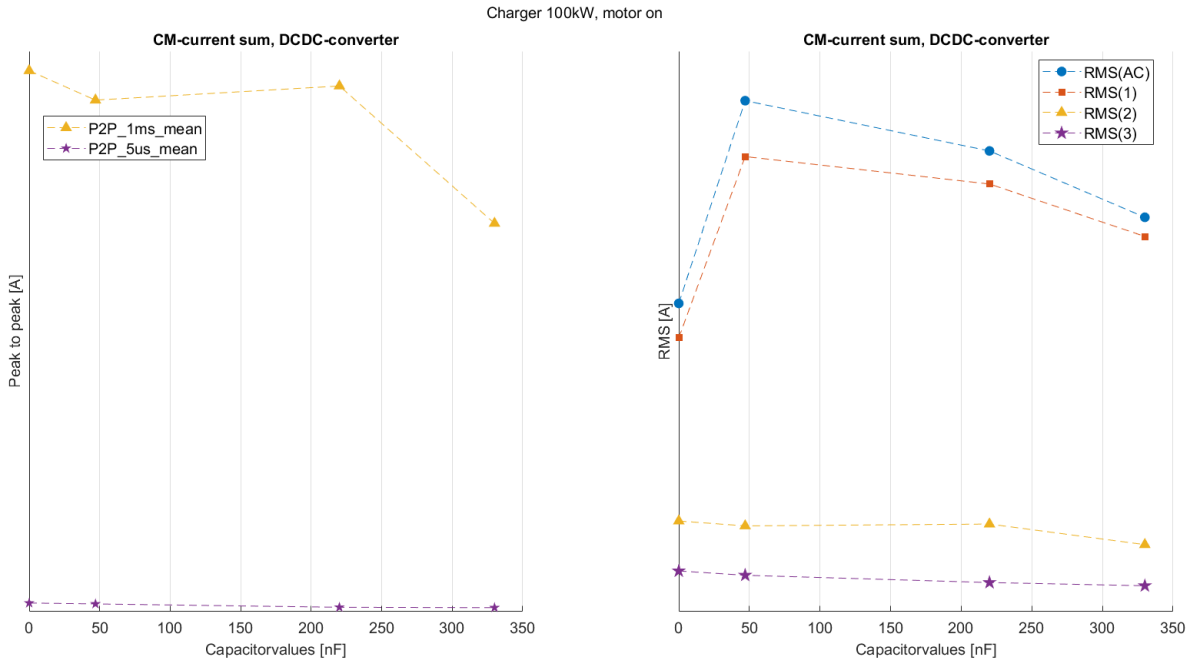

Figure A.55: RMS and peak-to-peak for the CM-currents in the DC/DC-converter with varying Y-capacitor filter. 100kW, motor on.

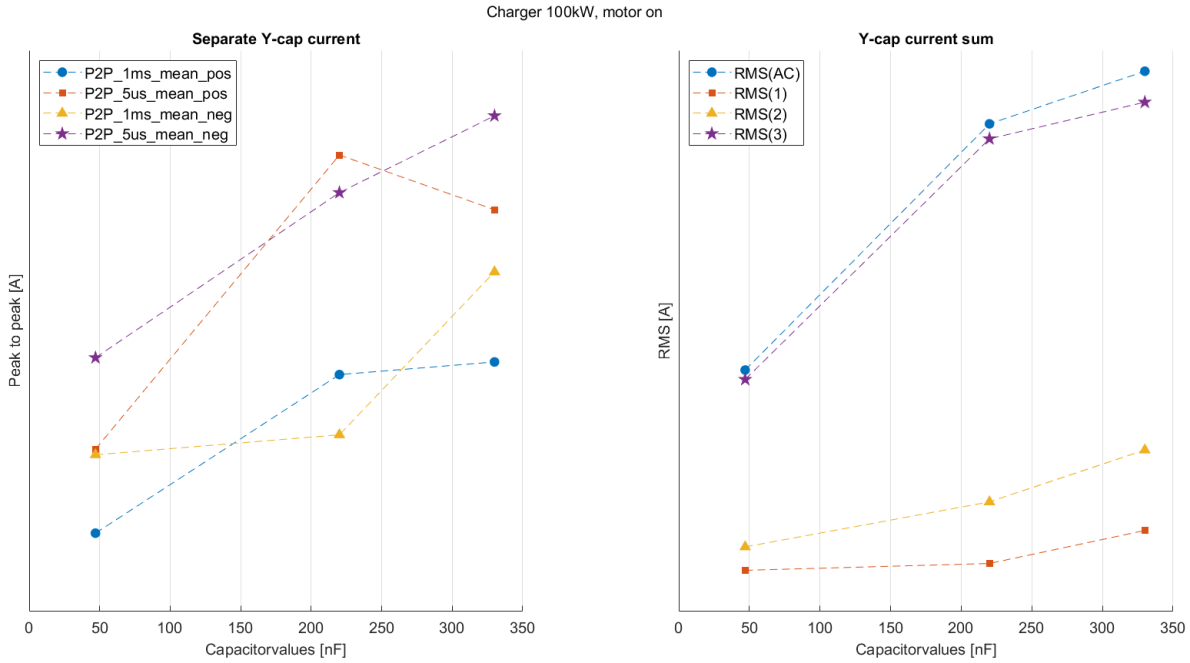

Figure A.56: RMS and peak-to-peak for the filtered Y-capacitor CM-current. 100kW, motor on.

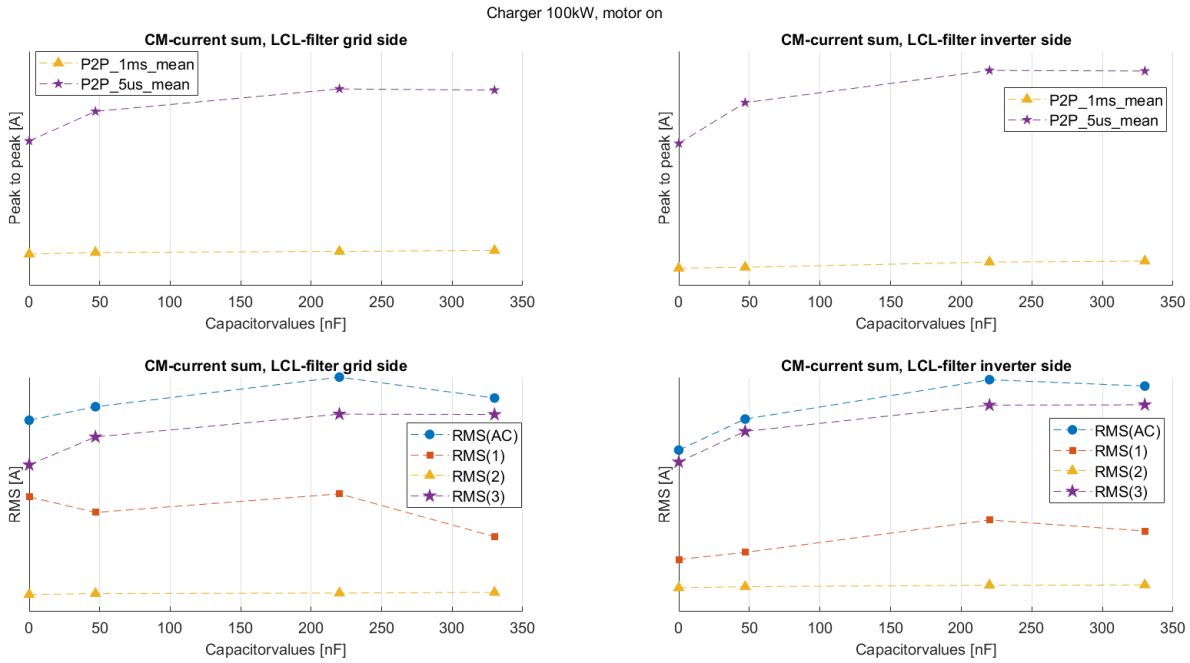

Figure A.57: RMS and peak-to-peak for the CM-currents with varying Y-capacitor filter before and after the LCL-filter. 100kW, motor on.

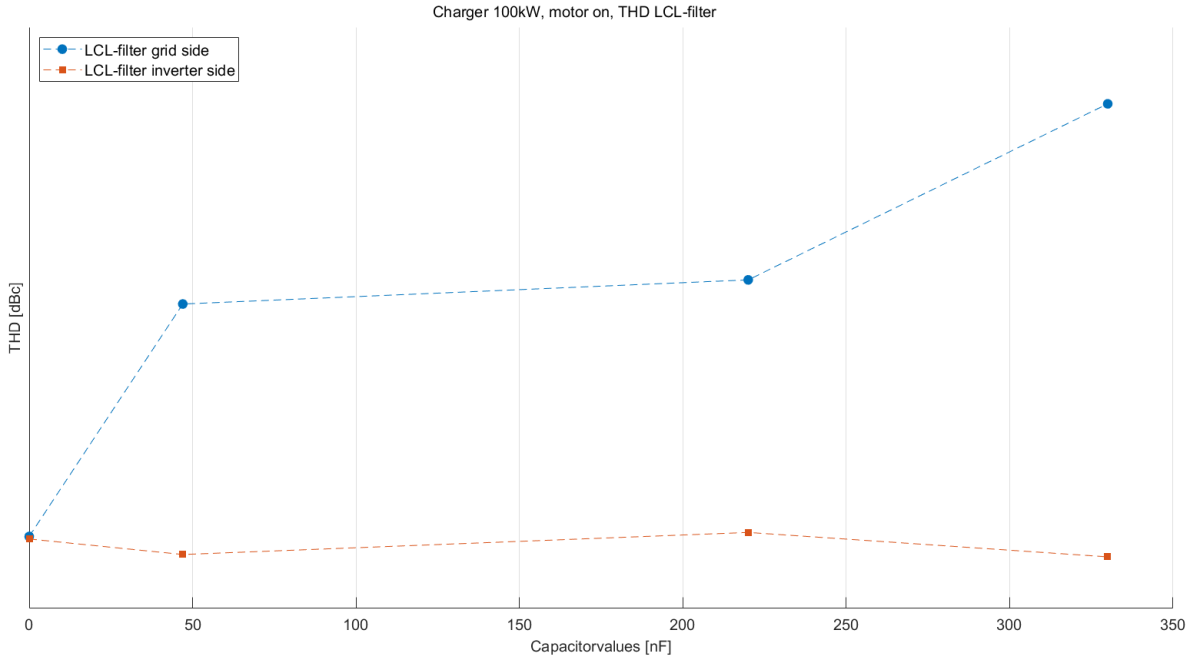

Figure A.58: THD before and after the LCL-filter, with varying Y-capacitor values. 100kW, motor on.

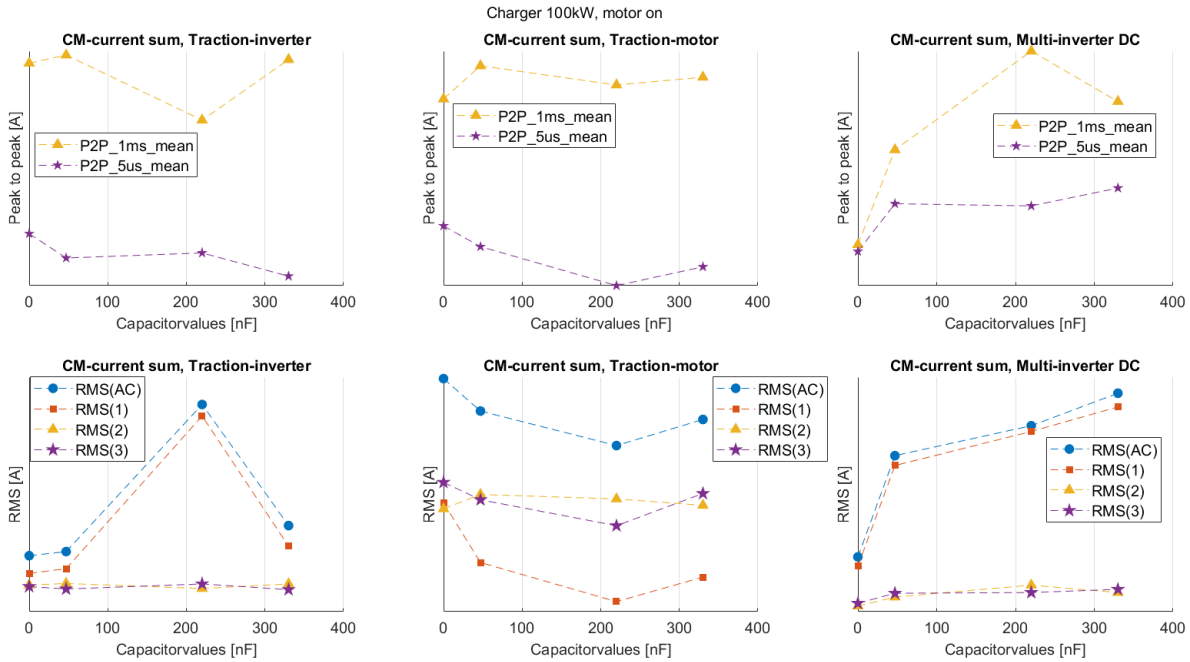

Figure A.59: RMS and peak-to-peak for the CM-currents with varying Y-capacitor filter and measuring points. 100kW, motor on.

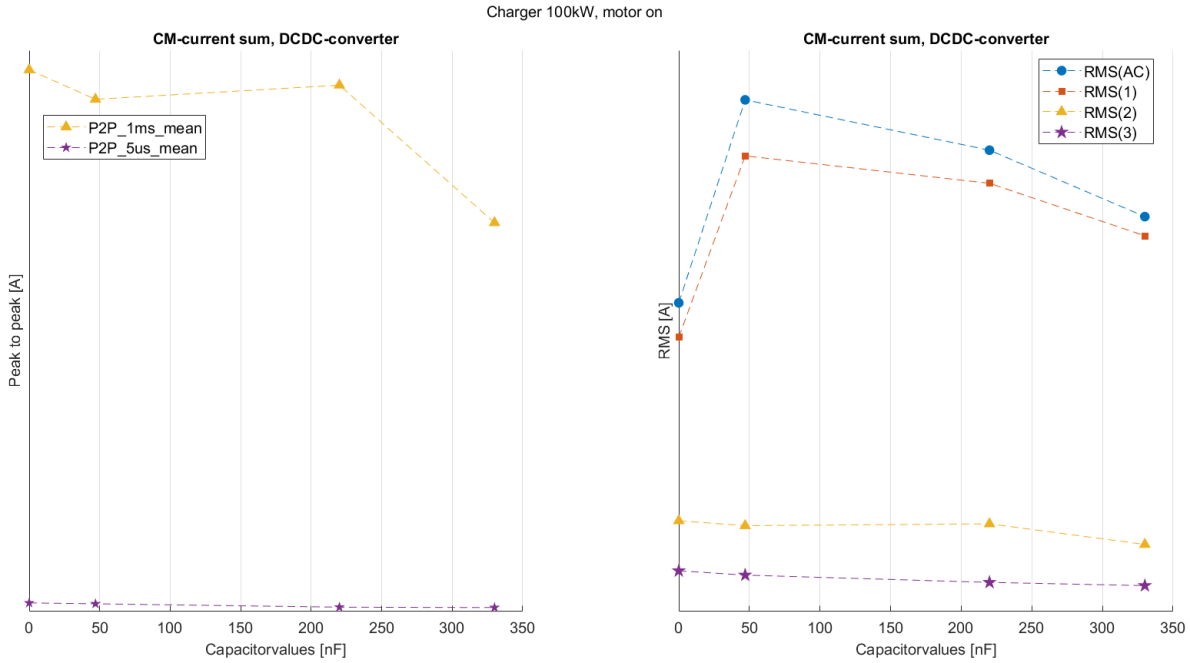

Figure A.60: RMS and peak-to-peak for the CM-currents in the DC/DC-converter with varying Y-capacitor filter. 100kW, motor on.

DEPARTMENT OF SOME SUBJECT OR TECHNOLOGY
CHALMERS UNIVERSITY OF TECHNOLOGY
Gothenburg, Sweden
www.chalmers.se

CHALMERS